ORIGIN OF THE MEMBRANE COMPARTMENT FOR COWPEA MOSAIC VIRUS RNA REPLICATION

Promotor: Prof. Dr. A. van Kammen
Emeritus hoogleraar in de Moleculaire Biologie
Wageningen Universiteit

Co-promotor: Dr. Ir. J. Wellink
Universitair docent
Laboratorium voor Moleculaire Biologie
Wageningen Universiteit

Samenstelling promotiecommissie:

Prof. Dr. J.F. Bol, Universiteit Leiden
Prof. Dr. R. Goldbach, Wageningen Universiteit
Dr. W. Melchers, Katholieke Universiteit Nijmegen
Dr. E.J. Snijder, Universiteit Leiden

ORIGIN OF THE MEMBRANE COMPARTMENT FOR COWPEA MOSAIC VIRUS RNA REPLICATION

Jan Eduard Carette

Proefschrift
Ter verkrijging van de graad van doctor
op gezag van de rector magnificus
van Wageningen Universiteit
prof. dr. ir. L. Speelman
in het openbaar te verdedigen
op vrijdag 1 februari 2002
des namiddags om 16:00 in de Aula

Origin of the membrane compartment for cowpea mosaic virus replication

Carette, Jan

Thesis Wageningen University, The Netherlands
With references - with summary in Dutch

ISBN 90-5808-557-0

Stellingen behorende bij het proefschrift getiteld "Origin of the membrane compartment for cowpea mosaic virus replication".
Jan Carette, Wageningen 2002.

1. Het endoplasmatisch reticulum is donor van de membraanblaasjes waarmee in cellen de replicatie van cowpea mozaïek virus (CPMV) is geassocieerd.
Dit proefschrift.

2. Het celdodend vermogen van de door CPMV gecodeerde eiwitten 32K en 60K wordt tijdens infectie van planten onderdrukt door snelle aggregatie van de eiwitten in electronendichte structuren.
Dit proefschrift.

3. De geringe homologie van het door CPMV gecodeerde 32K eiwit met eiwitten van poliovirus en andere verwante virussen heeft geleid tot onderschatting van de rol van dit eiwit voor de replicatie van CPMV.
Dit proefschrift.

4. De observatie dat de lokalisatie van het door grapevine fanleaf virus gecodeerde eiwit 2A gefuseerd met het green fluorescent protein gedeeltelijk samenvalt met die van de replicatie eiwitten, is niet voldoende om te concluderen dat het eiwit 2A een actieve rol speelt bij het dirigeren van RNA2 moleculen naar de plaats van replicatie.
Gaire *et al.* (1999) Virology **264**, 25-36

5. Budding uit het ER via het COPII mechanisme en niet autofagie is betrokken bij de formatie van vesicles geïnduceerd in met poliovirus geïnfecteerde cellen.
Suhy *et al.* (2000) J. Virol. **74**, 8953-8965
Rust *et al.* (2001) J. Virol. **75**, 9808-9818

6. Het gebruik van het gist two-hybrid systeem voor onderzoek naar eiwit-eiwit interacties is niet aan te raden nu de resultaten verkregen met dit systeem weinig reproduceerbaar blijken te zijn.
Uetz *et al.* (2000). Nature **403**, 623-627
Ito *et al.* (2001). Proc. Natl. Acad. Sci. USA **98**, 4569-4574

7. Zolang het effect van een vaccin tegen beta amyloide op gedrag en geestelijk welzijn van mensen niet te testen is, moet het gebruik van zo'n vaccin om de ziekte van Alzheimer te voorkomen, ontraden worden.
Schenk *et al.* (1999). Nature **400**, 173-177

8. Het tegenhouden van veldproeven met genetisch gemodificeerde gewassen door de Nederlandse regering is onredelijk en frustreert het publieke debat over het nut en de risico's van genetisch gemodificeerde gewassen voor de landbouw en de voedselproductie.

9. Gezien de economische ontwikkelingen is zelfs op de markt je euro geen dollar waard.

10. Wageningen is een mooie stad maar het mooiste uitzicht heb je toch als je er met je rug naar toe staat.

Aan mijn vader

CONTENTS

OUTLINE OF THIS THESIS

Replication of many positive-strand RNA viruses takes place in association with intracellular membranes. Often these membranes are induced upon infection by vesiculation or rearrangement of membranes from different organelles including the early and late endomembrane system. Upon infection of cowpea cells with cowpea mosaic virus (CPMV) typical cytopathological structures are formed which consists of an amorphous matrix of electron-dense material traversed by rays of small membranous vesicles. The membranous vesicles are closely associated with CPMV RNA replication. CPMV, a bipartite positive-stranded virus, is the type member of the *Comoviruses*, which bear strong resemblance to animal *Picornaviruses* both in gene organization and in amino acid sequence of replication proteins. RNA1 and RNA2 are separately encapsidated and code for large polyproteins, which are proteolytically cleaved into different proteins by a virus-encoded proteinase. CPMV RNA1 is able to replicate in cowpea protoplasts independently from RNA2, and in such RNA1-infected protoplasts vesiculation and electron-dense material is also found suggesting that RNA1-encoded proteins are responsible for the formation of the vesicles. This thesis describes the studies that were undertaken to define the cellular components involved in the establishment of the site of viral RNA replication consisting of vesiculated membranes and electron-dense material. Furthermore, the role of individual viral proteins as well as host proteins in this process was investigated.

The significance of vesiculated intracellular membranes for the replication of different positive-stranded RNA viruses is reviewed in **chapter 1**. Special attention is given to CPMV-induced membrane rearrangements.

Chapter 2 describes the severe effect that CPMV-infection exerts on the morphology of the endoplasmic reticulum (ER) as was observed using the green fluorescent protein (GFP) specifically targeted to ER membranes. Rearranged ER membranes were found in close association with replication proteins suggesting that the ER produced the vesicles involved in replication. Furthermore lipid biosynthesis was found to be essential for CPMV-replication.

In **chapter 3** we have visualized viral RNA in CPMV-infected protoplasts to study the distribution of viral replication complexes during the course of a CPMV-infection. The actin cytoskeleton appeared to play an important role in the establishment of the site of replication.

To identify host proteins interacting with the 60K protein a yeast two-hybrid screen was performed in **chapter 4**. Initial characterization of the interactor proteins took place by transient expression in CPMV-infected protoplasts.

In **chapter 5** individual RNA1-encoded proteins were expressed separately from CPMV-infection using the tobacco rattle virus vector. The 32K and 60K proteins were found to

associate with membranes mainly derived from the ER. Prolonged expression of these proteins resulted in cell death.

Chapter 6 describes a mutational analysis of the VPg protein to discern the structural requirements necessary for proper functioning of VPg.

Finally, in **chapter 7**, we discuss how the experiments described in the preceding chapters added to the knowledge on CPMV-replication and we present a model how viral replication in association with rearranged cellular membranes is effected.

CHAPTER 1

INTRODUCTION

Introduction

Viruses are amongst the smallest pathogens known and are the causative agent of many clinically and economically important diseases. Because viruses contain only limited genetic information, they must rely on existing or modified cellular machineries for many steps of macromolecular synthesis including protein translation and RNA replication. Replication of positive-stranded RNA viruses occurs in the cytoplasm of the infected cell and is often associated with rearranged intracellular membranes. These modified membranes appear to play a key role in the viral replicative cycle.

Cowpea mosaic virus (CPMV) infection induces the formation of numerous small membranous vesicles that are the site of viral replication. The aim of the investigations described in this thesis was to explore the interactions of CPMV-encoded proteins with these membranes and to discover host components involved in the formation of the membranous site of viral replication. In this chapter we will first give an overview of the remarkable diversity of intracellular membranes that are used by different positive-stranded viruses and the complex interactions of viral replication proteins with these membranes. In the last paragraphs we will briefly summarize the knowledge on CPMV-induced membrane alterations that was available at the start of the project.

Virus-induced rearrangements of intracellular membranes

It has long been recognized that infection with positive-strand RNA viruses induces clear morphological changes of intracellular membranes to promote efficient replication of the virus. The membrane alterations involve vesiculation of a wide variety of different organelles depending on the infecting virus. Poliovirus, mouse hepatitis virus, equine arteritis virus, Kunjin virus and Semliki Forest virus (SFV) induce rearrangements of membranes from the early and late endomembrane system (88, 102, 128, 161, 173, 186), pea enation mosaic virus modifies the nuclear envelope (34), cymbidium ringspot virus the peroxisomal membrane (22), turnip yellow mosaic the chloroplast outer membrane (179), carnation Italian ringspot virus the mitochondrial membrane (22) and alfalfa mosaic virus the vacuolar membrane (104). Cytological studies, where replication proteins, double-strand RNA (dsRNA) species or metabolically labeled RNA molecules were found to colocalize with the vesiculated membranes, pointed to a role of these membrane in viral replication. For example, the smooth, double-membraned vesicles that are induced upon poliovirus infection are associated with both the 2BC protein and newly synthesized RNA molecules as was shown using immunocytology and autoradiography (14). Kunjin flavivirus induces formation of vesicle packets of smooth membranes that dual label with anti-dsRNA and anti-NS1 or anti-NS3 antibodies (199). Already in 1968 Grimley et al (58) recognized that in SFV-infected cells cytoplasmic vacuoles (denoted CPV-I) were formed that could be pulse-labeled with tritiated

uridine indicating that RNA synthesis took place at CPV-I. Only recently it was demonstrated that all the nonstructural proteins of SFV localized to the CPV-I (88).

Viral replication activity is associated with intracellular membranes

The notion that replication complexes are tightly associated with membranes was further established in biochemical experiments aimed at isolating the viral RNA dependent RNA polymerase (RdRp). For many positive-strand viruses replication complexes isolated by differential centrifugation of homogenates of infected cells were exclusively found in the crude membrane fraction (for a review see 20, 31). Generally, RNA synthesis by such complexes consisted of the completion of strands already initiated *in vivo*. Often solubilization of the replication complexes did not result in loss of the RNA synthesis activity, which indicates that a membranous environment is not a prerequisite for *in vitro* RNA-elongation. There are however indications that for complete, template dependent *in vitro* replication membranes are important. Replication complexes that are able to initiate *de novo* RNA synthesis programmed by an added RNA template were produced for a number of viruses by removal of endogenous RNA from the replication complexes with micrococcal nuclease (31). In most of these systems only negative-strand RNA was synthesized with the positive-strand RNA as template. Synthesis of both negative- and positive-strands RNA *in vitro* was demonstrated for tobacco mosaic virus (TMV) using an RNA polymerase preparation obtained from a crude membrane fraction of TMV-infected tomato leaves (123). The template dependent activity was lost after solubilization of the polymerase preparation. For Flockhouse virus addition of certain phosphoglycerolipids (PGL) to the polymerase preparations isolated from a crude membrane fraction was required to obtain *in vitro* synthesis of both negative- and positive-strands while in the absence of PGL only negative-strand synthesis occurred (205) (206). These results strongly suggest that for complete *in vitro* replication a membranous environment is essential. For cucumber mosaic virus (CMV) however it was demonstrated that a highly purified, solubilized polymerase preparation isolated from infected *N. tabacum* leaves was capable of catalyzing the complete replication of CMV RNA (66). It should be noted that replication in this system was very inefficient with only a small fraction of the template being copied and the ratio of positive- to negative-strands was much lower than the ratio observed *in vivo*.

For poliovius complete replication in a cell-free translation/replication system was almost completely inhibited in the presence of cerulenin, an inhibitor of *de novo* lipid biosynthesis, whereas the translation was unaffected (114). The effect of cerulenin on poliovirus replication was noted before *in vivo* suggesting that newly formed membranes are important for viral replication (60). Also addition of oleic acid, that alters membrane fluidity, inhibited polioviral replication both in the *in vitro* system and *in vivo* (59, 114). Fractionation of the translation/replication mixture further revealed that the replication activity was present in the

pellet sedimented at 15,000 x g and not in the supernatant fraction indicating that the *de novo* generated replication complexes were physically associated with membranes (9).

Virus-encoded replication proteins interact with membranes

Many viruses encode membrane-associated nonstructural proteins that in some cases have been further characterized by expression of individual proteins separately from viral infection. As summarized in table 1 transient expression of these proteins often leads to vesiculation of different intracellular membranes resembling the morphological changes occurring in virus-infected cells. These nonstructural proteins often contain one or more transmembrane α-helices that consist of a stretch of approximately 20 amino acids with mostly hydrophobic side chains. For example poliovirus 3A contains a 22 amino acid hydrophobic domain, conserved amongst the *Enterovirus* and *Rhinovirus* genera, that by mutational analysis was shown to mediate membrane binding of 3A *in vitro* (177). For some nonstructural proteins an amphipathic helix domain was identified that can mediate membrane binding by insertion of the hydrophobic part of the helix in the lipid membrane and by interaction of the hydrophilic part with the aqueous face (43, 187). Mutational analysis of the amphipathic helix of coxsackie protein 2B showed that this domain is required for RNA replication (187). These membrane-associated proteins may play a dual role. Firstly, the induction of membrane rearrangements by these proteins could compartmentalize viral RNA synthesis. Secondly, these proteins could promote the interaction of viral RdRp with the rearranged membranes.

The targeting of viral membrane associated proteins to specific organelles seems to determine the origin of the virus-induced membranes that are the site of RNA replication. A striking example of this is the formation of multivesicular bodies (MVBs) that occurs upon infection of *N. benthamiana* cells with the tombusviruses cymbidium ringspot (CymRSV) and carnation Italian ringspot (CIRV). While the origin of the MVBs induced by wild-type CIRV is exclusively the mitochondrial membrane and by CymRSV the peroxisomal membrane, in plant cells infected with chimeric CIRV/CymRSV viruses where a small part of the N-proximal region of ORF1 is exchanged, MVBs are formed that are derived from both organelles (22, 150). This demonstrates the diversity of intracellular membranes that can be modified by different viruses, even when these viruses are closely related.

Table 1. Viral non-structural proteins that induce vesiculation of target membranes.

Virus	Protein	Target membrane*	Other properties	Reference
Brome mosaic virus	1a	ER	m^7G Methyltransferase, nucleotide binding	(26, 141)
Carnation Italian ringspot virus	36K	Mitochondria (trans)		(150, 151)
Cymbidium ringspot virus	33K	Peroxisomes (trans)		(150)
Equine arteritis virus	NSP2-3	ER	Protease	(170)
Hepatitis C virus	NSP4B	ER		(69)
	NS4A	ER	Co-factor protease	(201)
Poliovirus	2B	ER (amph)		(3, 27, 173)
	2BC	ER (amph)	Nucleotide binding	(3, 27, 173)
	3A	ER (trans)		(40, 173)
Semliki Forest virus	NSP1	Plasma membrane, endosomes and lysosomes (palm)	m^7G Methyltransferase	(88, 91, 130)
	NSP3	?	Phosphoprotein	(129)
Tobacco etch virus	6kDa	ER (trans)		(160)

*Between brackets motif responsible for membrane association: trans, transmembrane domain; amph, amphipathic helix; palm, palmitylation site

In some cases the origin of the membrane-induced vesicles is not obvious. Poliovirus-induced vesicles are not attached to membranes of a particular organelle and bear protein markers from the ER, the Golgi apparatus and the lysosomes (161). Individual expression of polioviral proteins in different cell types has revealed that proteins from the 2BC3AB region were responsible for the extensive vesiculation. 2BC and 2C induced formation of small membranous vesicles probably derived from the ER that were morphologically similar to poliovirus-induced vesicles (3, 7, 27). The 3A protein, when expressed in isolation, associated with ER membranes causing swelling of these membranes but no small membranous vesicles were formed (40, 41). Recently it was reported by Suhy *et al* that co-expression of 3A and 2BC resulted in formation of vesicles that were similar in both ultrastructure and in biochemical properties as the vesicles induced in a poliovirus infection (173).

COWPEA MOSAIC VIRUS INFECTION INDUCES A MASSIVE PROLIFERATION OF ER BUT NOT GOLGI MEMBRANES AND IS DEPENDENT ON *DE NOVO* MEMBRANE SYNTHESIS

Abstract

Replication of cowpea mosaic virus (CPMV) is associated with small membranous vesicles that are induced upon infection. The effect of CPMV replication on the morphology and distribution of the endomembrane system in living plant cells was studied by expressing the Green Fluorescent Protein (GFP) targeted to the endoplasmic reticulum (ER) and the Golgi. CPMV infection was found to induce an extensive proliferation of the ER whereas the distribution and morphology of the Golgi stacks remained unaffected. Immunolocalization experiments using fluorescence confocal microscopy showed that the proliferated ER membranes were closely associated with the electron-dense structures that contain the replication proteins encoded by RNA1. Replication of CPMV was strongly inhibited by cerulenin, an inhibitor of *de novo* lipid synthesis, at concentrations where the replication of the two unrelated viruses alfalfa mosaic virus and tobacco mosaic virus were largely unaffected. These results suggest that proliferating ER membranes produce the membranous vesicles formed during CPMV infection and that this process requires continuous lipid biosynthesis.

Carette, J.E., Stuiver, M., Van Lent, J., Wellink, J. and Van Kammen, A. (2000) *J. Virol.* **74**, 6556-6563

replication (60). Furthermore, poliovirus infection stimulated the biosynthesis of phosphatidylcholine (191).

To study the effect of CPMV replication on the morphology and distribution of membranes of the secretory pathway we have expressed the Green Fluorescent Protein (GFP) targeted to the ER and the Golgi and used confocal microscopy to visualize the organelles in living plant cells infected by CPMV. Furthermore, we have tested the action of cerulenin on virus replication.

Results

Morphological changes of the ER but not the Golgi apparatus upon CPMV infection

Transgenic *Nicotiana benthamiana* plants, expressing GFP targeted to the lumen of the ER (65), were mechanically inoculated with CPMV. Three days p.i. the leaves were examined by confocal fluorescence microscopy and compared to mock inoculated leaves. As was to be expected, in epidermal cells of mock inoculated leaves green fluorescence was detected in the typical stationary cortical ER network (Fig. 2A), the nuclear envelope (Fig. 2B) and the ER tubules traversing the cytoplasmic threads (data not shown). In contrast, in the epidermis of CPMV-infected leaves clusters of cells were found which contained, in addition to the ER structures as occurring in the mock inoculated cells, a large GFP containing structure often located near the nucleus. High-resolution imaging showed that this structure was connected to the cortical ER network and consisted of a ball of tubular ER (Fig. 2C). Once formed, this structure remained present in the infected cell for two weeks, which was the duration of the experiment. To obtain insight in morphological changes of the ER preceding the formation of this large fluorescent structure, a cluster of infected cells four days p.i. was examined. From the center to the periphery such a cluster of infected cells represents an approximate time course of infection because CPMV infection starts at a single epidermal cell and subsequently spreads to neighboring cells within two days p.i. ((198); unpublished results). Newly infected cells at the periphery of the cluster showed several small, highly mobile, bodies of fluorescence, which were connected to the cortical ER network (Fig. 2D for a close-up). In these cells the large stationary fluorescent body present in cells infected for a longer period, more inward to the cluster of infected cells, was absent. It should be noted that the cortical ER network in both newly infected cells (Fig. 2D) and cells infected for a longer period (Fig. 2C) remained intact despite the formation of these highly fluorescent bodies, suggesting that they are formed by a process of proliferation of pre-existing ER membranes rather than aggregation of these membranes.

To confirm that CPMV induced ER proliferation also takes place in cells from the natural host plant *Vigna unguiculata* L., cowpea mesophyl protoplasts were isolated and transfected with pUC-mGFP5-ER alone or together with CPMV RNA. Typically 40% of the protoplasts

showed GFP fluorescence whereas over 80% of the protoplasts were infected as was tested two days p.i. by immunofluorescence with antibodies directed against the RNA1 encoded 110K protein. The organization of the ER in uninfected living cowpea protoplasts was examined 42 h post transfection, and differed somewhat from the epidermal cells in the transgenic *Nicotiana benthamiana* plants. Again the cortical ER network and nuclear envelope were readily visible but the majority of fluorescence was seen in disordered ER tubules in the cytoplasm surrounding the nucleus and the chloroplasts (Fig. 2E). In the CPMV-infected protoplasts, additionally a large body of fluorescence often near the nucleus was observed in the majority of the pUC-mGFP5-ER transfected cells (Fig. 2F). Observation of the infected protoplasts at an earlier timepoint (18 h p.i.) did not reveal changes of the ER structure in comparison to uninfected cells although the disorderly nature of the ER in the cytoplasm could have obscured minor changes in ER structure. Next it was tested whether RNA1 replication alone, without expression of the viral capsid proteins and movement proteins encoded by RNA2, was able to induce the observed changes in ER structure. For this purpose RNA transcripts of an infectious cDNA clone of RNA1 were co-transfected with pUC-mGFP5-ER and 2 days p.i. observed with a fluorescence microscope. Again the large regions of proliferated ER membranes were apparent in protoplasts infected with RNA1 alone (data not shown).

Since in plant cells the Golgi stacks are closely associated with the endoplasmic reticulum (16), it was of interest to study the distribution of the individual Golgi stacks and the possible proliferation of Golgi derived membranes in CPMV-infected cells. For this purpose two different Golgi markers were used *in vivo*: An *Arabidopsis thaliana* homologue of the yeast HDEL receptor fused to GFP, which accumulates mainly in the Golgi stacks and partly in the ER (pMON-ERD2-smYFP) (16), and the N-terminal transmembrane domain of the rat sialyl transferase fused to GFP, which accumulates exclusively in the Golgi stacks (pMON-STtmd-eYFP) (16). In uninfected cowpea protoplasts the numerous Golgi stacks as visualized by both ERD2-smYFP and STtmd-eYFP were scattered uniformly throughout the cytoplasm, mainly surrounding the chloroplasts and in cytoplasmic threads (ERD2-smYFP: Fig. 2G, 2G'; STtmd-eYFP: data not shown). Using the faint background staining of the ER by ERD2-smYFP it was verified that the Golgi stacks were associated with ER tubules as was reported previously ((16); data not shown). In CPMV-infected protoplasts the amount and distribution of the Golgi stacks did not differ from uninfected cells (ERD2-smYFP: Fig. 2H, 2H', 2H''; STtmd-eYFP: data not shown) in spite of the presence of the large region of proliferated ER observed with ERD2-smYFP (Fig. 2H'').

The data indicate that CPMV infection causes a strong proliferation of ER membranes starting at the cortical ER network ultimately leading to a large region of densely packed ER membranes often near the nucleus. The changes in ER morphology can be induced by infection with RNA1 alone suggesting a role of these structures in viral RNA replication. The distribution and morphology of the Golgi stacks remains unaffected in CPMV-infected cells.

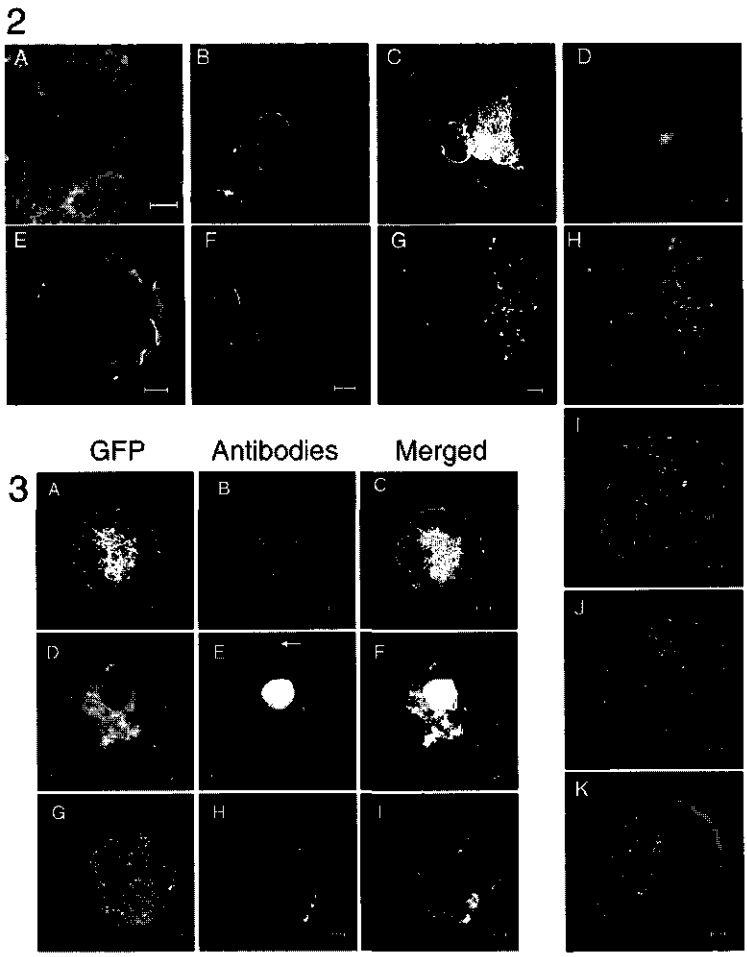

Figure 2 Confocal fluorescence micrographs of healthy (A, B, E, G, G') and CPMV-infected (C, D, F, H, H', H'') plant cells expressing GFP/YFP targeted to the ER (A-F) or the Golgi (G-H''). The confocal images were collected with focal depth of 1 μM using standard FITC filter settings to detect GFP or YFP (pseudo-colored green) and standard rhodamine filter settings to detect autofluorescence of the chlorophyll (pseudo-colored red). (A-D) *Nicotiana benthamiana* mGFP5-ER epidermal cells. (A) Reticulate pattern of cortical ER network. (B) Fluorescent halo of mGFP5-ER in nuclear envelope. (C) Large body of proliferated ER adjacent to nucleus in CPMV-infected cell. (D) Small cortical body of proliferated ER early in infection. (E-H'') Cowpea mesophyll protoplasts. (E) Disorganized ER tubules in cytoplasm surrounding chloroplasts and nucleus in uninfected cells. (F) Large body of proliferated ER in CPMV-infected cell. (G, G') Golgi stacks in uninfected cell scattered through cytoplasm visualized by ERD2-smYFP fluorescence, shown in combination with autofluorescence of chloroplasts (G) or alone (G'). (H, H', H'') Similar distribution in CPMV-infected cells using ERD2-smYFP shown in combination with autofluorescence of chloroplasts (H) or alone (H'). ERD2-smYFP faintly stains the ER showing the nuclear envelope and the CPMV induced large body of proliferated ER (H''). (Bars =5μm).

Figure 3. Immunofluorescence double-labeling showing the intracellular distribution of mGFP5-ER targeted to the ER (A, B) and STtmd-eYFP targeted to the Golgi (C) and viral proteins in CPMV-infected cowpea protoplasts. Cells were fixed 48h p.i. and processed for indirect immunofluorescence using rabbit antibodies against the viral proteins followed by anti-rabbit antibodies conjugated to Cy3. GFP/YFP retained its fluorescence throughout the procedure. Rows show GFP/YFP (left), viral protein (middle), and their superposition (right) of a representative cell. The antibodies used were raised against the replication proteins 110K (A') and VPg (C') and the 48K movement protein (B'). Arrow indicates the tubular structure formed by the movement protein 48K. (Bars =5μm)

RNA1 proteins involved in replication colocalize with the ER but not the Golgi stacks

CPMV RNA replication occurs on clusters of smooth membranous vesicles located near the large electron-dense structures that contain the bulk of the replication RNA1 encoded proteins (33). To determine whether the observed bodies of proliferated ER membranes colocalize with this cytopathological structure, CPMV-infected cowpea protoplasts transfected with pUC-mGFP5-ER were fixed and immunostained with antibodies raised against the RNA1 encoded proteins VPg and 110K. In the infected cells intermediate cleavage products accumulate of which the anti-VPg antibodies recognizes the 170K, 112K, 84K and 60K proteins and the anti-110K recognizes the 170K, 112K, 87K, and the 84K proteins (see Fig. 1). Furthermore, an antibody was used against the RNA2 encoded 48K movement protein to determine possible colocalization with the proliferated ER membranes.

GFP retained its green fluorescence during the immunostaining procedure, and the antibodies raised against the viral proteins were stained with red fluorescence by treatment with goat-antirabbit-Cy3 as secondary antibody. Confocal microscopy showed that in the majority of cells the replication proteins were localized in one or several large fluorescent bodies per cell (Fig. 3A', 3C') probably corresponding to the matrix of electron-dense structures observed by electron microscopy. The proliferated ER membranes stained by mGFP5-ER were always found to surround and traverse these bodies (anti-110K: Fig. 3A-3A''; anti-VPg: data not shown). A small proportion of the proteins recognized by the anti-48K antibodies colocalized with the proliferated ER membranes but the majority was localized in the nucleus and in the typical tubular structures formed by the movement protein (Fig. 3B-3B''). On the other hand no colocalization was found of the replication proteins visualized with anti-VPg and the Golgi markers STtmd-eYFP and ERD2-smYFP (STtmd-eYFP: Fig. 3C-3C''; ERD2-smYFP: data not shown).

To further analyze the presence of proliferated ER in the cytopathological structures, leaf tissue of CPMV-infected *Nicotiana benthamiana* plants transgenic with ER-GFP were prepared for electron microscopy. ER tubules could be distinguished based upon their morphology and were shown to be present near the electron-dense structures and the small membranous vesicles (Fig. 4A). Immunolabeling with anti-GFP confirmed that ER-GFP was present in ER tubules near these structures (Fig. 4B). No specific labeling of ER-GFP was found in the small membranous vesicles.

These data show that the cytopathological structures are enriched with proliferated ER membranes but not with Golgi membranes suggesting that the ER produces the small membranous vesicles which are the sites of viral RNA replication.

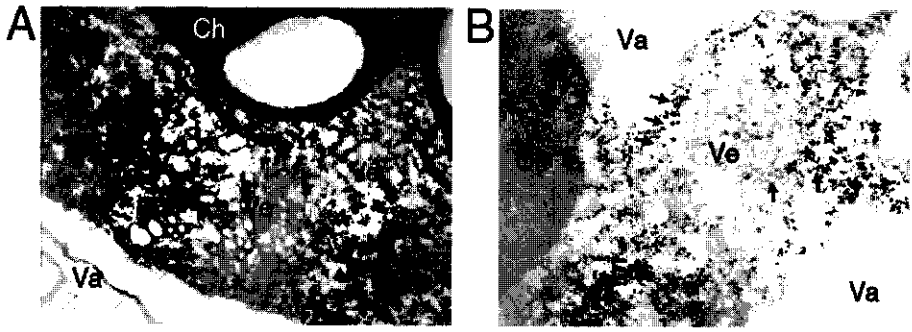

Figure 4. Electron microscopy of cytopathological structures in CPMV-infected *Nicotiana benthamiana* mesophyll cells carrying the mGFP5-ER transgene. (A) ER tubules (arrows) located near electron-dense structures (Eds) and small membranous vesicles (Ve). (B) Immunolabeling with anti-GFP shows labeling of the ER tubules (arrows) and not the vesicles. (Ch=chloroplasts, Va=vacuole; Bars =300nm)

Replication of CPMV requires continuous lipid biosynthesis

To examine whether the proliferation of ER membranes is essential for viral RNA replication, the effect of cerulenin, an inhibitor of *de novo* lipid synthesis (124, 162), on the replication of CPMV was tested.

For this purpose cowpea protoplasts were infected with virus, divided in four portions and cerulenin was added in different concentrations to the incubation medium. Two days p.i. the protoplasts were fixed and stained with antibodies raised against the viral proteins and the percentage of fluorescent cells was calculated. Because viral proteins only accumulate to detectable levels when replication of the virus takes place, the percentage of fluorescent cells is considered to correspond to the percentage of infected cells (183). Fig. 5 summarizes the results of 2 independent experiments. The infection percentage of the sample in which no cerulenin was added was normalized to 100 percent. The presence of 15 μM cerulenin in the incubation medium markedly decreased the infection rate to 50% while concentrations of 30 μM and 50 μM further decreased the infection rate to 10% and 0% respectively. These results show that CPMV replication is strongly inhibited by cerulenin. To exclude the possibility that the observed inhibitory effect is due to a reduced viability of the protoplasts and not the inhibition of *de novo* lipid synthesis per se, the effect of cerulenin on the replication of the unrelated viruses TMV and AMV was tested using identical concentrations of cerulenin. As shown in Fig. 5 cerulenin slightly decreased the infection rate of AMV and TMV to 65% at the highest concentration of 50 μM. The requirement of continuous lipid biosynthesis for CPMV replication suggests that the formation of new membranes plays an essential role in the viral replicative cycle.

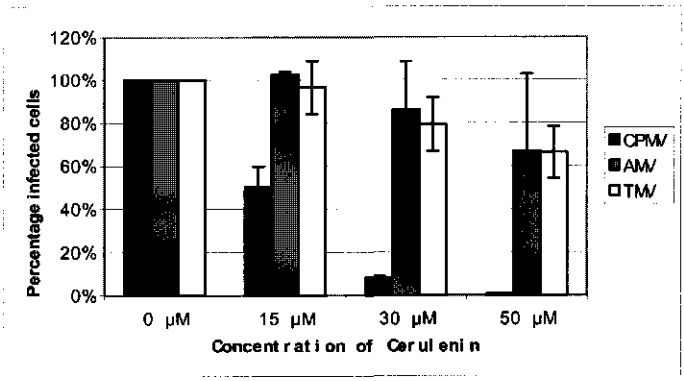

Figure 5 Cerulenin inhibits CPMV but not TMV or AMV replication in cowpea protoplasts. Infected protoplasts were divided in 4 equal portions and were incubated 48h in the presence of 0, 15, 30 or 50 µM cerulenin. Subsequently the protoplasts were processed for indirect, immunofluorescence using antisera against CPMV 110K, TMV CP and AMV CP and the percentage of infected cells was determined. For each virus two independent experiments were performed and error bars indicate the standard deviation.

Discussion

In this study we have shown with confocal fluorescence microscopy using living tissue expressing GFP targeted to the ER and the Golgi, that CPMV infection induces a massive proliferation of ER resulting in the formation of a cytopathological structure highly enriched in ER membranes but not Golgi stacks. The Golgi stacks were moving in close association with the cortical ER network, which remained intact during the whole infection process. Remarkably, they were excluded from the region of proliferating ER membranes indicating that this region is a distinct sub domain of the ER disturbed in its normal function of protein trafficking through the secretory pathway. The rapid formation of such a sub-region of the ER specialized in viral replication exemplifies the remarkable versatility and adaptability of this organelle. In plants as much as 16 ER domains can be distinguished based on morphological features and their known or postulated functional properties (172).

The proliferated ER membranes were present in the cytopathological structure as was shown with immunolabeling experiments using confocal microscopy and electron microscopy. The enrichment of ER membranes in this region suggests that they produce small membranous vesicles, which are the sites of viral replication (33). Since in plant cells the endoplasmic reticulum is the site where the synthesis of the majority of the phopsholipids takes place (121), CPMV might stimulate this synthesis leading to ER proliferation and vesiculation. ER membranes are implicated in viral replication due to their intimate association with replication proteins for many positive-stranded RNA viruses including tobamoviruses (106), bromoviruses (141, 142), flaviviruses (57), potyviruses (160) and

nidoviruses (128). The Golgi membranes did not proliferate and the amount and distribution of Golgi stacks did not differ from uninfected cells, suggesting at most a minor role for this organelle in CPMV induced vesiculation. In contrast, poliovirus infection causes a complete disassembly of the Golgi stacks (157) and isolated membranous vesicles involved in replication were shown to contain molecular markers from throughout the secretory pathway including the ER, trans-Golgi stacks, trans-Golgi network and lysosomes (161). The clusters of vesicles in the cytopathological structures in CPMV-infected tobacco leaf cells transgenic with mGFP5-ER, did not show this marker in electron microscopy. Also the poliovirus-induced vesicles proven to originate from the ER (14) contained a relatively low amount of the lumenal ER marker protein-disulfate isomerase (PDI) (161). This indicates that during the generation of these vesicles lumenal ER proteins are excluded.

Investigation of a cluster of infected cells on transgenic *Nicotiana benthamiana* leaves expressing GFP targeted to the ER allowed us to observe different stages of the infection cycle. At the border of infection sites, several fluorescent bodies at the cortical ER were found to be the first signs of proliferation of ER membranes. These bodies then aggregate into one large fluorescent body usually near the nucleus. Also for poliovirus it has been described that RNA replication starts at small clusters of membranous vesicles distributed through most of the cytoplasm, and that viral RNA associated with these vesicles later in infection migrate to the center of the cell (18).

The unique opportunity to observe virus-mediated changes of ER *in planta* using mGFP5-ER has been exploited for several viruses including potato virus X (PVX), tobacco etch virus (TEV) and TMV (17, 140, 160). The morphological changes of the ER induced by infection with these viruses all involved the formation of large fluorescent structures as seen with CPMV but comparison brings to light some remarkable differences. For TMV and TEV infection, it was reported that the formation of the large fluorescent structures coincides with the disappearance of the typical cortical ER network (140, 160) suggesting that pre-existing ER membranes aggregate to form the structure. In contrast during PVX (17) and CPMV infection the typical cortical ER network remains present indicating that the fluorescent bodies are formed by proliferation of membranes. Our results that CPMV, but not TMV replication requires formation of new membranes as was tested with the inhibitor cerulenin, is consistent with this observation. Furthermore, TMV-induced changes of the ER network are transient and seem to coincide with the synthesis and subsequent degradation of the movement protein (106, 140), while the CPMV-induced changes are permanent and independent from expression of the movement protein of CPMV. The latter was shown in cowpea cells where infection with RNA1 alone showed ER proliferation. Previous experiments using electron microscopy already showed that in RNA1 infected protoplasts small membranous vesicles were formed (143).

Although the movement protein plays no role in the induction of the modified ER membranes, a small proportion of the proteins recognized by anti-48K colocalized with this

structure in CPMV-infected protoplasts. It should be noted that the anti-48K recognizes both the 48K movement protein and the co-C-terminal 58K protein that has been implicated in replication of RNA2 (183). Possibly the observed colocalization with proliferated ER membranes reflects primarily 58K proteins present in replication complexes at the site of viral replication. Previous experiments however indicate that the bulk of the 58K proteins accumulates in the nucleus (83). Alternatively the colocalization reflects 48K and 58K proteins, which are recently synthesized and not yet distributed to the tubules and the nucleus, as it is likely that the site of replication corresponds to the site of translation of viral proteins (180). Like the 58K protein, the N-terminal 2A protein of grapevine fanleaf virus (GFLV), another member of the *Comoviridae*, is required for RNA2 replication (49). Moreover, it was shown that a 2A-GFP fusion protein, transiently expressed from a plant expression vector, partly colocalized with the sites of viral replication. This observation led the authors to suggest that this domain within the polyprotein is responsible for targeting RNA2 to the replication site (49).

The observation of this radical virus-induced proliferation of ER membranes, which the virus uses for its replication, raises the question on how the virus accomplishes the disturbance of a normal function of healthy cells. The CPMV-induced ER proliferation resembles the drastic changes in ER morphology which occur after over-expression of certain endogenous ER resident membrane proteins in yeast and in animal cells (e.g. HMG-CoA reductase (80, 84), cytochrome P-450 (120) and malfolded cytochrome P-450 (71)). It was shown in these cases that overcrowding of the ER membrane and/or improper folding of the over-expressed integral ER membrane proteins affected the triggering of the so-called unfolded protein response (UPR). This is a mechanism to relieve ER stress by both the up-regulation of ER resident chaperone proteins like the heavy-chain binding protein (BiP), PDI and KAR2 and an increase in phospholipid synthesis (for a review: (164)). We speculate that CPMV infection triggers this UPR, which leads to the observed CPMV-induced proliferation of ER membranes and rationalizes the requirement of CPMV replication on *de novo* phospholipid biosynthesis. The viral protein responsible for triggering this response might be the RNA1 encoded 60K protein because it was shown that this protein expressed in insect cells using the baculovirus expression system induces the formation of small vesicles (181).

Materials and methods

Construction of the plasmids

pMON-ERD2-smYFP: This construct contains a plant optimized mutant of the Green Fluorescent Protein (GFP) fused to the coding sequence of the *Arabidopsis* ERD2 homologue (94) in pMON999. The plant expression vector pMON999 contains a multiple cloning site (MCS) between the double CaMV 35S promoter and a terminator sequence of the nopaline

synthase gene (Tnos) (183). pMON-smYFP1 (generously provided by G. van der Krogt, Wageningen University, Wageningen, The Netherlands) contains an *Eco*RI site immediately downstream of the ATG start codon of the coding sequence of the soluble modified Yellow Fluorescent Protein (smYFP), constructed by PCR overlap extension introducing the S65T, V68L, S72A, T203Y mutations in smGFP (30) which improve the fluorescence intensity of the GFP using standard FITC settings. The coding sequence of the *Arabidopsis* ERD2 homologue (94) was PCR amplified from an *Arabidopsis* two-hybrid cDNA library (Clontech) using the following primers, which created additional restriction sites (bold); the start codon is underlined. : GG**TCTAGA**TCAACC<u>ATG</u>AATATCTTTAGATTTG and GG**GAATTC**AGCCGGAAGCTTAAGTTTGGTG. This PCR fragment was digested with *Xba*I and *Eco*RI and cloned in pMON-smYFP1 digested with the same enzymes. The resulting clone was designated pMON-ERD2-smYFP.

pMON-STtmd-eYFP: This construct contains the first 53 amino acids of the rat sialyl transferase gene containing the transmembrane domain fused to a mutant of the green fluorescent protein. pMON-eYFP (generously provided by G. van der Krogt, Wageningen University, Wageningen, The Netherlands) contains an *Nco*I site overlapping the start codon of the coding sequence of eYFP obtained by PCR using yellow cameleon-2 (112) (generously provided by R.Y. Tsien, University of California, San Diego, USA) as template. The complete cDNA of the rat sialyl transferase (ST) was released from pSMH4 (generously provided by S. Munro, Cambridge University, Cambridge, UK) using *Hind*III and *Xba*I and subcloned in pBSK(-) creating a *Cla*I recognition site directly upstream of the 5' nontranslated region (NTR) of ST. Subsequent digestion with *Cla*I and *Nco*I created a fragment containing the 5' NTR and the coding region for the first 53 amino acids of ST and this fragment was cloned in pMON-eYFP digested with the same restriction enzymes. The resulting clone was designated pMON-STtmd-eYFP.

pUC-mGFP5-ER: pUC-mGFP5-ER contains the plant optimized GFP5 (165) with an N-terminal *Arabidopsis thaliana* basic chitinase signal sequence and a C-terminal HDEL ER retention signal (65).This region was released from pBIN m-GFP5-ER (generously provided by J. Haseloff, Cambridge University, Cambridge, UK) and cloned as an *Xba*I *Sst*I fragment in the smBFP vector (30) (obtained from the *Arabidopsis* Biological Research Centre at the Ohio State University) replacing the GFP present in the original construct. The resulting clone contains m-GFP5-ER between a CaMV 35S promoter and a Tnos in the high copy plasmid pUC118 and is referred to as pUC-mGFP5-ER.

Fluorescence microscopy

The Zeiss LSM 510 confocal microscope was used to obtain images. Standard filter for FITC and rhodamine were used to detect GFP5/YFP and Cy3 in fixed protoplasts or GFP5/YFP and the chlorophyll in living protoplasts (FITC: ex. 488nm em. BP505-550; rhodamine: ex 543nm em LP560)

Transfection of cowpea protoplasts and infection of plants

Cowpea (*Vigna unguiculata* L.) mesophyll protoplasts were prepared and transfected by PEG mediated transformation as described previously (183).

Five week old *Nicotiana benthamiana* plants carrying the mGFP5-ER transgene (152) (generously provided by D. Baulcombe, John Innes Centre, Norwich, UK) were dusted with carborundum and inoculated with a homogenate of CPMV-infected leaves.

Immunofluorescent analysis of transfected protoplasts

Immunofluorescent detection of accumulation of viral proteins to determine the number of infected cells using the inhibitor cerulenin was performed as described previously (183).

For the double-labeling experiments a different method of fixation was used to retain the GFP fluorescence as follows:

42 h post transfection the protoplasts were harvested for immunofluorescent staining. The protoplasts were allowed to settle on poly-L-lysine coated coverslips and one volume of fixing solution (4% paraformaldehyde; 0.1% glutaraldehyde; 0.25M mannitol; 50mM sodiumphosphate) was added to the protoplast suspension. After an incubation of 15 min the liquid was removed, replaced with fixing solution and allowed to incubate another 30 min. The cells were washed three times with PBS and permeabilized with a 0.5% Triton X-100 solution in PBS for 10 min. Aspecific antibody binding was reduced using an incubation step of 10 min in blocking solution (1% BSA, 0.8% gelatine from cold water fish skin in PBS). Subsequently, the protoplasts were incubated for one hour with dilutions of the primary anti-48K (197), anti-VPg (44) or anti-110K (181) in blocking solution. After three washes with PBS, the protoplasts were incubated with goat anti-rabbit antibodies conjugated to Cy3 (Sigma) for another hour. After two washes with PBS the coverslips were mounted on microscope slides using Citifluor.

Electron microscopy analysis of Nicotiana benthamiana mesophyll cells infected with CPMV

For electron microscopy, samples were cut from infected leaf tissue and fixed in glutaraldehyde/paraformaldehyde, followed by post-fixation with osmium tetroxide and uranyl acetate, dehydration with ethanol and embedding in LR White as described by van Lent *et al.* (190). For immunogold staining, thin sections were treated with saturated sodium metaperiodate for 1 h at room temperature, washed with distilled water and subsequently labeled and stained as described by van Lent *et al.* (190) using commercially available polyclonal antibodies to GFP (Molecular Probes).

Acknowledgements

We are grateful to David Baulcombe, Jim Haseloff, Gerard van der Krogt, Sean Munro and Roger Tsien for providing the biological material indicated in the Materials and Methods section. Ton Bisseling is acknowledged for critically reading the manuscript. This work was supported by The Netherlands Foundation of Chemical Research with financial aid from The Netherlands Organisation for Scientific Research.

THE COALESCENCE OF THE SITES OF COWPEA MOSAIC VIRUS RNA REPLICATION INTO A CYTOPATHIC STRUCTURE

Abstract

Cowpea mosaic virus (CPMV) replication induces an extensive proliferation of endoplasmic reticulum (ER) membranes and leads to the formation of small membranous vesicles where viral replication takes place. Using fluorescent *in situ* hybridization we found that early in infection of cowpea protoplasts, CPMV plus-strand RNA accumulates at numerous distinct subcellular sites distributed randomly throughout the cytoplasm which quickly coalesce to a large body located in the center of the cell often near the nucleus. The combined use of immunostaining and of a GFP ER-marker revealed that during the course of an infection CPMV RNA and the 110K viral polymerase colocalize and are always found in close association with proliferated ER membranes indicating that these sites correspond to the membranous site of viral replication. Experiments with the cytoskeleton inhibitors oryzalin and latrunculin B pointed to a role of actin filaments in establishing the large central structure. Induction of ER-membrane proliferations in CPMV-infected protoplasts did not coincide with increased levels of BiP mRNA indicating that the unfolded protein response was not involved in this process.

Jan Carette, Kerstin Gühl, Joan Wellink and Ab Van Kammen
Submitted for publication

Introduction

Infection of positive-stranded RNA viruses often causes extensive membrane rearrangements in the host cell to establish a distinct compartment where viral RNA synthesis occurs. The viral replication complexes are associated with these membranes, which can originate from different intracellular membranes including the late and early endomembrane system (88, 102, 128, 161, 173, 186). Despite the central role of such virus-induced membranous compartment in the replicative cycle, the cellular components that are involved in the formation of this compartment are largely unknown.

Cowpea mosaic virus (CPMV), a bipartite positive-stranded RNA virus, is the type member of the *Comoviruses* which bear strong resemblance to animal *Picornaviruses* both in gene organization and in amino acid sequence of replication proteins (4, 47). Both RNA1 and RNA2 are translated into large polyproteins, which are proteolytically cleaved into the different cleavage products by the 24-kDa (24K) proteinase (Fig. 1). The proteins encoded by RNA1 are necessary and sufficient for replication, whereas RNA2 codes for the capsid proteins and the movement protein.

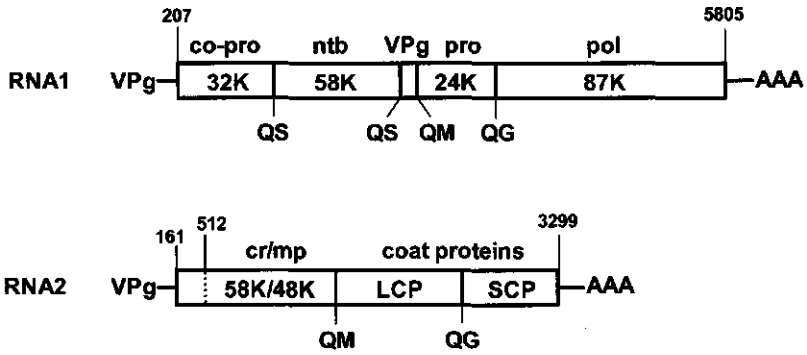

Figure 1 Genetic organization of the CPMV genome. Open reading frames in the RNA molecules are indicated by open bars. Nucleotide positions of start and stop codons are shown above and cleavage sites in the polyproteins are shown below the open reading frame. Abbreviations: co-pro, cofactor for proteinase; ntb, nucleotide binding protein; pro, proteinase; pol, core polymerase; cr, cofactor for RNA2 replication; mp, movement protein; LCP, large coat protein; SCP, small coat protein.

Upon infection of cowpea plants with CPMV, a typical cytopathic structure is formed often adjacent to the nucleus, consisting of an amorphous matrix of electron-dense material, which is traversed by rays of small membranous vesicles (33). Autoradiography in conjunction with electron microscopy on sections of CPMV-infected leaves treated with [^{3}H]uridine revealed that the membranous vesicles are closely associated with CPMV RNA

replication (33). Additional support for that view came from analyzing different fractions of homogenates of CPMV-infected leaves in which the double-stranded, replicative form of CPMV RNA was mainly present in the microsomal fraction (5). Also the viral RNA dependent RNA polymerase activity was found to cofractionate with the crude membrane fraction of CPMV-infected leaves (44, 174). However, using electron microcopy, the bulk of the replication proteins was immunolocalized in CPMV-infected cells not to the vesicles but to the adjacent electron-dense structures, suggesting that only a small subset is present in active replication complexes (196).

The membranous vesicles induced upon CPMV infection may originate from the endoplasmic reticulum (ER). Experiments using transgenic *N. benthamiana* plants expressing the green fluorescent protein (GFP) targeted to the lumen of the ER showed that CPMV infection leads to a strong proliferation of ER membranes and that these membranes are associated with the viral cytopathic structure (24). Also for poliovirus the ER has been suggested to serve as source for the virally induced membranous vesicles although immunoisolated vesicles were found to contain marker proteins of both the ER and of the late endomembrane system (161). It has been proposed that the small membranous vesicles in CPMV-infected cells are due to the unfolded protein response (24), a well described cellular reaction occurring after overcrowding of ER membranes which results in both a proliferation of ER membranes and the upregulation of ER chaperones like protein disulphide isomerase and the lumenal binding protein (BiP) (63).

In this study, the intracellular distribution of CPMV RNA during virus infection was visualized using fluorescent *in situ* hybridization (FISH). The combined use of FISH and immunofluorescence detection of viral proteins allowed us to determine the spatial relationship of CPMV RNA accumulation and accumulation of CPMV proteins involved in replication and encapsidation, and to establish the role of cellular components in formation of the cytopathic structure. Furthermore it was tested whether the unfolded protein response was involved in the proliferation of ER membranes in CPMV-infected cells by monitoring the level of BiP mRNA accumulation.

Results

Localization of CPMV RNA in infected protoplasts

The intracellular accumulation of CPMV viral RNA during CPMV infection in cowpea protoplasts was visualized by fluorescence *in situ* hybrization using a plus-strand-specific probe corresponding to nt 2894 to 3857 of CPMV RNA1 labeled with FITC-UTP by *in vitro* transcription. The earliest time point at which viral proteins and infectious viral particles can be detected in cowpea protoplasts using immunofluorescence and a local lesion assay respectively, is 12 hours post infection (hpi) and between 12 and 24 hpi, the number of

infected cells and the production of infectious particles increase rapidly to reach a maximum at 36 hpi (68). This implies that viral RNA synthesis peaks between 12 and 24 hpi in these cells. Cowpea protoplasts were infected with CPMV RNA1 and RNA2, collected at 16 hpi, and hybridized with the probe. The fluorescent signals were measured with a focal depth of 1 μm by confocal microscopy. The majority of the plus-strand RNA was localized in a large irregularly shaped body often near the nucleus (Fig. 2C). Similar localization patterns were observed with protoplasts harvested at 24 hpi (data not shown) and 36 hpi (fig 3B). Since typically 40% of the protoplasts became infected, the background staining could be evaluated on the same microscope slide. As shown in Fig 2D no background staining was observed when identical settings were used for the confocal. This was confirmed using mock-infected protoplasts (data not shown). To determine the localization of plus-strand RNA early in infection, protoplasts were harvested 12 hpi. At this time point the plus-strand RNA labeling was still weak and signals higher than background (Fig. 2B) could be observed only in a small percentage of the protoplasts (typically 5%). Approximately half of these protoplasts displayed the accumulation of plus-strand RNA in large irregular bodies located near the nucleus as was observed at later time points. In the other half, the fluorescence pattern differed markedly and plus-strand RNA was observed in multiple smaller bodies scattered over the cytoplasm (Fig. 2A). At later time points (14-36 hpi) this fluorescence pattern was no longer observed suggesting that the smaller bodies occur as a preliminary stage, preceding the large juxtanuclear amorphous structure.

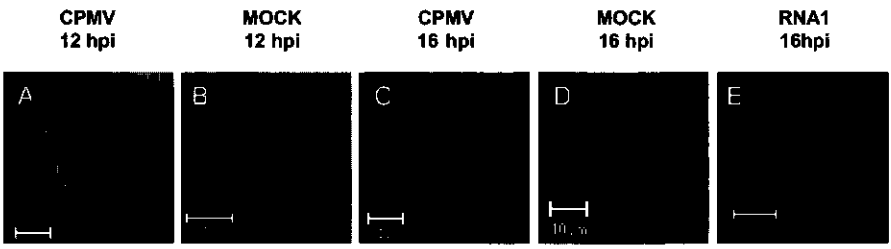

Figure 2 Intracellular distribution of plus-strand viral RNA in protoplasts infected with CPMV RNA. Protoplasts were collected at the indicated time points after infection with CPMV RNA1 and RNA2 (CPMV), CPMV RNA1 (RNA1) or water (MOCK) and hybridized with a fluorescein-RNA probe that recognized plus-strand CPMV RNA1. Fluorescent signals were visualized by confocal microscopy, measuring optical sections with a focal depth of 1 μm. (A) At 12 hours post infection (hpi) viral RNA is localized in multiple small bodies dispersed over the cytoplasm. (C and E) At 16 hpi viral RNA is observed in one or several large, amorphous bodies of fluorescence located in the center of protoplasts infected with CPMV (C) or with CPMV RNA1 alone (E). (B + D) Background fluorescence was evaluated in mock-infected protoplasts using identical settings at 12 hpi (B) and 16 hpi (D). Bars, 10μm.

In order to visualize the accumulation of minus-strand RNA, a minus-strand-specific probe was prepared corresponding to nt 2305 to 3857 of RNA1. With this probe a fluorescent signal above background could not be observed at 12 hpi, 16 hpi and 36 hpi (data not shown) even

when the samples were denatured thermally at 65^{0}C prior to hybridization, a treatment reported to be necessary for detection of poliovirus minus-strand RNA (18). Also with probes spanning different regions of RNA1 or RNA2 no specific signal corresponding to minus-strand RNA was observed (data not shown). This suggests that minus-strand RNA accumulation in CPMV infected protoplasts is much lower than plus-strand accumulation, which is in line with earlier findings using Northern hybridization studies (35).

Taken together these results suggest that plus-strand CPMV RNA accumulates at multiple sites early in infection, which quickly coalesce to a large irregular shaped body located juxtanuclear.

Combined localization of plus-strand RNA and CPMV proteins

The accumulation of plus-strand viral RNA in a large amorphous structure resembles the immunofluorescence pattern observed using antibodies against the viral replication proteins (24, 183). On the ultrastructural level, the replication proteins accumulate in electron-dense material that is found in close proximity to the small membranous vesicles, which are the site of RNA synthesis and presumably RNA accumulation. To examine the spatial relationship between the site of viral plus-strand RNA accumulation and the location of CPMV proteins involved in replication, CPMV-infected protoplasts were immunostained with different antibodies prior to *in situ* hybridization. The distribution of the 110-kDa polymerase (110K), visualized with Cy3-conjugated secondary antibody (Fig. 3B; red) was almost exactly similar to that of viral plus-strand RNA (Fig. 3B; green) at 36 hpi as is clearly visible in the digitally superimposed image (Fig. 3B; merged) where green and red signals that coincide together produce a yellow signal. Also at 12 hpi, when the large amorphous structure in the center of

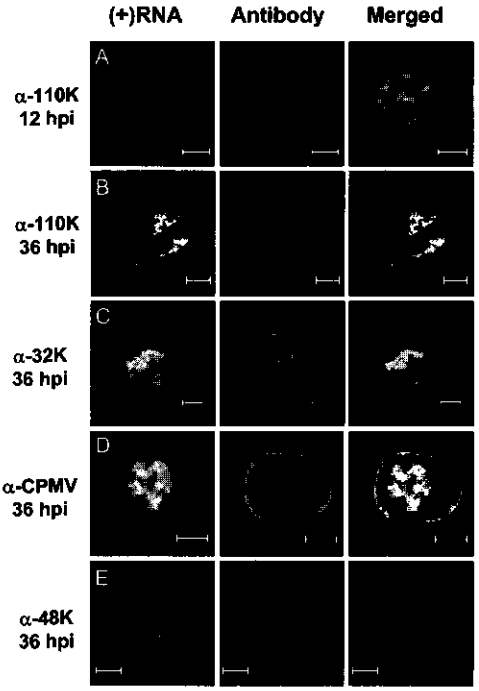

Figure 3 Dual localization of plus-strand viral RNA with different viral proteins in CPMV-infected protoplasts. Protoplasts were collected at the indicated time points after infection with CPMV RNA, hybridized with a fluorescein-RNA probe that recognized plus-strand CPMV RNA1 (green signal) and immunostained with the indicated antisera (red signal). (A and B) At 12 hpi and 36 hpi, the 110K polymerase was localized almost exclusively in sites where viral RNA accumulated. Colocalization of the two signals is shown in the merged image as yellow. (C) The 32K cofactor for the proteinase also colocalized substantially with viral RNA. (D) Viral particles localized to the periphery of the cell and did not colocalize with sites of viral RNA accumulation. (E) The 58K protein recognized by the anti-48K serum localized mainly in the nucleus and did not colocalize with viral RNA. Bars, 10μm.

the cell is not yet formed, 110K colocalizes with the plus-strand RNA (Fig. 3A). Using antibodies raised against the RNA1 encoded VPg and 32K a similar colocalization was found (Fig 3C and data not shown) at 36 hpi although with slightly more variation in intensity of the red and green fluorescence than with the anti-110K serum. At present we do not know whether these differences reflect real differences in the localization of minor portions of the replication proteins recognized by anti-32K and anti-VPg serum and the viral RNA.

After synthesis, plus-strand RNA is encapsidated in viral particles. To investigate the spatial relationship between plus-strand RNA visualized by FISH and the particles, immunolabeling was performed using an antibody raised against purified virus particles. As shown in Fig. 3D, the viral particles accumulate at the periphery of the cell at 36 hpi whereas plus-strand RNA is found centrally, near the nucleus. It is clear from the merged image that colocalization of viral RNA and viral particles is not observed, which is somewhat surprising because the viral particles contain plus-strand RNA. This suggests that encapsidated plus-strand RNA does not hybridize to the probe under these experimental conditions. Using anti-48K serum that recognizes both the 48K movement protein (MP) and the co-C-terminal 58K protein, the majority of the anti-48K signal was present in the nucleus at 36 hpi whereas only a faint signal was present diffusely in the cytoplasm, which only partly overlapped with the fluorescently-labeled viral RNA (Fig. 3E). The signal in the nucleus is in agreement with earlier studies localizing 58K, an RNA2-encoded protein essential for RNA2 replication, in the nucleus (197). The lack of colocalization of plus-strand RNA with the 58K, MP or the capsid proteins may suggest that these RNA2-encoded proteins play no role in the establishment of the sites of viral RNA accumulation. This was strengthened by the observation that the localization of viral RNA in cowpea protoplasts infected with RNA1 alone was similar to the localization observed in cells infected with both RNA1 and RNA2 (Fig. 2E).

Effects of cytoskeletal inhibitors on establishment of the site of replication

As shown above, both viral RNA and the 110K polymerase colocalize in multiple bodies early in infection, which later in infection coalesce to a large irregular shaped body. To test the possible involvement of the plant cytoskeleton in the formation of this structure, the cytoskeletal inhibitors latrunculin B and oryzalin were used. The highly specific toxin latrunculin B, isolated from a red sea sponge, has been shown to effectively depolymerize actin filaments in all eukaryotic cells ((6) and references therein). Oryzalin is an herbicide, which has been shown to bind strongly to plant tubulin monomers thereby stimulating the complete disassembly of the microtubular network ((10) and references therein). Protoplasts were infected with CPMV and then divided in three equal portions. One sample was left untreated whereas either oryzalin (10μM) or latrunculin B (20μM) was added to the incubation medium of the other two samples, directly after infection. The protoplasts were

collected at 16 hpi and 36 hpi and prepared for immunofluorescent staining using antibodies raised against the 110K polymerase. The percentage of infected protoplasts did not differ in the treated and untreated samples. In the untreated or the oryzalin treated protoplasts the polymerase was present in the large juxtanuclear body at 16 hpi (Fig. 4A and 4B) and at 36 hpi (data not shown). The pattern of distribution of the polymerase in latrunculin B treated protoplasts was strikingly different. Fluorescence was present in numerous small bodies that were randomly scattered through the cytoplasm (Fig. 4C). A similar pattern was observed at 36 hpi (Fig 4D). The multiple smaller bodies resembled the pattern of polymerase distribution observed early in infection suggesting that latrunculin B arrests the movement of these bodies to a juxtanuclear position. In parallel experiments it was verified that both inhibitors were active at the used concentrations. For this purpose the cowpea protoplasts were transfected either with a plant expression vector encoding a fusion of GFP with the tubulin binding part of mammalian MAP4 (GFP-MBD; (103)), or with an expression vector encoding a fusion of the yellow fluorescent protein (YFP) with the actin binding part of the Dictostelium talin gene (Talin-YFP; (85)). In protoplasts treated with oryzalin, the typical microtubular network labeled by GFP-MBD was rigorously disturbed as was observed in live protoplasts 16 and 36 hours post transfection using confocal microscopy (Fig 4E and 4F). Also the actin cytoskeleton labeled with Talin-YFP was severely disturbed upon treatment with latrunculin B and only very small fluorescent strands that were not interconnected remained (Fig. 4G and 4H).

Taken together these data suggest that integrity of the actin but not the microtubular cytoskeleton is required for formation of the juxtanuclear large shapeless body.

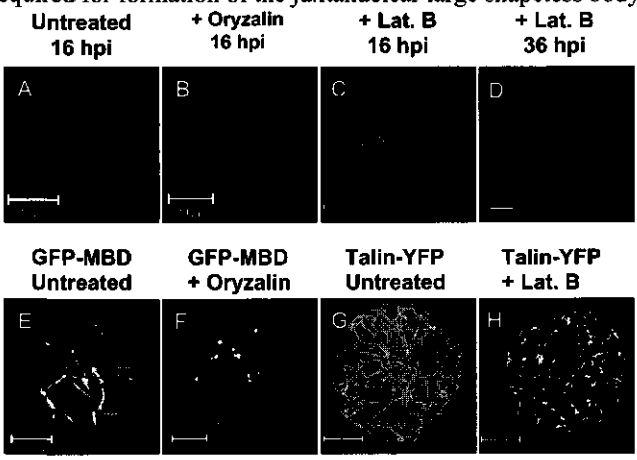

Figure 4 Disruption of the actin but not the microtubular network induces changes in the localization of the viral 110K polymerase in CPMV infected protoplasts. Immediately after infection, protoplasts were treated with oryzalin (10mM) (B), latrunculin B (20mM) (C, D) or left untreated (A) and harvested at the indicated time points followed by immunostaining using anti-110K serum. In untreated (A) and oryzalin (B) treated protoplasts the polymerase was present in a central large amorphous structure at 16 hpi. In cells treated with latrunculin B the polymerase was present in numerous small spots scattered through the cytoplasm both at 16 hpi (C) and 36 hpi (D). Protoplasts transiently expressing GFP-MBD to visualize the microtubules (E, F) and YFP-Talin to visualize the actin cytoskelton (G, H) show that oryzalin (F) and latrunculin B (H) were active at the used concentration. Bars, 10μm.

CPMV-induced membrane proliferation

CPMV infection results in formation of proliferated ER membranes that are surrounding and traversing the site of RNA replication stained with anti-110K serum at 36 hpi (Fig. 5B; (24)). To determine whether the proliferated ER membranes are formed already early in infection when the replication complexes are present dispersed over the cytoplasm, cowpea protoplasts were transfected with CPMV RNA together with pUC-mGFP5-ER, a plant expression vector that encodes the green fluorescent protein targeted to the lumen of the ER (65). The protoplasts were harvested 12 hpi and prepared for immunostaining with anti-110K serum. It should be noted that mGFP5-ER remains fluorescent during immunostaining procedures and the GFP fluorescence could be separated from the fluorescence of Cy3 used for staining the viral polymerase. As shown in figure 5A, the smaller bodies stained with anti-110K serum were closely associated with proliferated ER membranes.

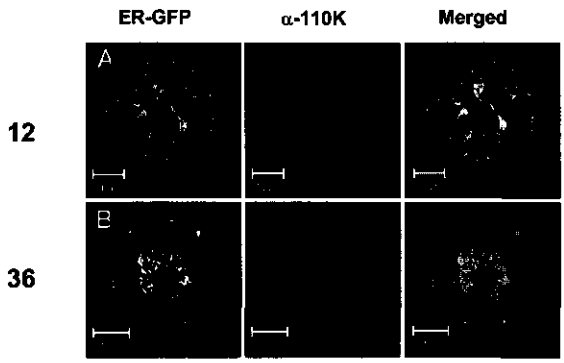

Figure 5 Dual localization of ER targeted GFP (ER-GFP) and the viral 110K polymerase (α-110K) in CPMV-infected protoplasts. Cells were fixed at 12 hpi (A) and 36 hpi (B) and processed for immunofluorescence using antibodies raised against the 110K polymerase. ER-GFP retained its fluorescence throughout the procedure. Proliferated ER membranes surround and traverse the sites of 110K accumulation both early (12 hpi) and late (36 hpi) in infection. Bars, 10μm.

It has been suggested that the ER membrane proliferation occurs as a result of the unfolded protein response triggered by CPMV-infection (24). We now tested this hypothesis in cowpea protoplasts by monitoring the mRNA levels of an ER resident binding protein (BiP), which has been reported to be strongly upregulated in yeast, mammalian and plant cells during the unfolded protein response (63, 78). Northern blot analysis with a tobacco BiP probe revealed that the level of BiP mRNA in CPMV-infected protoplasts was not elevated compared to uninfected protoplasts at 36 hpi when the CPMV-induced membrane proliferation was at its maximum (Fig. 6) Similar results were obtained at earlier time points (data not shown). As a control that the unfolded protein response could be induced in our cowpea protoplasts system, tunicamycin, a drug that inhibits N-glycosylation of ER membrane proteins and potently elicits the unfolded protein response, was used. Treatment of the protoplasts with this drug led a sharp increase in BiP mRNA levels (Fig. 6). These results suggest that the ER membrane proliferations associated with CPMV-replication are probably not due to the unfolded protein response.

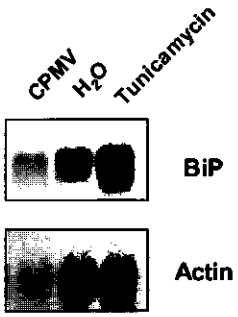

Figure 6 Effect of CPMV-infection on BiP mRNA levels in cowpea protoplasts. Cowpea protoplasts were infected with CPMV (CPMV) or uninfected (H_2O, Tunicamycin). Prior to the harvesting of the protoplasts (36 hpi) the sample designated tunicamycin was treated with tunicamycin (20 µg/mL) for 2.5 h. Total RNA was extracted, separated on a agarose gel and blotted on paper. The blots were probed for BiP, and an actin probe (Actin) was used as a control for loading differences. CPMV infection did not lead to an increase in BiP mRNA levels (CPMV) compared to uninfected protoplasts (H_2O). Treatment with tunicamycin resulted in upregulation of BiP expression (Tunicamycin).

Discussion

The use of fluorescent *in situ* hybridization and immunolocalization allowed us to better define the subcellular sites of viral RNA replication during the course of a CPMV infection. Early in infection the fluorescent probe that recognizes plus-strand RNA was present at numerous subcellular sites distributed over the cytoplasm that quickly coalesced to a large structure located in the center of the cell. Strikingly, almost no fluorescence was present in the cytoplasm at the periphery of the cells, which was the site where the viral particles were shown to accumulate indicating that only unencapsidated plus-strand RNA hybridizes with the fluorescent probe. This observation, together with previously reported experimental data showing that unencapsidated plus-strand RNA is readily degraded in cowpea protoplasts (35), suggests that the signal observed with FISH corresponds to recently synthesized RNA implying a direct correlation of the FISH signal with the site of viral replication. This is in agreement with the observation that the FISH signal colocalized almost perfectly with the viral 110K polymerase during infection. The subcellular sites where 110K and the viral RNA were found to colocalize are believed to correspond, on the ultrastructural level, with the cytopathic structure consisting of electron dense material and clusters of small membranous vesicles.

The numerous sites where the viral RNA and the 110K colocalized early in infection were closely associated with proliferated ER membranes, supporting the view that ER membranes act as source for the small membranous vesicles. This is in agreement with earlier observations in live *N. benthamiana* cells using ER-GFP in which multiple, highly mobile bodies consisting of proliferated ER were observed in newly infected cells (24). Also for poliovirus it has been shown that vesiculation of intracellular membranes starts early in

infection at multiple sites in the cytoplasm of infected cells (18). In CPMV-infected protoplasts, the smaller bodies containing viral RNA could be detected from 12 hpi onwards but they rapidly (within 2 hours) coalesce to a large irregular shaped body located in the center of the cell, often near the nucleus. The majority of viral RNA synthesis occurs between 12 and 24 hpi, which suggests that formation of this cytopathic structure early in infection is important to promote efficient RNA replication. Consistent with this are the findings that also in cells infected with poliovirus or tobacco mosaic virus (TMV) formation of a large juxtanuclear structure containing viral RNA, nonstructural proteins and ER membranes precedes bulk RNA synthesis (18, 106). Many positive-stranded RNA viruses induce the formation of a membranous compartment in the cytoplasm where viral replication occurs and it has been proposed that such compartmentalization increases the local concentrations of virus-encoded proteins and viral RNA (21).

Based on the effects of latrunculin B and oryzalin on the distribution of the viral polymerase, we suggest that in CPMV-infected protoplasts intracellular trafficking of replication complexes to the large juxtanuclear structure occurs via association with the actin cytoskeleton and not the microtubular network. Actin-based movement in plant cells has also been reported recently for individual Golgi stacks in live plant cells using GFP constructs specifically targeted to the Golgi apparatus (16, 119). In contrast to CPMV, for the movement of TMV replication complexes to a juxtanuclear position early in infection, the integrity of both the actin as the microtubular cytoskeleton is required as was demonstrated using cytochalasin D and oryzalin (106).

After the formation of the large cytopathic structure, unencapsidated viral RNA remained in the center of the cell and was not redistributed to the periphery of the cell. In contrast, viral particles did accumulate in the periphery of the cell, presumably to be transported to the neighboring cell via plasmodesmata. These results suggest that encapsidation occurs at the site of RNA synthesis and precedes intercellular transport. The 48K MP did not colocalize with viral RNA and the distribution of viral RNA was similar in protoplast infected with both RNA1 and RNA2 or RNA1 alone, suggesting that the MP does not influence the distribution of viral RNA. In contrast, the TMV 30K MP colocalized with viral RNA at all points during infection and was essential for establishment of the large body near the nucleus observed in midstages of infection (106). Furthermore, at late stages of infection viral RNA was dispersed over the cytoplasm and at the periphery of the cell (106). These differences between CPMV and TMV might reflect the different mechanism these viruses use for their cell-to-cell movement since TMV RNA spreads from cell-to-cell as a ribonucleoprotein complex of TMV RNA and 30K MP (for a review (12)) whereas CPMV RNA is encapsidated before intercellular transport and moves from cell-to-cell as viral particles through tubules formed by the MP in plasmodesmata (189, 195, 198).

CPMV-infection induces an extensive rearrangement of intracellular membranes but the cellular mechanism underlying this vesiculation is unclear. Based on the observation that

poliovirus-induced vesicles share cytological characteristics (a double membrane and cytosolic content) with autophagic vacuoles that are formed in non-infected cells in response to nitrogen or amino acid starvation, autophagy has been proposed as a mechanism of induction of the vesicles (161, 173). At the other hand, CPMV-induced vesicles do not posses similar features, which makes it unlikely that autophagy is involved for CPMV. Another mechanism that has been proposed for poliovirus is that poliovirus-infection interferes with ER to Golgi transport leading to the accumulation of membranous vesicles (108). This view is supported by a recent study that, by using immunofluorescence confocal microscopy combined with deconvolution analysis to enhance the resolution of the acquired images, showed that the small membranous vesicles, that occur during poliovirus infection, bud from the ER and colocalize with the COPII components Sec13 and Sec31 suggesting that poliovirus-induced vesicles are homologous to the vesicles of the anterograde membrane transport pathway (153). The extensive ER-proliferation observed in CPMV-infected cells has not been reported for poliovirus-infected cells, which may suggest that CPMV uses a different cellular mechanism to induce vesiculation. CPMV-infection did not result in an increase of the level of BiP mRNA in protoplasts, which is a marker for the unfolded protein response. The reliability of this marker was tested with tunicamycin that elicited a clear response in protoplasts. Since in yeast, animal and plant cells upregulation of BiP is a hallmark in the unfolded proteins response (63, 78) it is unlikely that this stress response is responsible for the ER membrane proliferations. Further studies will be necessary to unravel the molecular pathways leading to CPMV-induced ER proliferation and vesiculation.

Materials and methods

Plasmids

Plasmid pTB1552(+) was used as template to produce the fluorescein labeled probes used in *in situ* hybridization experiments. To create pTB1552(+), the Sst1-BamHI fragment of the coding region of RNA1 (comprising nucleotides 2305 to 3857) was released from pTB1G and subcloned into the plasmid vector Bluescript SK+ (Stratagene Inc.). The construction of pUC-mGFP5-ER that contains the plant optimized GFP5 with an N-terminal *Arabidopsis thaliana* basic chitinase signal sequence and a C-terminal HDEL ER retention signal under control of a CaMV35S promotor was described earlier (24). pMON talin-YFP (generously provided by Gerard van der Krogt, Wageningen University, Wageningen, the Netherlands) contains the actin binding domain of Dictyostelium talin fused to YFP (Pouwels et al submitted). The construction of GFP-MBD (generously provided by Richard Cyr, The Pennsylvania State University, Pennsylvania, USA) has been described (103). Plasmid pBLP2 (generously provided by Jürgen Denecke, University of Leeds, Leeds, UK) was used to determine BiP mRNA levels and contains tobacco BiP as described earlier (37).

Transfection of cowpea protoplasts and immunofluorescent labeling

Cowpea (*Vigna unguiculata L.*) mesophyll protoplasts were prepared and transfected by polyethylene glycol-mediated transformation as described previously (183). Protoplasts were harvested at different time points post infection for immunofluorescent staining. One volume of fixing solution (4% paraformaldehyde, 0.1% glutaraldehyde, 0.25 M mannitol, 50 mM sodium phosphate pH 6) was added to the protoplast suspension. After incubation for 15 min, the liquid was removed, replaced with fixing solution, and allowed to incubate for another 30 min. The cells were washed three times with phosphate-buffered saline (PBS) and spotted on polylysine-coated microscope slides. The protoplasts were permeabilized with a 0.5% Triton X-100 solution in PBS for 10 min. In the case that the protoplasts were used for *in situ* hybridization the slides were immersed in cold methanol for 10 min to reduce background staining of the chlorophyll. This step was omitted when the GFP organellar markers were used since this step abolishes GFP fluorescence. Nonspecific antibody binding was reduced by incubation for 10 min in blocking solution (5% bovine serum albumin in PBS). Subsequently, the protoplasts were incubated for 1 h with dilutions of the primary anti-48K (197), anti-CPMV (196), anti-32K (48), or anti-110K (181) serum in blocking solution. After three washes with PBS, the protoplasts were incubated with goat anti-rabbit antibodies conjugated to Cy3 (Sigma) for another hour. After two washes with PBS the cells were either mounted with coverslides using Citifluor or prepared for *in situ* hybridization.

In situ hybridization

In situ hybridization was performed essentially as described by (106) with some minor modifications. After acetylation, the dehydration step was omitted. The fluorescent probe that recognizes CPMV plus-strand RNA was obtained by *in vitro* transcription of pTB1552(+) linearized with SpeI in the presence of fluorescein-12-UTP (Roche Diagnostics Gmbh) according to the manufactures recommendations.

Fluorescence microscopy

A Zeiss LSM 510 confocal microscope was used to obtain images. Optical sections were made at 1μm intervals and projections of serial optical sections were obtained using the software provided by the manufacturer. GFP and fluorescein fluorescence was observed using standard settings (excitation wavelength 488 nm, emission band pass filter 505 to 550 nm). Cy3 fluorescence was detected using the settings: excitation wavelength 543 nm, emission band pass filter 560-615 nm. In experiments of dual localization, both fluorophores were scanned independently to reduce the possibility of crossover between the cannels. Furthermore, single immunodetection controls verified the absence of fluorescence crossover.

Northern Blotting

At various times post infection, protoplasts were harvested and centrifuged at low speed (600g). Total RNA was isolated from the cell pellet using Trizol reagent (Gibco BRL) according to the instructions of the manufacturer. Standard procedures were followed to denature the RNA with glyoxal, electroforese in a 1% agarose gel, blot to a GeneScreen membrane (NEN Research Products) and hybridize with a 32P-labelled probe prepared by random-primer labeling of an EcoRI fragment of pBLP2 to detect BiP mRNA.

Acknowledgments

We thank Jürgen Denecke, Richard Cyr and Gerard van der Krogt for generously providing the biological material indicated in the Materials and Methods section. We gratefully acknowledge Jeroen Pouwels for useful comments and technical assistance. This work was supported by The Netherlands Foundation of Chemical Research with financial aid from The Netherlands Organization for Scientific Research.

CHARACTERIZATION OF PLANT PROTEINS THAT INTERACT WITH COWPEA MOSAIC VIRUS 60K PROTEIN IN THE YEAST TWO-HYBRID SYSTEM

Abstract

Cowpea mosaic virus (CPMV) replication occurs in close association with small membranous vesicles in the host cell. The CPMV RNA1-encoded 60-kDa nucleotide-binding protein (60K) plays a role in the formation of these vesicles. In this study, five cellular proteins were identified that interacted with different domains of 60K using a yeast two-hybrid search of an *Arabidopsis* cDNA library. Two of these host proteins (termed VAP27-1 and VAP27-2), with high homology to the VAP33 family of SNARE like proteins from animals, interacted specifically with the C-terminal domain of 60K and upon transient expression colocalized with 60K in CPMV-infected cowpea protoplasts. eEF1-β, picked up using the central domain of 60K, was also found to colocalize with 60K. The possible role of these host proteins for the viral replicative cycle is discussed.

Carette, J.E., Verver, J., Martens, J., van Kampen, T., Wellink, J. and van Kammen, A. (2002) *J. Gen. Virol. in press*

Introduction

Cowpea mosaic virus (CPMV), the type member of the *Comoviruses* possesses a bi-partite, plus-sense RNA genome and bears strong resemblance to animal *Picornaviridae* both in gene organization and in amino acid sequence of replication proteins (4, 47). Translation of both RNAs (designated RNA1 and RNA2) results in formation of large polyproteins from which functional proteins are generated by proteolytic processing by the RNA1-encoded proteinase. RNA1 encodes the viral nonstructural proteins required and sufficient for CPMV replication whereas RNA2 encodes the capsid proteins and the movement protein involved in viral spread. Replication of CPMV is inhibited in protoplasts treated with actinomycin D early in infection, which suggests that viral RNA replication also involves host proteins (148).

CPMV replication occurs on typical cytoplasmic vesicles that are formed during CPMV-infection (33). Based on the observation that CPMV-infection is accompanied by an extensive proliferation of the endoplasmic reticulum (ER) it was proposed that the vesicles originate from the ER (24). The RNA1-encoded 60-kDa protein (60K) induces the formation of similar vesicles when expressed separately from other CPMV proteins in insect cells suggesting that 60K is involved in the membrane rearrangements that occur during CPMV infection (181). Expression of polioviral 2BC, which contains amino acid homology to 60K, also induces characteristic membrane rearrangements when expressed in human or yeast cells (7, 27). The 60K protein contains a Walker nucleotide-binding domain (NTBM) reminiscent of helicases (56). Mutations in the NTBM reduced the ability of 60K to bind ATP *in vitro* and when introduced in an infectious clone, abolished RNA replication (134). Besides, 60K may play a role in the initiation of replication acting as the precursor protein for a small protein, denoted VPg which is covalently attached to the 5'-terminal pU of each viral RNA molecule. For poliovirus, the generation of uridylated VPg species (VPg-pU, VPg-pUpU and VPg-poly(U)) has been demonstrated *in vitro* in a membrane fraction of infected cells (176) and in a cell-free system consisting of synthetic VPg, purified 3Dpol, UTP and poly(A) template (127), which strongly suggest that uridylylated VPg acts as primer for RNA transcription.

To identify host proteins, which might assist 60K in inducing the membranous vesicles or play a role in early steps of RNA replication, a yeast two-hybrid screen was performed using different domains of the 60K proteins as bait. Initial characterization of the potential interactors was performed by immunolocalization studies in CPMV-infected protoplasts transiently expressing the interactors.

Results

Identification of 60K-binding proteins using the yeast two-hybrid system

The CPMV 60K protein was used as bait in a yeast two-hybrid screen to identify interacting proteins encoded by a cDNA library derived from *Arabidopsis thaliana*. Although this is not a natural host plant of CPMV, protoplasts can be infected with the virus (197). Besides with full-length 60K, screens were performed with four different domains of 60K (Fig. 1B). 60KN comprises of the N-terminal half of 60K and contains a predicted amphipathic helix and the NTBM. 60KC comprises of the C-terminal half of 60K and contains a transmembrane domain and VPg, whereas Δ60K contains the central domain of 60K excluding the membrane binding domains. Furthermore, screens were performed with the 28 amino-acid VPg as a bait.

In an initial screen with 60KC, interaction was monitored in yeast strain HF7c by histidine prototrophic growth and β-galactosidase activity. On a total of 300,000 cDNAs one potential

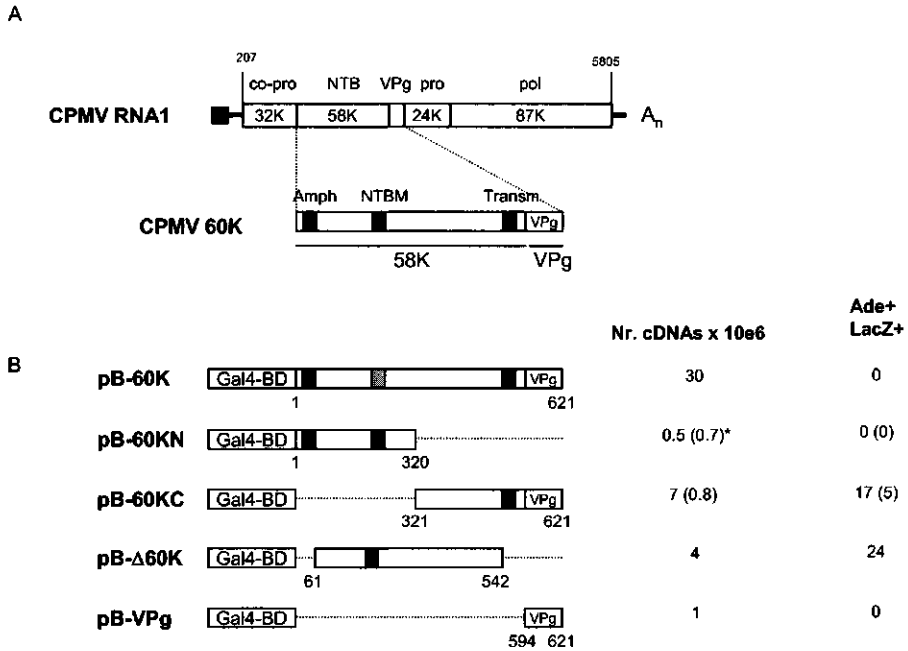

Figure 1 Schematic diagram of CPMV RNA1, the different domains present in 60K and of the bait constructs used to screen an *Arabidopsis* cDNA library. (A) Open reading frames in CPMV RNA1 (open bars), VPg (black square) and nucleotide positions of start and stop codons are indicated. Abbreviations: pro, proteinase; co-pro, cofactor for proteinase; NTB, nucleotide binding protein; pol, core RNA dependent RNA polymerase. CPMV 60K contains a predicted amphipathic helix (amph; aa 45-61), a nucleotide binding domain (NTBM; aa 168-219) and a transmembrane domain (transm; aa 544-565). (B) Summary of the number of cDNAs screened and the number of positive colonies using the bait proteins that contain different domains of 60K. *Between brackets the results are indicated obtained with the pODB8 vector instead of the pGBT9 vector that was used for most screens (See Materials and Methods)

interactor was found. The high background of colonies on the –His plates complicated the analysis. For this reason a different yeast strain (PJ69-4A) was used in subsequent screens. In this strain adenine prototrophic growth and β-galactosidase activity are reporters for protein interaction. The ADE2 gene of the yeast strain is under the control of the LAC2 promoter, which has been reported to display excellent sensitivity and extremely low background (76). The results of several screens in PJ69-4A with the different baits are summarized in Figure 1B. 60KC yielded 22 potential interactors out of the 8 million cDNAs that were screened in total. The central part of 60K, Δ60K, excluding the membrane binding domains, generated 24 possible interactors out of 4 million screened cDNAs. However, the full-length construct of 60K yielded no interactors after screening of thirty million cDNAs, which is ten times the amount of independent clones present in the *Arabidopsis* library. Also no interactors were obtained with 60KN and VPg.

The 47 candidate plasmids picked up with 60KC and Δ60K were rescued and characterized by DNA sequencing of the junction between the coding region of the GAL4 activation domain and the cDNA. Surprisingly, 37 of the potential interactors were found with the cDNA inserted in the reverse orientation, or in a different reading frame with regard to the activation domain. These clones were considered false positives and were excluded from further analysis. The remaining positives were retransformed in PJ69-4A with the corresponding bait plasmid used in the initial screen and tested for growth on medium lacking adenine to confirm the interaction. Three clones were not able to support growth in this retransformed yeast and one clone supported growth even in the absence of the bait plasmid and also these clones were discarded. After this selection 5 interactors remained that were all initially picked up with 60KC. Cotransformation of these clones with either the empty bait vector or a bait vector encoding the *Arabidopsis* Ran protein (61), a small soluble GTP-binding protein unrelated to 60K, did not result in a positive two-hybrid interaction demonstrating that the 5 clones specifically interacted with 60KC.

Sequence analysis of the 60K interacting proteins

The open reading frames encoded by the cDNA present in the 5 clones were compared to amino acid sequences deposited to the non-redundant database at NCBI using the BLASTp algorithm. Two clones (designated γ-TIP) were identical to the full-length sequence of a γ-tonoplast intrinsic protein, which is induced under salt stress (Accession number: AAB62692; *Arabidopsis* gene: At3g26520; (137)). γ-TIP is an abundant protein localized in the vacuolar membrane of plant cells and is a member of the aquaporin family (107). These proteins allow passive diffusion of water molecules across different cellular membranes (158).

One clone encoded a full-length protein of 240 amino acids, which showed 68% identity to NpVAP27 isolated from *Nicotiana plumbaginifolia* (AC: JC7234) and was therefore designated VAP27-1. NpVAP27 was reported to be a VAP protein on the basis of amino acid

sequence and structural homology (93). VAP was first identified in *Aplysia californica* as a member of the SNARE complex involved in vesicular docking and neurotransmitter exocytosis in nervous cells (168). The architecture of VAP proteins identified in different species is similar, with a highly conserved N-terminal region and a less conserved C-terminal region containing a transmembrane domain and a coiled-coil region. In plants, NpVAP27 is the only characterized VAP protein although a BLASTp search using the *Arabidopsis* database at The *Arabidopsis* Information Resource (TAIR; http://www.arabidopsis.org) revealed that VAP27-1 was identical to a putative protein (CAB82664; At3g60600) predicted from a BAC sequence. In addition, 6 putative proteins were present in the *Arabidopsis* database that are highly homologous (E value < 10e-30) to VAP27-1.

One clone encoded a protein of 121 amino acids with 16% and 17% identity to the C-terminal part of NpVAP27 and VAP27-1 respectively. Furthermore it contained a coiled coil as predicted by the COILS algorithm and a predicted transmembrane domain. These results suggest that this clone encodes the C-terminal part of an *Arabidopsis* VAP protein distinct from VAP27-1 and it was therefore named ΔVAP27-2. Comparison of ΔVAP27-2 with proteins in the *Arabidopsis* database revealed that it showed a perfect match over a stretch of 59 amino acids with a hypothetical protein (T00738;At1g08820). Because this hypothetical protein had almost twice the length of VAP proteins identified in different species and only 59 amino acids matched the translation product of our ΔVAP27-2 cDNA, it is likely that the hypothetical protein has been incorrectly predicted from the *Arabidopsis* genomic sequence.

One clone was identical to the C-terminal 223 amino acids of a thylakoid-bound ascorbate peroxidase and was designated ΔthAPX. The full-length protein is 426 amino acids long and contains an N-terminal signal sequence of 48 amino acids to target the protein to the stromal site of the thylakoid membrane (CAA67426;At1g77490) (79). Ascorbate peroxidases are haem proteins that efficiently scavenge H_2O_2 in the cytosol and chloroplasts of plants. They protect the cells from the deleterious effects of H_2O_2 generated as by-product during photosynthesis and respiration (169).

Although none of the candidates picked up in a screen using Δ60K, comprising of the central domain of 60K, could be confirmed to bind 60K upon retransformation, the sequence data of one (designated ΔeEF1-β), tempted us to use the clone for further analysis. It encoded the last 33 aminoacids of eukaryotic elongation factor 1β (P48006;At1g30230 (51)). Translation elongation factors have been shown to be components of the replication complex of several positive-stranded RNA viruses including phage Qβ, vesicular stomatitis virus (VSV) and poliovirus (15, 29, 64). The potential association of the CPMV 60K protein with eEF-1β might indicate that this cellular protein is an integral part of the CPMV replicase complex.

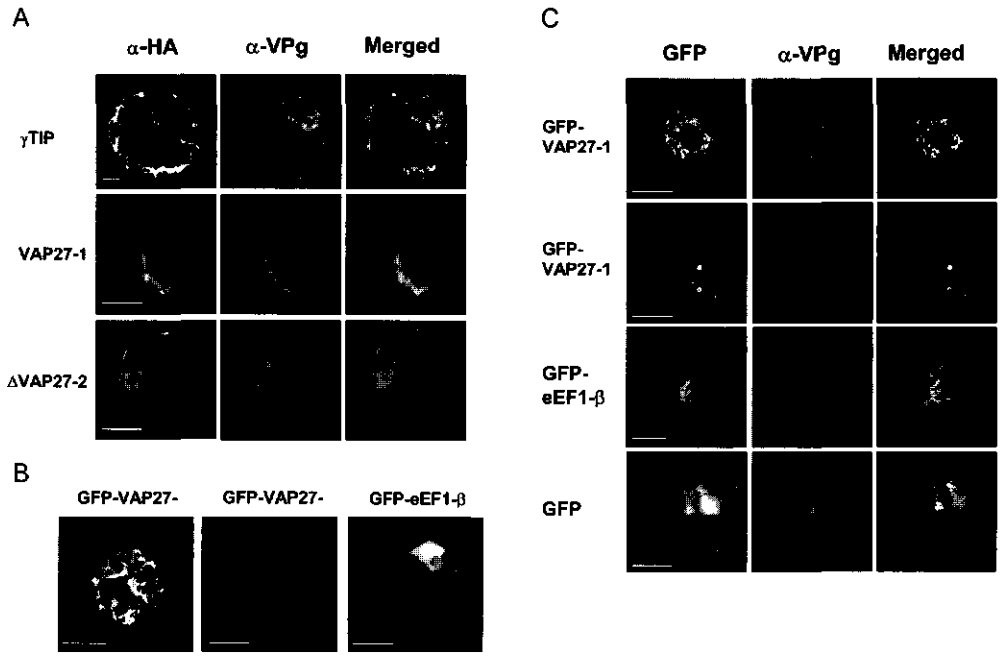

Figure 3 Subcellular localization of the interactor proteins fused to GFP or the HA-epitope tag transiently expressed in cowpea protoplast infected with CPMV (A and C) or in uninfected protoplasts (B). The interactor proteins (green) were visualized using immunofluorescence staining with anti-HA antibodies (A) or using the direct fluorescence of GFP (B and C). 60K (red), was immunostained in CPMV infected protoplasts using anti-VPg serum and localized to a large shapeless body in the cytoplasm. HA-tagged γ-TIP, was present exclusively in the vacuolar membrane (A). In uninfected cells, GFP-VAP-27-1 was present in ER-tubules (B; left panel) or in some cases in highly fluorescent vesicles (B; middle panel). In CPMV infected cells, HA-tagged VAP27-1, ΔVAP27-2 (A) and GFP-VAP27-1 (C; first row) was present in ER tubules colocalizing with 60K. The highly fluorescent vesicles observed sometimes with GFP-VAP27-1 did not colocalize with the 60K (C; second row). GFP-eEF1-β fluorescence was present in a diffuse pattern in the cytoplasm and nucleus of uninfected cells (B). In infected cells, GFP-eEF1-β was additionally present in the cytopathic structure (C). Unfused GFP displayed a similar localization pattern (C). Bar= 10μm.

in the cytopathic structure. This indicates that soluble proteins in general tend to accumulate in the cytopathic structure and that the presence of GFP-eEF1-β in the cytopathic structure is not necessarily due to association with the 60K protein.

Western Blot analysis of extracts of protoplasts transfected with the different HA-tagged host proteins showed proper expression of γ-TIP, VAP27-1, ΔVAP27-2, eEF1-β whereas ΔthAPX, thAPX and ΔeEF1-β were not detected (Fig. 4; γ-TIP, thAPX and eEF1-β: data not shown). In the lane of ΔVAP27-2 two prominent bands near the predicted length of 17 kDa were present and a prominent band of approximately twice the size of ΔVAP27-2. The fastest migrating band might be a degradation product while the slower migrating band may be a dimer. Additionally a third rather faint band is present at triple the size of ΔVAP27-2 suggesting that a small proportion of ΔVAP27-2 can form trimers. Expression of HA-tagged

VAP27-1 was somewhat lower than ΔVAP27-2 but a clear band was present running at the expected length of 33-kDa. The presence of an 66-kDa endogenous cowpea protein interacting with the HA-antibody prevented us to determine whether VAP27-1 also forms a dimer but at approximately 100-kDa a faint band was present suggesting that a trimer was formed.

Discussion

The CPMV 60K protein was used as bait in a yeast two-hybrid screen to identify interacting proteins encoded by a cDNA library derived from *Arabidopsis thaliana*. Four host proteins were found that interacted specifically with the C-terminal half of 60K. Based on amino acid sequence comparisons with (predicted) proteins deposited in the sequence database, these proteins could be identified as a γ-TIP aquaporin, a thylakoid-bound peroxidase and two VAP proteins, which all were predicted to be membrane associated. This is in line with the proposed role of 60K in inducing intracellular membrane rearrangements. A screen with the central domain yielded 24 putative interactors but only one clone contained cDNA in the proper reading frame compared to the activation domain. Although this clone did not interact upon retransformation it was further analyzed since it contained cDNA encoding the translation elongation factor eEF1-β that has been shown to be a component of the replication complex of several positive-stranded RNA viruses including phage Qβ, vesicular stomatitis virus (VSV) and poliovirus (15, 29, 64). Screening of the *Arabidopsis* cDNA library with the full-length 60K yielded no interactors despite several attempts. It has been reported earlier in experiments using well-defined protein combinations that in the yeast two-hybrid system full-length proteins sometimes do not interact whereas smaller domains of these proteins do give interaction (46).

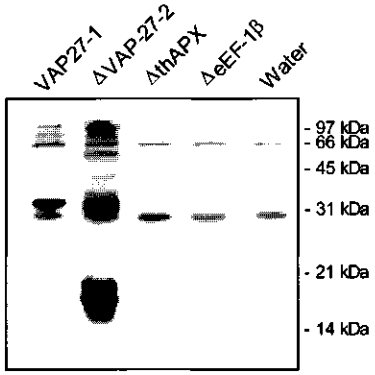

Figure 4 Immunoblot analysis of HA-tagged interactor proteins transiently expressed in cowpea protoplasts. Protoplast lysates were prepared 40 hpt, and the proteins were electrophoresed in 10% polyacrylamide gels. Detection of the proteins was with mouse monoclonal HA antibodies. Water: no DNA added. Positions of molecular size markers are indicated.

Even though several host proteins were found that specifi cally interacted with different domains of 60K in the yeast two-hybrid system it is conceivable that they are not physiologically relevant in the context of CPMV infection because they will never actually meet in a cell. We have used localization studies of transiently expressed 60K interactors in CPMV-infected protoplasts as a first step to differentiate between true interactors and physiological irrelevant ones. CPMV replication is compartmentalized and occurs in a cytopathic structure

consisting of small, probably ER-derived vesicles and electron dense material that contains the majority of the nonstructural proteins including 60K (24, 33, 196). Only the VAP proteins and eEF1-β were shown to colocalize with the cytopathic structure suggesting that these proteins have the opportunity to interact with 60K during CPMV infection. The VAP proteins localized in ER membranes, including the proliferated ER membranes that surround and traverse the cytopathic structure in CPMV-infected cells. GFP-eEF1-β behaved as a soluble, cytoplasmic protein and was found to be present in the cytopathic structure. Unfused GFP however displayed a similar localization pattern, which may suggests that cytoplasmic proteins in general are present in the cytopathic structure. Despite this, on the basis of the localization studies eEF1-β cannot be ruled out as a true interactor with 60K and additional experiments are required to demonstrate a functional role of eEF1-β in the viral life cycle. γ-TIP localized in the vacuolar membrane in non-infected protoplasts and was not relocated to the site of CPMV replication in infected protoplasts. Therefore it is unlikely that this protein is involved in CPMV replication. thAPX is predicted to localize in the thylakoid membrane of chloroplasts but we were unable to determine the localization of the protein in CPMV-infected cells since it was not expressed to detectable levels in cowpea protoplasts. Additional experiments are required to determine the significance of the interaction of 60K with thAPX in the two-hybrid system. It should be noted however that redox control proteins are frequently found as false positives in the yeast two-hybrid system (163).

The localization of transiently expressed eEF1-β in protoplasts diffusely distributed in the cytoplasm was somewhat surprising. Subcellular localization studies of components of eEF1 in Xenopus and human cells revealed that endogenous eEF1-β is present in a complex with eEF1-γ and eEF1-δ in association with ER whereas eEF1-α is present in higher amounts and is distributed diffusely over the cytoplasm (111, 156). In our transient expression system, the eEF1-β subunit may be expressed to such a high level that only a small part forms ER-associated complexes with endogenous eEF1-β while the bulk of the proteins is present freely in the cytoplasm.

The two *Arabidopsis* VAP proteins that we have identified as interactors with 60K are homologous to Alypsia VAP33 that has been originally identified in a yeast two-hybrid screen with the SNARE protein VAMP (168). VAP33 has been proposed to be a SNARE-like protein that functions in a complex with VAMP in the fusion of synaptic vesicles with the plasma membrane (168). Characterization of mammalian and yeast homologues of VAP33 has suggested a more general role in vesicle trafficking because VAP proteins were expressed in many different tissues and were found to localize mainly to ER membranes and to microtubules (82, 167, 194). Although the *Arabidopsis* genome contains a large number of SNARE proteins for many of which the intracellular localization has been determined (reviewed in (155)), this is the first report of a SNARE-like protein that localizes to the ER

membrane, which may suggests that VAP27-1 and VAP27-2 play an important role in vesicular transport to or from the ER.

The occurrence of multimers of VAP27-1 and ΔVAP27-2 in protoplasts is consistent with the finding that SNARE proteins interact strongly either with themselves or with other SNARE proteins usually via the C-terminal coiled coil region and transmembrane region (90, 194); (23). These region may also be involved in the interaction with the 60K region.
It has been reported that human VAP binds promiscuously to many members of the SNARE family including VAMP, syntaxin 1A, rbet1, rsec22, alphaSNAP, and NSF (168, 193, 194). Using the two-hybrid system, VAP was also found to interact with proteins that are not related to SNARE proteins including the gene product of cf9 that confers resistance to a pathogenic fungus in tomato plants (93) and occludin, a transmembrane protein located at tight junctions between epithelial and endothelial cells (92). The role of VAP for these systems is unclear. Recently VAP was identified in a two-hybrid screen to interact with the hepatitis C virus (HCV) nonstructural proteins NS5A and the viral polymerase (178). For most positive-stranded RNA viruses including HCV and CPMV, replication occurs closely associated with intracellular membranes. VAP may act as membrane anchor for the viral replication complex. Alternatively, since 60K was shown to induce the dramatic vesiculation of membranes probably derived from the ER, it is tempting to speculate that this vesiculation is mediated by interference of 60K with VAP function.

Materials and methods

Plasmid construction

(i) Two-hybrid constructs. The cDNAs encoding full-length 60K or parts of 60K (Fig. 1B) were amplified by PCR using gene-specific primers containing EcoRI and BamHI restriction sites. The PCR product was digested with EcoRI and BamHI and ligated into pGBT9 (Clontech) or pODB8 (100) digested with the same enzymes. Plasmid pGBT9 contains a truncated ADH1 promoter leading to low levels of fusion protein expression whereas pODB8 contains the full-length ADH1 promoter leading to high levels of fusion protein expression. The *Arabidopsis thaliana* cDNA library was cloned in the pGAD10 (Clontech) vector.

(ii) Plant expression constructs. The constructs used to transiently express the interactor proteins were based on pMON999 that contains a CaMV 35S promotor and a nopaline synthase terminator (183). The construction of pMON-HA, that contains a start codon followed by the coding sequence of the HA epitope tag (YPYDVPDYA) and a multiple cloning site, has been described earlier (185). The cDNAs of the positive clones were excised from the pGAD10 vector using EcoRI and ligated in the EcoRI site of pMON-HA to allow expression of the interactors tagged with HA at the N-terminus. pMON-GFP* was constructed by amplification of the GFP5 coding region (65) without the stop codon from

pM19GFP10 (55) using gene-specific primers containing XbaI and EcoRI restriction sites and ligation in pMON999. To allow expression of the interactors with GFP fused to the N-terminus, the cDNAs of the positive clones were excised from the pGAD10 vector using EcoRI and ligated in the EcoRI site of pMON-GFP*. The coding region of full-length eEF1-β was PCR amplified from the *Arabidopsis* cDNA library used for the two- hybrid screen with gene-specific primers that introduce an EcoRI site at the 5'-end and BamHI site at the 3'-end and ligated in pMON-HA and pMON-GFP*. The coding region of full-length ThAPX was PCR amplified from the *Arabidopsis* cDNA library used for the two-hybrid screen with gene-specific primers that introduce an XbaI site at the 5'-end and the HA-tag and BamHI site at the 3'-end. This PCR frament digested with XbaI and BamHI and ligated in pMON999 digested with the same enzymes to allow expression of ThAPX with the HA tag fused to the C-terminus. pMON-GFP was constructed by amplification of the GFP coding region including the stop codon from pM19GFP10 (55) using gene-specific primers containing EcoRI restriction sites and BamHI. Full-length ThAPX was PCR amplified from the *Arabidopsis* cDNA library used for the two-hybrid screen with gene-specific primers that introduce an XbaI site at the 5'-end and the EcoRI site at the 3'-end. Ligation in pMON-GFP allowed expression of ThAPX fused at the C-terminus with GFP.

Yeast two-hybrid screening

In initial experiments, yeast strain HF7c was sequentially transformed with pGBT9-60KC and with an *Arabidopsis thaliana* cDNA library in the vector pGAD10 (Clontech). This library was constructed using 3-week-old green vegetative tissue of cv. Columbia and contains 3 million independent cDNAs. Colonies were selected on agar plates lacking histidine, tryptophan, and leucine over a 7-day period. Positive yeast transformants were picked up and replated for β-galactosidase assay by colony-lift filter procedure. A positive interaction was determined by the appearance of blue colonies and the plasmid was isolated and analyzed by nucleotide sequencing. In subsequent experiments, yeast strain PJ69-4A (76) was sequentially transformed with bait constructs containing full-length 60K or domains of 60K and with the *Arabidopsis thaliana* cDNA library. Plasmids were isolated from Ade+ and Gal+ colonies and were characterized by DNA sequencing. The plasmids containing a reading frame in frame with the Gal4 activation domain were retransformed with or without the bait plasmid into yeast strain PJ69-4A, followed by testing for adenine prototrophy. Plasmid clones that grew on adenine lacking medium only in the presence of the bait plasmid were chosen and transformed in yeast strain SFY526 for liquid β-gal assays. β-galactosidase assays were performed according to the protocols described in the Clontech MATCHMAKER manual. Briefly, overnight cultures grown in selective medium were diluted 5 times and grown to an optical density at 600 nm of 0.5-0.8. Cells were pelleted by centrifugation, resuspended Z buffer (60 mM Na_2HPO_4, 40 mM NaH_2PO_4, 10 mM KCl, 1 mM $MgSO_4$, 50 mM -mercaptoethanol [pH 7.0]) and subjected to three freeze/thaw cycles using liquid nitrogen.

After addition of o-nitrophenyl--D-galactopyranoside (ONPG) to a concentration of 0.7 mg/ml, the reaction mixture was incubated at 30°C until a yellow color developed. The reaction was stopped by the addition of Na_2CO_3, and the cells were pelleted by centrifugation. The A_{420} of the supernatant was measured, and β-galactosidase activity units were calculated as described previously (110). Nucleotide and predicted amino acid sequences were compared with known protein sequences deposited in the GenBankTM by BLAST analysis.

Transfection of cowpea protoplasts and immunofluorescent labeling

Cowpea (*Vigna unguiculata* L.) mesophyll protoplasts were prepared and transfected by polyethylene glycol-mediated transformation as described previously (183).
Immunofluorescence labeling was performed essentially as described previously (24). Briefly, protoplasts were harvested at 40 hours post transfection and fixed with 4% paraformaldehyde and 0.1% glutaraldehyde. After permeabilization with a 0.5% Triton X-100 solution, nonspecific antibody binding was reduced by incubation with 5% bovine serum albumin. Subsequently, the protoplasts were incubated for 1 h with dilutions of the primary anti-VPg (44) rabbit serum and mouse monoclonal anti-HA (Boehringer) antibodies, followed by incubation with goat anti-rabbit antibodies conjugated to Cy3 (Sigma) and donkey anti mouse conjugated to fluorescein isothiocyanate (Sigma) for another hour. After two washes with PBS the cells were mounted with coverslides using Citifluor.

Fluorescence microscopy

A Zeiss LSM 510 confocal microscope was used to obtain images. Images shown are single optical sections made at 1μm interval. Fluorescein and GFP fluorescence was observed using standard settings (excitation wavelength 488 nm, emission band pass filter 505 to 550 nm). Cy3 fluorescence was detected using the settings: excitation wavelength 543 nm, emission band pass filter 560-615 nm. In experiments of dual localization, both fluorophores were scanned independently to reduce the possibility of crossover between the channels. Furthermore, single immunodetection controls verified the absence of fluorescence crossover.

Acknowledgements

The authors thank Philip James, Olivier Louvet and Ferenc Nagy for generously providing yeast strain PJ69-4A, vector pODB8 and pGBT9RAN/pGBT9RANBP and Jeroen Pouwels and Maurice van der Heijden for useful comments. J.C. was supported by the Netherlands foundation for chemical research (CW) with financial aid from the Netherlands Foundation for Scientific Research (NWO).

CHAPTER 5

COWPEA MOSAIC VIRUS REPLICATION PROTEINS 32K AND 60K TARGET TO AND CHANGE THE MORPHOLOGY OF ENDOPLASMIC RETICULUM MEMBRANES

Abstract

Cowpea mosaic virus (CPMV) replicates in close association with small membranous vesicles that are formed by rearrangements of intracellular membranes. To determine which of the viral proteins are responsible for the rearrangements of membranes and the attachment of the replication complex, we have expressed individual CPMV proteins encoded by RNA1 in cowpea protoplasts using transient expression and in *N. benthamiana* plants using the tobacco rattle virus (TRV) expression vector. The 32K and the 60K proteins, when expressed individually, accumulate only in low amounts, but are found associated with membranes mainly derived from the endoplasmic reticulum (ER). The 24K and 110K are freely soluble and accumulate to high levels. Using the TRV vector, expression of 32K and 60K results in rearrangement of ER membranes. Besides, expression of 32K and 60K results in necrosis of the inoculated *N. benthamiana* leaves suggesting that 32K and 60K are cytotoxic proteins. At the other hand, during CPMV-infection 32K and 60K accumulate to high levels without causing necrosis and are localized both in electron-dense structures and the small membranous vesicles as shown by immuno-electron microscopy.

Jan Carette, Jan van Lent, Stuart MacFarlane, Joan Wellink and Ab Van Kammen

Submitted for publication

Introduction

It has become increasingly clear that replication of positive-strand RNA viruses takes place in association with intracellular membranes (for a review (20)). Often these membranes are induced upon infection by vesiculation or rearrangement of membranes from different organelles including the early and late endomembrane system (102, 128, 161). The importance of membranes for viral replication is evident from various studies. *In vitro* synthesis of positive-strand RNAs of picornaviruses and nodaviruses depends on membranes (114, 205). Poliovirus, Semliki Forest virus and cowpea mosaic virus (CPMV) RNA replication is inhibited in cells treated with cerulenin, an inhibitor of lipid biosynthesis (24, 60, 131). Brome mosaic virus RNA replication is severely inhibited in yeast cells that carry a mutation in the host Δ9 fatty acid desaturase, which affects the lipid composition of the membranes (95). Despite the central role of membranes in viral replication, it remains poorly understood how viral replication complexes are targeted to and assembled on specific membrane sites.

Upon infection of cowpea cells with CPMV typical cytopathological structures are formed which consists of an amorphous matrix of electron-dense material traversed by rays of small membranous vesicles (33, 68). The membranous vesicles are closely associated with CPMV RNA replication as was revealed by autoradiography in conjunction with electron microscopy on sections of CPMV-infected leaves treated with ^{3}H-uridine (33). Fractionation of homogenates from infected leaves further demonstrated that the viral replicase activity is present in the crude membrane fraction, which corroborated the notion that viral replication complexes are physically associated with membranes (44). Based on the observation that the endoplasmic reticulum (ER) undergoes a drastic proliferation upon CPMV-infection and that the rearranged ER membranes co-localize with the cytopathological structure, we have proposed that the small membranous vesicles originate from the ER (24).

CPMV is the type member of the *Comoviruses* and bears strong resemblance to animal *Picornaviruses* both in gene organization and in amino acid sequence of replication proteins. Both RNA1 and RNA2 express large polyproteins, which are proteolytically cleaved into different proteins by the 24-kDa proteinase (24K) (Fig. 1A). The proteins encoded by RNA1 are necessary and sufficient for virus replication, whereas RNA2 codes for the capsid proteins and the movement protein. Based on amino acid sequence comparison with other viruses and different experimental data, functions have been attributed to the different RNA1-encoded proteins. The 32-kDa protein (32K) is a hydrophobic protein, which contains no motifs common to other positive-stranded RNA viruses outside the *Comoviridae*. It is involved in regulation of the RNA1 polyprotein processing and is required as a cofactor in the cleavage of the RNA2 polyprotein (136). The 60-kDa (58K + VPg) protein (60K) is able to bind ATP via a conserved Walker nucleotide-binding motif and has been proposed to be a viral helicase (134). The 87-kDa protein (87K) has a domain specific to RNA-dependent RNA polymerases (RdRp), however 110K (87K +24K) is the only viral protein present in highly purified RdRp

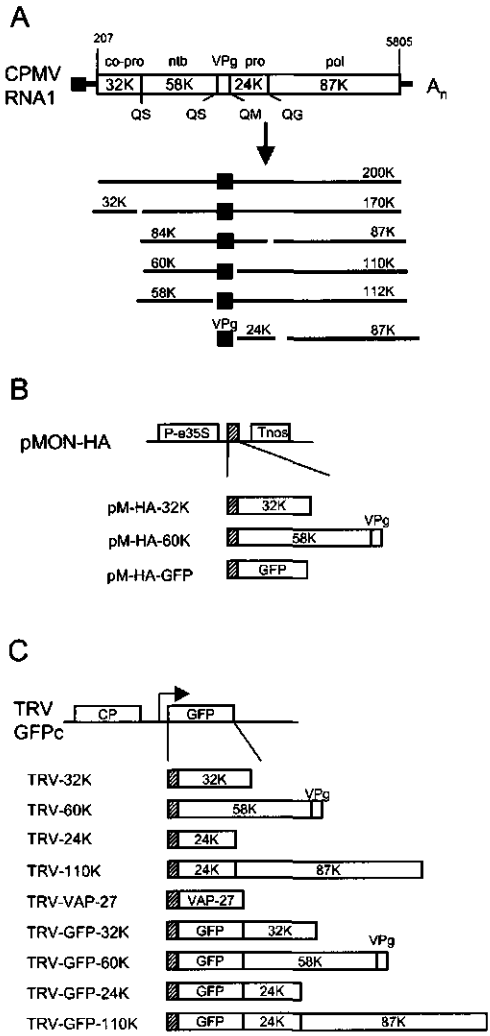

Figure 1 Schematic diagram of CPMV RNA1 and the TRV RNA2 based expression vector used to express the CPMV non-structural proteins. (A) Genetic organization and translational expression of CPMV RNA1. Open reading frames in the RNA molecules (open bars), VPg (black square), cleavage sites (Q/G, Q/M and Q/S) and nucleotide positions of start and stop codons are indicated. Abbreviations: pro, proteinase; co-pro, cofactor for proteinase; NTB, nucleotide binding protein; pol, core RNA dependent RNA polymerase. (B) Organization of the constructs in the plant expression vector pMON-HA used to transiently express CPMV RNA1-encoded proteins in cowpea protoplasts via an enhanced CaMV 35S promoter (P-e35S). An HA-epitope tag was added to facilitate immunodetection of the expressed proteins (hatched box). 60K is composed of the 58K nucleotide binding protein and VPg. (C) Organization of the expression vector TRV-GFPc and the TRV constructs used to express CPMV RNA1-encoded proteins in *N benthamiana* leaves. The duplicated promoter region with downstream cloning sites (arrow) permits transcription of a subgenomic RNA for expression of foreign gene inserts. The 110K polymerase is composed of the 24K proteinase and the 87K core polymerase as indicated. Additional constructs were made that contain a fusion with GFP. VAP-27 is an *A. thaliana* protein that inserts in the ER membrane. The position of the HA-epitope tag is indicated with a hatched box.

capable of elongating nascent viral RNA chains (44), suggesting that fusion to the 24K proteinase is required for replicase activity.

During infection, the bulk of the nonstructural proteins encoded by RNA1 is present in electron-dense structures adjacent to the small membranous vesicles (196). It was proposed that the replication complexes are deposited to these electron-dense structures after taking part in RNA replication located on the membranes (183). Aggregation of the virus nonstructural proteins in this structure complicates the analysis of the membrane binding properties of the individual proteins during normal CPMV infection. Expression of RNA1-encoded proteins in insect cells, using the baculovirus expression system, showed that 60K, but not 110K is able to induce and associate with small membranous vesicles in the cytoplasm in these cells (181).

In this study, the nature of the interaction of different RNA1-encoded proteins and membranes was further explored in plant cells. Using a virus vector-based expression system, selected RNA1 proteins were expressed alone or in a fusion with a reporter protein, which allowed us to identify and visualize specific membranes interacting with the viral proteins in live plant cells. In addition, expression of certain viral proteins led to drastic rearrangements of intracellular membranes and ultimately cell death.

Results

Expression of individual CPMV RNA1-encoded proteins in plant cells

In previous studies several individual CPMV proteins were transiently expressed in cowpea protoplasts using the plant expression vector pMON999 that carries the enhanced CaMV 35S promoter (133, 183). Those studies concerned the viral RdRp and therefore were focused on the C-terminal 110K region of the 200K polyprotein. In the present study the proteins encoded in the N-terminal region were included also. For this purpose, the coding sequences for the 32K proteinase cofactor and the 60K NTP binding protein were inserted into the multiple cloning site of pMON999 to produce pM-32K and pM-60K. The constructs were used to transfect protoplasts, which were then harvested 16 hours post transfection (hpt). Homogenates of the protoplasts were subjected to centrifugation at 30,000 g crudely separating soluble proteins from membrane-bound proteins. It was shown previously using immunoblotting procedures that 110K and 87K accumulate to high levels in protoplasts and are found mainly in the soluble fraction (S30) (183). The 32K and 60K were not detectable in either the S30 or the pellet fraction (P30) using anti-32K and anti-VPg sera (data not shown). The failure to detect 32K and 60K might be due to low expression levels of these proteins and/or to low titers of the anti-sera. To avoid the latter possibility, constructs were made with the haemagglutinin (HA) epitope tag fused to the N-terminus of 32K and 60K (Fig. 1B). As a positive control the HA epitope was also fused to the green fluorescent protein (GFP).

Western blot analysis of extracts from transfected protoplasts using mouse monoclonal antibodies raised against the HA-epitope revealed that HA-GFP accumulated to readily detectable levels and was present mainly in the S30 fraction (Fig. 2). HA-60K accumulated to much lower levels and was present mainly in the P30 fraction (Fig. 2) whereas 32K was not detectable in either S30 or P30. Comparison of the expression levels of the three HA-tagged proteins suggests that 32K and 60K are unstable proteins.

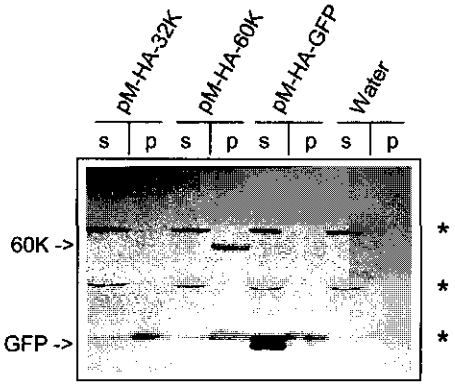

Figure 2 Immunodetection of CPMV RNA1-encoded proteins in different subcellular fractions of cowpea protoplasts transfected with transient expression vectors. Protoplasts were harvested 16 hpt and homogenates were separated in the supernatant (s) and pellet fraction (p) by centrifugation at 30.000g. Detection of the proteins was with a mouse monoclonal HA antibody. 60K and 32K are indicated by arrows to the left. Cowpea proteins that cross-react with this antibody are indicated by asterisks. Water: no DNA added.

Next, the individual CPMV RNA1-encoded proteins were expressed in *N. benthamiana* plants using the tobacco rattle virus (TRV) expression system (101). *N. benthamiana* is a systemic host for CPMV and the TRV based expression system was shown to give high levels of foreign protein expression in these plants. Since TRV does not cause visible morphological changes to the host endomembrane system as observed by electron microscopy (32) and is not related to CPMV, a TRV infection probably does not interfere with proper targeting of the CPMV proteins. Vector TRV-GFPc contains the coding sequence of GFP in a cDNA clone of TRV RNA2 in which GFP can be replaced with other genes of choice (Fig. 1C ; (101)). To facilitate immunodetection of the CPMV proteins, TRV-GFPc was modified to encode the HA-epitope followed by a multiple cloning site. Subsequently, the coding sequences for the 24K proteinase, the 32K proteinase cofactor, the 60K NTP binding protein and the 110K polymerase were each inserted into the TRV vector immediately downstream of the HA tag thereby substituting the GFP gene (Fig. 1C). *In vitro* transcripts of these constructs were combined with TRV RNA1 and used as inoculum on *N. benthamiana*. Homogenates of infected leaves were separated into P30 and S30 fractions. SDS-PAGE was performed on samples of these fractions followed by Western blot analysis using mouse monoclonal antibodies recognizing the HA-epitope present at the N-terminus of the proteins. 24K and 110K were present predominantly in the soluble fraction whereas 60K was present in the crude membrane fraction (Fig. 3A). We were unable to detect 32K in either fraction (Fig. 3A). To confirm that membrane associated proteins are localized to the pellet during fractionation, cDNA of an *A. thaliana* integral membrane protein, VAP-27, was cloned into TRV as a fusion with the HA epitope tag. VAP-27 is a SNARE-like protein that inserts post-translationally into the ER membrane via a C-terminal transmembrane domain ((167).

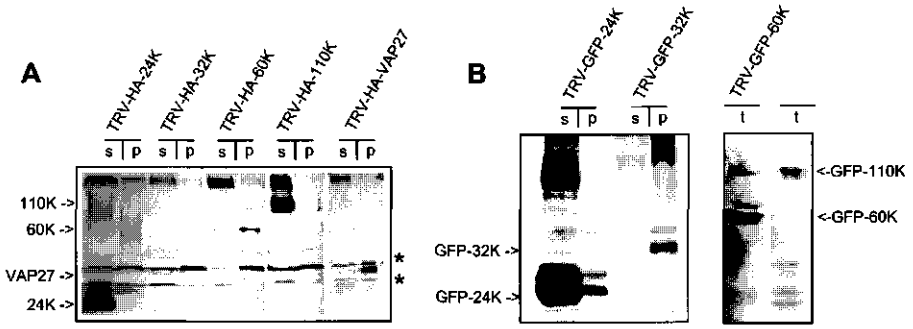

Figure 3 Immunodetection of CPMV RNA1-encoded proteins, either tagged with HA (A) or fused to GFP (B), in different subcellular fractions of *N. benthamiana* leaves infected with TRV expression vectors. Infected leaves were collected 1 dpi and total homogenates (t) were prepared that were either loaded directly for TRV-GFP60K and TRV-GFP-110K or were centrifuged at 30.000g to separate proteins from the supernatant (s) and pellet fraction (p) for the other constructs. Detection of the proteins was with mouse monoclonal anti-HA antibody (A) or with a rabbit polyclonal anti-GFP serum (B). The bands corresponding to the CPMV proteins are indicated by arrows while *N. bentamiana* proteins that cross-react with anti-HA are indicated by asterisks.

Homogenates of TRV-VAP-27-infected leaves were fractionated and, like 60K, VAP-27 was detected predominantly in the P30 fraction (Fig. 3A).

These data suggest that 60K associates with membranes when expressed in the absence of other CPMV encoded proteins whereas 24K and 110K behave as cytoplasmic, soluble proteins. We were unable to detect the 32K protein by immunoblotting either expressed in *N. benthamiana* leaves using the TRV expression system or transiently expressed in cowpea protoplasts.

Intracellular localization of the replication proteins

To visualize and characterize the protein-membrane interaction in live cells, TRV-expression vectors encoding fusions of the CPMV-proteins with the green fluorescent protein were constructed. First it was established that the constructs were properly expressed using immunoblotting. Homogenates of infected leaves were separated by centrifugation in the P30 and S30 fractions. Using anti-GFP serum, GFP-24K was found present mainly in the S30 fraction (Fig. 3B). In contrast to native 32K, GFP-32K was detectable using immunoblotting and was found to be present mainly in the P30 fraction (Fig. 3B). Expression of GFP-60K and GFP-110K was detected in the leaf homogenates (Fig. 3B) however after fractionation in the P30 and S30 fractions no specific bands could be visualized for unknown reasons (data not shown).

The intracellular localization of the fusion proteins was examined in infected leaf epidermal cells one day post inoculation (dpi) by confocal laser scanning microscopy. Cells containing GFP-24K (data not shown) or GFP-110K (Fig. 4A) displayed a pattern of fluorescence similar to that of non-fused GFP (Fig. 4B), and fluorescence was present diffusely in the cytoplasm and in the nucleus. Since GFP is excluded from the vacuole that

takes up more than 90% of the cell volume in epidermal cells, cytoplasmic GFP is confined to a small layer between the vacuole and the cell-wall (the cortex) and to a small region near the nucleus (Fig. 4B). The occurrence of GFP in the nucleus is in line with earlier reports that indicate that GFP alone or fused to a soluble protein, accumulates partly in the nucleus probably by means of passive diffusion through the nuclear pore (202). The fluorescence pattern of GFP-60K differed from that of non-fused GFP. GFP-60K fluorescence was most obvious in a ring surrounding the nucleus, in small rings surrounding spherical organelles in the cytoplasm and in one or several spherical aggregates often near the nucleus while no fluorescence was present in the nucleus (Fig 4C). The fluorescent ring around the nucleus was reminiscent of what we have observed in transgenic *N. benthamiana* plants expressing ER-GFP (24), a GFP fusion protein that contains an N-terminal cleavable signal peptide and a C-terminal HDEL retention signal and therefore is targeted to the lumen of the ER (65) (compare Fig. 4C with Fig. 5C). It thus appears that GFP-60K localizes to the ER membranes that are contiguous with the nuclear envelope. Red chlorophyll autofluorescence was observed in the small spherical organelles (Fig. 4C inset) suggesting that GFP-60K is also present in the outer membrane of plastids. The nature of the spherical aggregates near the nucleus (Fig. 4C, arrow) is unknown but it might be a structure derived from ER membranes as will be pointed out in the next paragraph. Also the fluorescence observed with GFP-32K differed markedly from non-fused GFP. The fluorescence was most obvious at the cortex of the infected cells and was present in a clear reticulate pattern (Fig. 4D) closely resembling the pattern observed with the ER-GFP in transgenic plants (compare Fig. 4D with Fig. 6A). It thus appears that GFP-32K localizes to the cortical ER network. In some cells the reticulate pattern was less bright and GFP-32K was additionally present in large highly fluorescent aggregates at the cortex, which may be derived from ER membranes (Fig. 4E). No fluorescence of GFP-32K was observed in the nuclear envelope (data not shown), which is in

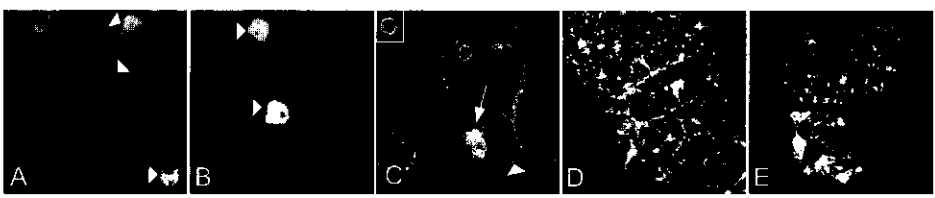

Figure 4 Subcellular distribution of CPMV proteins fused to GFP in *N. benthamiana* epidermal cells infected with TRV expression vectors. Fluorescent signals were visualized by confocal microscopy 1 dpi. GFP-24K (B) is present in the nucleus and in a diffuse pattern in the cytoplasm as is non-fused GFP (A). GFP-60K (C) localizes in a ring surrounding the nucleus, in one or several bodies often near the nucleus (arrow) and in a ring surrounding plastids that autofluoresce in red (inset). GFP-32K localizes in a cortical reticulated network (D) and in cortical fluorescent aggregates (E). Arrowheads indicate the position of the nucleus. The images shown in A to C correspond to single optical sections of 1 μm, while D and E correspond to projections of serial optical sections.

contrast to the fluorescence observed in transgenic plants that express ER-GFP or in TRV GFP-60K infected plants. It should be noted that GFP-32K fluorescence disappeared rather quickly from infected cells.

These data corroborate the cell fractionation data and indicate that individually expressed 24K and 110K are cytosolic, soluble proteins and that 32K and 60K associate with membranes mainly derived from the ER.

Previous studies using immunogold labeling on sections of CPMV infected protoplasts, that have been chemically fixed and embedded at low temperature in lowicryl K4M, showed that several of the replication proteins mainly accumulated in the electron-dense structures (48). Almost no label was found on or near the vesicles, and antibodies specific for the 32K protein were not used in that study. Cryo-fixation usually better preserves antigens and membranes, and on cryo-sections of CPMV-infected cowpea leaves treated with anti-32K, anti-VPg (which recognizes the 60K protein and other VPg containing intermediates, see Fig. 1A) and anti-110K sera, gold particles were found on or near the vesicles as well as in the electron-dense structures (Fig. 5). These results show that during an infection replication proteins accumulate both on vesicles and in electron-dense structures, and indicate that 32K and 60K might play a role in targeting the RdRp to membranes where replication takes place. The role of the electron-dense structures still remains unclear.

Expression of 32K and 60K modifies ER morphology

CPMV infection induces an extensive rearrangement of ER membranes, a process independent of RNA2-encoded proteins (24). To investigate whether a specific RNA1-encoded protein is responsible for these membrane modifications, the TRV-constructs each carrying an individual RNA-1 encoded protein (not fused to GFP) were used to infect *N. benthamiana* plants transgenic for GFP targeted to the lumen of the ER (65, 152). At 1 dpi the morphology of the ER membranes in infected epidermal cells was observed and compared to mock infected cells. TRV infection itself had no influence on ER membrane morphology since in plants infected with TRV, ER-GFP fluorescence in epidermal cells did not differ from mock-infected cells and fluorescence was detected in the typical cortical ER network (Fig. 6A), the nuclear envelope (Fig. 6B), and the ER tubules traversing the cytoplasmic threads (data not shown). In TRV-24K and in TRV-110K infected cells the fluorescence pattern of ER-GFP was also indistinguishable from mock-infected cells (data not shown). In contrast, the ER in cells infected with TRV-32K or TRV-60K differed radically from the ER in mock-infected cells. In TRV-32K infected cells, ER-GFP fluorescence was present in large amorphous aggregates that were connected with the cortical ER network (Fig. 6C) and in spherical aggregates (Fig. 6D) which were often near the nucleus. While in TRV-60K infected cells these spherical aggregates near the nucleus were also found (Fig. 6E) cortical ER aggregates were not observed (data not shown). Both types of aggregates resembled the regions of proliferated ER membranes induced in CPMV-infected cells although the extent of

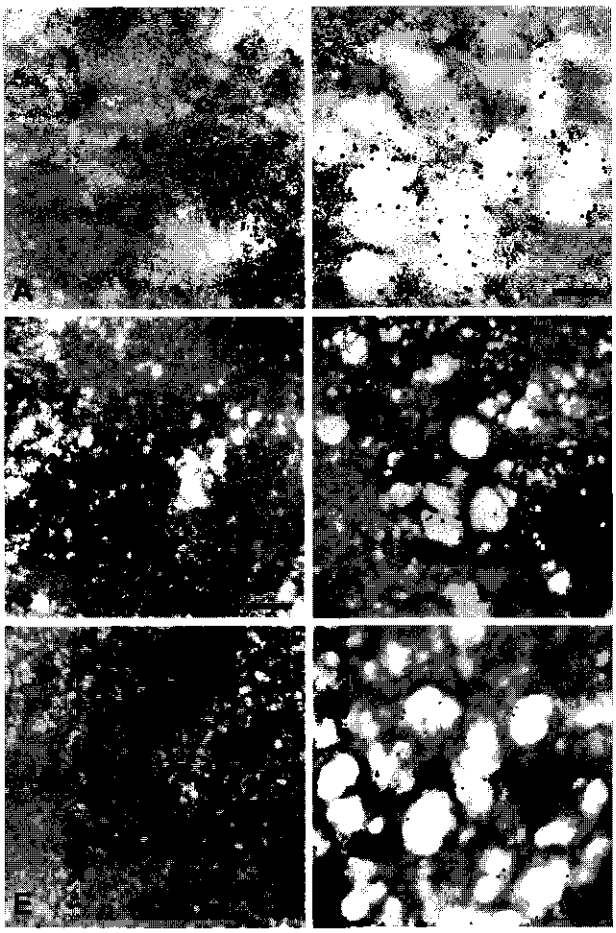

Figure 5 Immunogold labeling of electron-dense structures (A, C and E) and vesicles (B, D and F) in thin cryo-sections of CPMV infected cowpea leaves using anti 32K- (A, B), anti VPg- (C, D) and anti-110K sera (E, F). With all three antisera gold particles were found associated with both structures. Bar = 150 nm

ER proliferation in CPMV-infected cells was generally larger (Fig. 6F). The ER modifications seen with TRV-32K and with TRV-60K may be artifacts that occur upon expression of any ER membrane-associated protein using the TRV based expression system. This was tested by expressing the integral ER membrane protein VAP-27 with the TRV vector. When TRV-VAP-27 was used to infect ER-GFP transgenic plants no changes were found in the ER-GFP fluorescence pattern compared to mock infected cells (data not shown).

From these data we conclude that expression of 32K and 60K induced drastic morphological changes to the ER, resembling CPMV-induced ER membrane proliferation whereas 24K and 110K expression did not influence ER morphology.

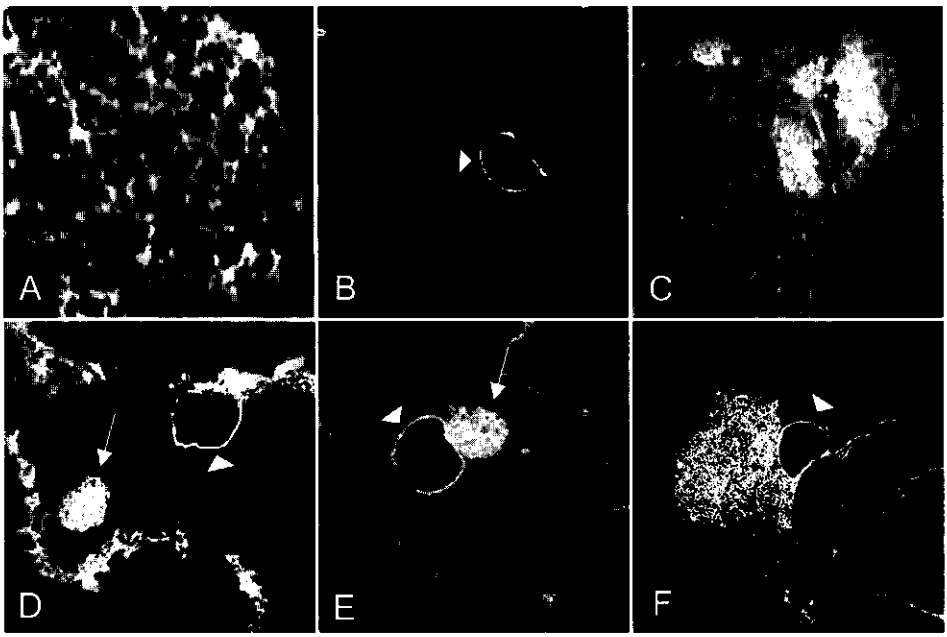

Figure 6 Effect of expression of different CPMV proteins on the morphology of the ER. *N. benthamiana* plants transgenic with GFP targeted to the lumen of the ER (ER-GFP) were infected with TRV expression vectors. Fluorescent signals were visualized by confocal microscopy 1 day post infection. In epidermal cells infected with TRV the pattern of ER-GFP fluorescence is not distinguishable from mock-infected cells and is present in a cortical reticulate pattern (A) and in a ring around the nucleus (B). In cells infected with TRV-32K ER-GFP fluorescence is additionally present in large aggregates connected to the cortical network (C) and in one or several spherical aggregates (arrow; D) often near the nucleus. In TRV-60K infected cells the latter structure is also present (arrow; E). Extensive ER-proliferation near the nucleus of a CPMV infected cell (F). Arrowheads indicate the position of the nucleus. The images shown in B, D, E and F correspond to single optical sections of 1 μm, while A and C correspond to projections of serial optical sections.

Expression of 32K and 60K induces necrosis

During the course of the experiments a severe effect of prolonged expression of 32K and 60K on cell viability was observed. TRV infection caused no visible symptoms on inoculated leaves of *N. benthamiana* but a slight curling of the systemically-infected leaves was apparent 4 dpi. Infection of leaves with TRV-GFP allowed us to monitor the spread of TRV from the initial infection sites to the systemic leaves using a handheld UV lamp. One day after infection GFP fluorescence was visible as green spots on inoculated leaves. With time these spots grew larger and 3 dpi fluorescence was observed in large patches and in the major veins of the inoculated leaves as well as in the veins of the systemic leaves (Fig 7A'). In contrast to TRV and TRV-GFP (Fig. 7A), infection with TRV-32K or TRV-60K triggered formation of necrotic spots on the inoculated leaves. The first sign of lesion formation occurred from

approximately 2 dpi onwards when infected tissue developed a glassy appearance. At 3 dpi the developing lesions were more distinct from the surrounding tissue appearing more clearly necrotic and collapsed (Fig. 7B and 7C). The necrotic tissue was typically confined to the inoculated leaves but occasionally some necrosis was observed in the upper, non-inoculated leaves at 4 to 6 dpi (data not shown). This suggests that movement of the recombinant TRV RNA2 is severely inhibited. Also the TRV construct carrying the GFP-32K fusion produced formation of necrotic spots but TRV-GFP-60K did not trigger necrosis (data not shown). Infection with TRV-24K, TRV-110K, TRV-GFP24K, TRV-GFP-110Ks and TRV-VAP-27 did not result in the formation of necrotic lesions although a slight yellowing of infection sites was observed for TRV-110K at 6 dpi (data not shown). These results suggest that prolonged expression of 32K, 60K or the fusion of 32K with GFP from the TRV expression vector leads to cell death. This was rather surprising since CPMV does not cause necrosis on *N. benthamiana* plants, moves systemically to the upper leaves and high amounts of 32K and 60K accumulate during the infection. To determine whether 32K and 60K expression also produced necrosis in other host plants, *N. clevelandii*, *N. tabacum* and *N. glutinosa* plants were infected with TRV-32K, TRV-60K and TRV-GFP as control. In all these *Nicotiana* species, necrosis was observed at 2-3 dpi on inoculated leaves infected with TRV-32K and TRV-60K whereas leaves infected with TRV-GFP were symptomless (Fig 7D-G and data not shown).

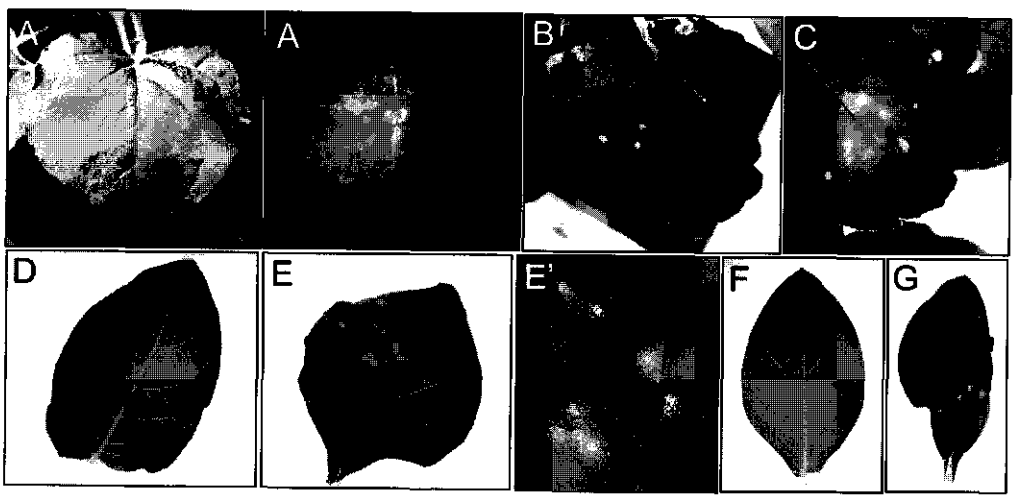

Figure 7 Necrosis of leaves infected with TRV-32K and TRV-60K in different host plants. Leaves were infected with the TRV constructs and photographed 3 days pi. (A-A') *N. benthamiana* leaf infected with TRV-GFP photographed either under normal light (A) or under UV light (A') where GFP fluorescence appears green. The red fluorescence in A' is due to chlorophyll. (B) *N. benthamiana* leaf infected with TRV-32K. (C) *N. benthamiana* leaf infected with TRV-60K. (D) *N. tabacum* leaf infected with TRV-GFP. (E) *N. tabacum* leaf infected with TRV-32K. (E') Close up of E. (F) *N. clevelandii* infected with TRV-GFP. (G) *N. clevelandii* infected with TRV-60K.

Discussion

In this study, the CPMV 32K and 60K replication proteins were shown to associate with membranes mainly derived from the ER, when expressed in isolation in plant cells. Moreover, expression of the 32K protein and to a lesser extent 60K effected proliferations of the ER resembling those that occur upon CPMV-infection. Other RNA1 encoded proteins, the 110K polymerase or the N-terminal cleavage product the 24K proteinase, behaved as freely soluble proteins when expressed in isolation. We propose that localization signals in 32K and 60K target the replication complexes to ER membranes and that this physical association causes an ER membrane rearrangement that may result in formation of the small membranous vesicles that are the site of CPMV RNA synthesis.

During CPMV infection the replication proteins accumulate both in electron-dense structures and the adjacent small membranous vesicles where CPMV replication occurs (33, 196). To analyze the properties of the individual RNA1-encoded nonstructural proteins, they were expressed separately using a transient expression system in cowpea protoplasts and using the tobacco rattle virus expression vector in *N. benthamiana*. In contrast to the 110K (87K + 24K) polymerase or the 24K proteinase that accumulated to high levels in both systems, the 60K NTB protein accumulated poorly while the 32K cofactor for the protease was not detectable by immunoblot analysis indicating that 32K and 60K have a high turnover rate. This is in line with previous findings where expression of 32K and 60K in insect cells or in *E. coli* cells yielded considerably lower protein levels than 110K (132, 145, 181, 182). The high levels of 32K and 60K accumulating during CPMV infection may be the result of aggregation in the electron-dense material. The role of the electron-dense structures in the viral life cycle and how the replication proteins end up in this structure still remains unclear. Fusion of GFP to 32K improved the expression levels and GFP-32K, like 60K, was found to be present mainly in the crude membrane fraction. Comparison of the GFP-32K fluorescence with that of GFP-60K revealed that 32K was present mainly in the cortical ER whereas GFP-60K was found mainly in the nuclear envelope, the plastidial membrane and in aggregates presumably derived from the ER. This suggests that 32K is more specifically targeted to and/or retained in the cortical ER compared to 60K that displays affinity for various intracellular membranes. It should be noted however that fusion of 60K to GFP abolished the ability of 60K to induce necrosis, which may suggest that 60K could not engage into the proper interactions when fused to GFP. Therefore the localization pattern observed with GFP-60K might not represent the actual localization of the non-fused 60K.

Expression of both 32K and 60K was shown to influence ER morphology with 32K inducing proliferation of the cortical ER and formation of one or several small bodies of proliferated ER near the nucleus whereas 60K induced only the latter structure. The alterations of the ER morphology resembled the proliferations that occur in CPMV-infected cells, although the regions of proliferated ER are generally larger in the latter case. Maybe the combined action of 32K and 60K is necessary to induce proliferations of the ER that mimic

those observed in CPMV infected cells. The observation that CPMV nonstructural proteins, when expressed in isolation target, to ER membranes and cause ER membrane rearrangements is in agreement with the previously proposed notion that the small membranous vesicles that are involved in virus replication originate from the ER (24).

Previous studies showed that 60K, when expressed in insect cells using the baculovirus expression system, induced formation of small membranous vesicles (181). Here we make the first report that 32K is also involved in the process of membrane attachment and rearrangement. Unlike the other replication proteins of CPMV, the 326-amino-acid hydrophobic 32K contains no conserved domains such as an NTP-binding motif (present in 60K), proteinase domain (24K) or polymerase domain (110K). *In vitro* translation studies pointed to a role of 32K as a cofactor required for processing of the RNA2 encoded polyprotein (136). Deletion of 32K from the RNA1 200K polyprotein resulted in more rapid cleavage of the 170K processing intermediate both *in vivo* and *in vitro* suggesting that 32K inhibits processing of 200K (136). It is likely that targeting to and insertion in the membrane of replicase proteins, polyprotein cleavage and the initiation of viral RNA synthesis occur in a coordinated fashion during CPMV replication. Since it was shown that 32K remains associated with 170K after cleavage from the 200K polyprotein (48), 32K might first target the 32K/170K complex to the membranous site of replication where, after further processing, initiation of replication occurs.

The properties of 32K and 60K in ER membrane attachment and modification resemble those of replication proteins encoded by different viruses of which poliovirus is the best-studied example. Membrane association of the polioviral proteins encoded by the 2BC3AB region was shown to be mediated by a stretch of hydrophobic amino acids (3AB) or by an amphipathic helix (2BC and 2C) (8, 125, 177). 32K contains three stretches of hydrophobic amino acids at the C-terminal end (unpublished observations) and 60K contains an amphipathic helix at the N-terminus (amino acids 45-61; (136)) and a 22 amino acid stretch of hydrophobic amino acids (amino acids 544-565; unpublished observations) at the C-terminus immediately upstream of VPg. These domains are conserved amongst different comoviruses. Further experiments will be necessary to verify that these regions are involved in membrane binding and the TRV expression system might provide a suitable experimental system for that purpose. Apart from binding to intracellular membranes, expression of polioviral proteins in different cell types has revealed that proteins from the 2BC3AB region could extensively modify the endomembrane system. 2BC and 2C induced formation of small membranous vesicles probably derived from the ER that were morphologically similar to poliovirus-induced vesicles (3, 7, 27). The 3A protein, when expressed in isolation, associated with ER membranes causing swelling of these membranes but no small membranous vesicles were formed (40, 41). Recently, it was reported that co-expression of 3A and 2BC resulted in formation of vesicles that were similar, both in ultrastructure and in biochemical properties, to the vesicles induced in a poliovirus infection (173). Also for the equine arteritis virus it was

shown that co-expression of the membrane proteins nsp2 and nsp3 induce the formation of double-membrane vesicles probably derived from the ER (170). The tobacco etch virus 6kDa protein was shown to localize specifically to ER membranes when expressed as a fusion with GFP or GUS and was proposed to cause the ER modifications that are observed during TEV infection (160). Such membrane-associated proteins may play a dual role. Firstly, the induction and accumulation of vesicles could compartmentalize viral RNA synthesis. Secondly, these proteins could promote the interaction of viral RdRp with the proliferating membranes.

Infection with TRV-32K and TRV-60K led to formation of necrotic tissue in inoculated leaves from *N. benthamiana* and other *Nicotiana* species suggesting that 32K and 60K are cytotoxic proteins that cause cell death. Fusion of 60K with GFP abolished its ability to induce necrosis for unknown reasons. The cytotoxic properties of 60K have been reported before in insect cells expressing 60K using the baculovirus system (182). These cells showed abnormal cytopathic effects and rapid cell lysis usually within 48 hpi. In the same system expression of 32K did not lead to clear effects on cell viability (181). It is remarkable that 32K and 60K induce necrosis only when expressed separately from other RNA1 encoded proteins, since CPMV infection on *N. benthamiana* leads to high accumulation of 32K and 60K but no visible necrosis. The aggregation of 32K and 60K in electron-dense structures during CPMV infection may somehow prevent induction of cell death by these proteins. The significance of the cytotoxic properties of 32K and 60K for the viral life cycle is unclear. Unlike animal viruses, plant viruses do not rely on lysis of host cells for their spread through the plant. It was reported that expression in mammalian cells of polioviral 2B and 2BC or 2B from the related coxsackievirus resulted in an increase in membrane permeability ultimately leading to cell lysis, suggesting that these proteins play an important role in the release of viral progeny (2, 188).

Recently it was reported that tobacco mosaic virus (TMV) modified to express the 2B protein of tomato aspermy virus (TAV) triggered the induction of a hypersensitive response (HR) resulting in tissue necrosis despite the fact that infection of this plant species with either wild type TMV or wild type TAV did not lead to necrosis (96). The HR is a plant defense mechanism that occurs upon attack of certain pathogens and involves rapid death of plant cells in association with the restriction of pathogen spread (for a review (67)). At the moment we cannot exclude the possibility that 32K and 60K are recognized by the plant and elicit an HR rather than that they cause cell death directly by increasing membrane permeability.

Materials and methods

Construction of the transient expression vectors

Plasmid pMON999 is a plant expression vector that contains the enhanced CaMV 35S promoter, followed by a multiple cloning site (MCS) and the terminator of the nopaline synthase gene (183). pMON-HA is derived from pMON999 and contains the coding region of the HA-epitope tag (YPYDVPDYA) between the promoter and terminator (185). The individual CPMV RNA1 proteins were PCR amplified using gene-specific primers (Table 1) and cloned in these vectors. Because the individual proteins are expressed in a polyprotein, the primers were designed to add a start codon at the 5'-end and a stop codon at the 3'-end of each gene when appropriate. Furthermore, the primers contained restriction sites to facilitate cloning. pM-HA-32K was constructed by amplification of the 32K coding region from pTB1G (45) using primers EcoRI_32K_F and BamHI_32K_R and insertion in pMON-HA. pM-HA-60K was constructed by PCR amplification of the 60K coding region from pTB1G using EcoRI_60K_F and BamHI_60K_R and pM-HA-GFP was constructed by amplification of the GFP coding region from pM19GFP10 (55) using primers EcoRI_GFP_F and BamHI_GFP_R. pM-60K was constructed by amplification of the 60K coding region from pTB1G (45) using primers XbaI_60K_F and BamHI_60K_R and insertion in pMON999. pM-32K was constructed by insertion of XbaI-SstI fragment of pTB32*, which contains the 32K coding sequence followed by a stop codon and the SstI restriction site (204), into pMB200K. pMB200K contains the entire RNA1 encoded 200K polyprotein followed by the SstI restriction site in pMON999 (183). The XbaI restriction site is present internally in the coding sequence of 32K.

Construction of TRV-expression vectors

Tobacco rattle virus (TRV)-vectors carrying CPMV RNA1-encoded proteins were constructed using TRV-GFPc. This plasmid contains cDNA from TRV RNA2 and an engineered subgenomic promoter followed by the GFP gene (101). First this plasmid was modified to contain a start codon followed by the coding sequence of the HA epitope tag and a MCS. This was achieved by substitution of the NcoI fragment released from TRV-GFPc with a PCR fragment amplified from pM-HA32K with primers NcoI_HA_F and SstI_TAA_32K_R digested with the same enzyme. This intermediate plasmid was designated TRV-HA-Δ32K and contains the SalI, PstI and EcoRI site directly following the coding sequence for the HA epitope. These restriction sites and the EcoRI, SstI or KpnI present at the 3'-end can be used to insert a gene of choice as an N-terminal fusion with the HA-tag.

TRV-HA-24K was constructed by PCR amplification of the 24K coding sequence from pTB1G using primers NcoI_24K_F and SstI_TAA_24K_R. This PCR product was digested with NcoI (filled in with Klenow polymerase) and SstI and cloned in TRV-HA-Δ32K digested with EcoRI (filled in with Klenow polymerase) and SstI. TRV-HA-32K was constructed by

PCR amplification of the 32K coding sequence from pTB1G using primers NcoI_32K_F and SstI_TAA_32K_R. This PCR product was digested with HindIII and SstI and was cloned in TRV-HA-Δ32K digested with HindIII and SstI. TRV-HA-60K was constructed by PCR amplification of the 60K coding sequence from pMON-HA-60K using primers NcoI_60K_F and EcoRI_TAA_60K_R. This PCR product was digested with EcoRI and cloned in TRV-HA-Δ32K digested with EcoRI. To construct TRV-HA-110K the 110K coding sequence was PCR-amplified from pTB1G using primers NcoI_110K_F and SstI_TAA_110K_R, digested with NcoI and SstI and cloned in TRV-GFPc digested with the same enzymes resulting in clone TRV-110K. Subsequently TRV-HA-24K was digested with KpnI and the released fragment was replaced with the KpnI fragment of TRV-110K to construct TRV-HA-110K. The fusion constructs of the different viral proteins with GFP were made using the SalI restriction site directly downstream of the HA-epitope sequence. The GFP coding sequence was PCR amplified from pM19GFP10 (55) using primers SalI_GFP5_F and SalI_GFP5_R. For the construction of TRV-HA-VAP27 the complete coding sequence of VAMP-associated protein of 27kDa (VAP27) was released as an EcoRI fragment from pGAD10-VAP-27, a clone isolated from an *A. thaliana* cDNA library. This fragment was ligated in TRV-HA-Δ32K digested with the same enzyme.

Transfection of cowpea protoplasts and infection of plants

Cowpea (*Vigna unguiculata* L.) mesophyll protoplasts were prepared and transfected by polyethylene glycol-mediated transformation as described previously (183). Five-week-old wild type *N. benthamiana* plants or *N. bentamiana* plants carrying the mGFP5-ER transgene (152) were dusted with carborundum and inoculated with TRV RNA1 together with transcripts of the TRV RNA2 recombinants as described (101).

Subcellular fractionation and immunoblotting

Protoplasts transfected with the transient expression vectors were collected 16 hours post transfection, centrifuged at 30.000g and proteins from the supernatant and pellet fraction were electrophoresed in 10% polyacrylamide gels and immunoblotted as described (13) using the mouse monoclonal antibody anti-HA (clone 12CA5; Boehringer) recognizing the HA-epitope tag.

For immunoblot analysis of the proteins produced by the TRV expression vector, infected leaves were collected 1 day post infection, and grinded with a mortar and pestle with 2 ml of extraction buffer (50 mM Tris-acetate, pH 7.4, 10 mM potassium acetate, 1 mM EDTA, 5 mM DTT, 0.5 mM phenylmethyl-sulfonyl fluoride) per 1 gram fresh weight). After extraction, the homogenates were centrifuged, electrophoresed and immunoblotted as described earlier (13) using anti-HA or anti-GFP (Clontech). In some cases, homogenates were not centrifuged but total protein was extracted using sample buffer (10% glycerol, 5% β-

Table 1. Oligonucleotides used in this study to insert coding sequences of CPMV replication proteins and GFP in different expression vectors.

Primer	Sequence
EcoRI_32K_F	GAGAATTCGGTCTCCCAGAATATGAGG
BamHI_32K_R	GGGGATCCTCACTGTGCATTGTTCTTTTCAC
EcoRI_60K_F	CGGAATTCAGTAGTCCTGTTATCCTCTTAG
BamHI_60K_R	CCGGATCCTTATTGTGCGTCTGCCCAAA
EcoRI_GFP_F	CGGAATTCATGAGTAAAGGAGAAGAACTTTTCACT
BamHI_GFP_R	CCGGATCCTTATTTGTATAGTTCATCCATGC
NcoI_HA_F	GGGACCATGGCTTATCCATACGATGTTCCA
NcoI_24K_F	GGGGCCATGGCTTCTTTGGATCAGAGTAGTGTT
SstI_24K_R	CCCGAGCTCTTATTGCGCTTGTGCTATTGG
NcoI_32K_F	GGGGCCATGGGTCTCCCAGAATAT
EcoRI_TAA_32K_R	CCCGAATTCTTACTGTGCATTGTCCTTTTCACC
NcoI_60K_F	GGGGCCATGGCTAGTAGTCCTGTTATCCTCTTA
EcoRI_TAA_60K_R	CCCGAATTCTTATTGTGCGTCTGCCCAAACTC
SstI_TAA_110K_R	CCCGAGCTCCTAAACATCAGAAAAAGCGAAATTGA
SalI_GFP5_F	GGGGGGTCGACGATGAGTAAAGGAGAAGAACTTTTC
SalI_GFP5_R	CCCCCGTCGACTCTTTGTATAGTTCATCCATGC

mercaptoethanol, 2% SDS, 0.01% bromophenol blue, 75 mM Tris-Hcl, pH 6.8), boiled for 3 min and loaded on the gel.

Fluorescence microscopy and immunogold labeling

A Zeiss LSM 510 confocal microscope was used to obtain images. GFP fluorescence was observed using standard settings (excitation wavelength 488 nm, emission band pass filter 505 to 550 nm). Red chlorophyll fluorescence was detected using an excitation wavelength 543 nm and emission long pass filter 560 nm.

For immunogold electron microscopy, small (0.5 x 0.5 mm) samples were cut from young trifoliate leaves of uninfected and CPMV-infected plants at 14 day post inoculation. The samples were fixed with 0.5% (w/v) glutaraldehyde/4% (w/v) paraformaldehyde in phosphate-citrate buffer (0.1 M $Na_2HPO_4.2H_2O$, 9.7 mM citric acid H_2O, 1.5 mM $CaCl_2$), pH 7.2 for 2 h at 4°C. The samples were then infiltrated with 2.3M sucrose in phosphate-citrate buffer for 16h at 4°C and cryo-fixed by plunge-freezing in liquid propane at –160°C with a Leica KF80 plunge-freezer. Cryo-sections with a thickness of 80 nm were cut using a Leica Ultracut FCS cryotome at –110°C. Sections were collected onto formvar-coated gold grids and incubated for 1h on drops of 0.01M glycine in phosphate buffered saline (PBS). The grids were then transferred to drops of 1% (w/v) bovine serum albumin (BSA) in PBS and blocked

for 30 min at room temperature. The sections were immunogold labeled using different antibodies and protein A-gold (10 nm) as described (190). Sections were negatively stained with 2% (w/v) ammonium molybdate for 15 sec, blotted and viewed with a Philips CM12 transmission electron microscope.

Acknowledgments

We gratefully acknowledge Jan Verver and Jeroen Pouwels for technical assistance and comments and Janneke Saaijer and Aart van Ommeren for growing the *N. benthamiana* plants. J.C. was supported by the Netherlands foundation for chemical research (CW) with financial aid from the Netherlands Foundation for Scientific Research (NWO).

MUTATIONAL ANALYSIS OF THE GENOME-LINKED PROTEIN OF COWPEA MOSAIC VIRUS

Abstract

In this study we have performed a mutational analysis of the cowpea mosaic comovirus (CPMV) genome-linked protein VPg to discern the structural requirements necessary for proper functioning of VPg. Either changing the serine residue linking VPg to RNA in a tyrosine or in a threonine or changing the position of the serine from the N-terminal end to position 2 or 3 abolished virus infectivity. Some of the mutations affected the cleavage between the VPg and the 58K ATP binding protein *in vitro*, which might have contributed to the lethal phenotype. RNA replication of some of the mutants designed to replace VPg with the related cowpea severe mosaic comovirus was completely abolished whereas others were not or only mildly affected showing that amino acids that are not conserved between the different comoviruses can be critical for the function of VPg. The replication proteins of one of the mutants failed to accumulate in typical cytopathic structures and this might reflect the involvement of VPg in protein-protein interactions with the other replication proteins.

Carette, J.E., Kujawa, A., Gühl, K., Verver, J., Wellink, J. and Van Kammen, A. (2001) *Virology* **290,** 21-29

Introduction

The genome of cowpea mosaic virus (CPMV) consists of two positive-stranded RNA molecules, denoted RNA1 and RNA2, which are separately encapsidated in particles containing 60 copies each of the two capsid proteins. Both RNA1 (5,889 nucleotides (nt)) and RNA2 (3,481 nt) are translated into large polyproteins from which the functional proteins are generated by proteolytic cleavages by the RNA1-encoded 24K proteinase. The two genomic RNA's are further characterized by a 3'-terminal poly(A) tail and a small protein, denoted VPg (viral protein genome-linked) covalently attached to the 5'-end of each RNA chain.

VPg is an RNA1-encoded, 28-amino-acid oligopeptide that is linked to RNA by a phosphodiester bond between the β-OH group of its N-terminal serine residue and the 5'-terminal uridyl residue of the RNA (75). Although many RNA viruses that belong to the *Picornavirus*-like supergroup possess a VPg, the amino acid that links the VPg to the RNA has been identified for only a few of them. A tyrosine residue was shown to link the VPg to the viral RNA for poliovirus (147) and encephalomyocarditis virus (192), both animal picornaviruses, and the plant potyvirus tobacco vein mottling virus (TVMV) (118) while the comovirus CPMV (75) and the related nepoviruses tobacco ringspot virus (175) and grapevine fanleaf virus (138) use a serine residue. Linkage of VPg to RNA via a threonine residue has not been reported although the side chain of this amino acid contains a hydroxyl group, which is required to form the phosphodiester bond.

A role for VPg in translation is not likely since full-size *in vitro* transcripts lacking the protein, and viral RNA from which the VPg has been proteolytically removed, are infectious and retain their messenger activity for most studied RNA viruses (42, 159, 171, 203). Rather VPg might have a role in the initiation of viral RNA synthesis as VPg is found covalently linked to the 5'-end of both positive- and negative-strands in the replicative forms isolated from virus infected tissue (99, 200). For poliovirus, the generation of uridylated VPg species (VPg-pU, VPg-pUpU and VPg-poly(U)) has been demonstrated *in vitro* in a membrane fraction of infected cells (176) and in a cell-free system consisting of synthetic VPg, purified 3Dpol, UTP and poly(A) template (127), which strongly suggest that uridylylated VPg acts as primer for RNA transcription. The proposed role of VPg in RNA replication is similar to the role of terminal proteins (TPs) in the initiation of DNA replication of DNA viruses. The TPs of adenovirus, bacteriophage PRD1 and bacteriophage Cp-1 were shown to be linked to genomic DNA via a serine, tyrosine and a threonine respectively (for a review see (154)).

The serine residue linking the CPMV VPg to the RNA is part of the Gln/Ser cleavage site between 58K and VPg implying that proteolytic cleavage and RNA-attachment may be interrelated. Figure 1 shows the processing scheme of the CPMV RNA1-encoded 200K polyprotein based on *in vivo* and *in vitro* translation and processing studies ((54) and references therein). The RNA1-encoded 24K proteinase has been shown to be responsible for all the cleavages. Both 60K and 58K proteins are present in extracts of CPMV-infected leaves indicating that 60K might be the direct precursor of VPg (53). 60K is an ATP-binding protein

that has been implicated in induction of typical small membranous vesicles associated with RNA replication (134, 181). Presumably 60K acts as a membrane anchor for the replication complex and as a donor of VPg. Alternatively, 112K either directly or via the 26K intermediate product acts as direct precursor for VPg (Fig. 1). When transiently expressed in cowpea protoplasts, 112K is readily processed either to VPg and 110K, which is a stable end product, or to 26K and 87K whereupon the 26K is further cleaved in 24K and VPg (133). These results are in line with findings that cleavages *in cis* of the 200K protein occur much more efficiently than cleavages *in trans* (28).

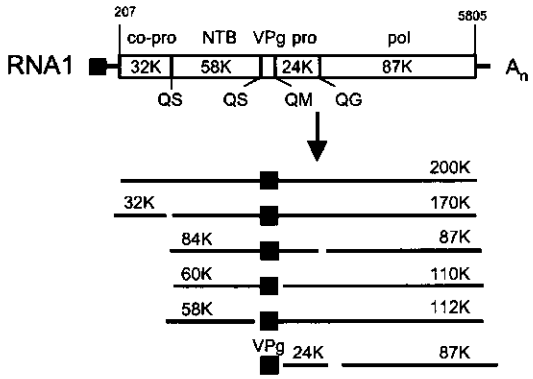

Figure 1 Genetic organization and translational expression of the CPMV genome. Open reading frames in the RNA molecules (open bars), VPg (black square) and nucleotide positions of start and stop codons are indicated. Abbreviations: pro, proteinase; co-pro, cofactor for proteinase; NTB, nucleotide binding protein; pol, RNA dependent RNA polymerase

In an attempt to delineate the function(s) of VPg in virus replication, we performed a mutational analysis of the VPg region in the RNA1-encoded polyprotein. Mutant constructs in which the serine residue that links VPg to the viral RNA was changed to different amino acids or the position of the serine relative to the cleavage site was altered, lost the ability to replicate in cowpea mesophyll protoplasts. We have employed an *in vitro* translation system to study whether proteolytic processing was disturbed in these mutants. We have also characterized a chimeric virus in which the coding region for CPMV VPg was substituted with that of another comovirus cowpea severe mosaic virus (CPSMV) and a set of intermediate mutants. RNA replication of some of the mutants was completely abolished whereas others were not or only mildly affected.

Results

Mutations directed at the serine linking the RNA with VPg

We have constructed five mutants that involve changes in the serine residue (Ser1) that links the VPg to the viral RNA as well as changes within the vicinity of the linking amino acid (Fig. 2). In mutant SR->Q/TR Ser1 has been replaced by threonine, a structurally conserved substitution that could provide a hydroxyl group for formation of the phosphodiester bond with RNA. Another mutant was designed to change Ser1 to a tyrosine residue, the residue linking VPg to genomic RNA in picornaviruses and potyviruses. Besides the intended S1Y mutation another mutation was fortuitously introduced changing the basic

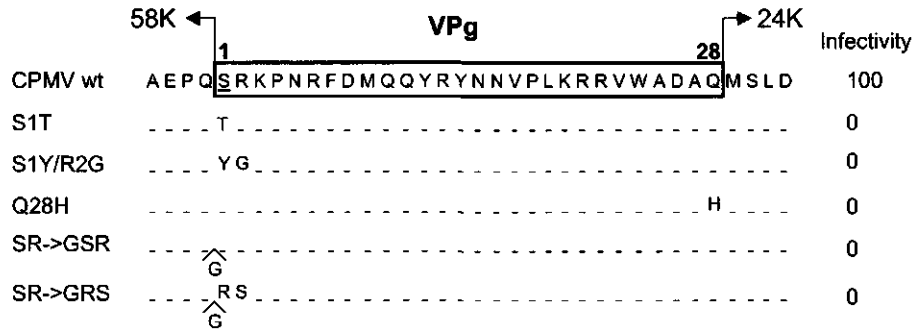

Figure 2 Sequence of CPMV VPg mutants that contain mutations near or at the serine linking VPg to RNA or at the C-terminal Q/M cleavage site. The amino acid sequence of the wild-type CPMV VPg is given by the one-letter amino acid code within the boxed region and the serine linking VPg to RNA is underlined. The names of the mutants are given to the left side, and their appropriate changes are shown replacing the wild-type sequence (- - - -). Clone SR->Q/GSR contains an insertion of a glycine residue at the indicated position. Indicated to the right are the percentages of infected cowpea protoplasts upon transfection with the mutants as determined by immunofluorescence. The experiment was repeated at least twice and the percentage of infected cells obtained with wild-type RNA1 (typically 15% to 30%) was set to 100%.

arginine residue at position 2 to a glycine (this mutant was designated SR->Q/YG). Two other mutants were made to investigate the necessity of the linking serine residue to be at the N-terminal position 1 of VPg. For mutant SR->Q/GSR insertion of a glycine residue at position 1 led to a change of the cleavage site from Q/S to Q/G and a VPg molecule with the linking serine at position 2. In mutant SR->Q/GRS the linking serine residue was introduced at position 3 replacing the arginine residue while the serine residue at position 1 was changed to a glycine.

For the potyvirus tobacco etch virus (TEV), cleavage of the VPg part (24-kDa) of the VPg-proteinase from the entire VPg-proteinase (49-kDa) seems not essential as both forms are found attached to TEV genomic RNA isolated from infected plants (117). For encephalomyocarditis virus it was shown that a mutant disturbed in the cleavage between 3B (VPg) and 3C (proteinase) produced infectious virus particles containing 3BC that was probably linked to viral RNA (62). An additional CPMV VPg mutant was made to investigate the necessity of VPg to be cleaved from the 24K proteinase in order to function in RNA replication. The mutation comprised of a change of the C-terminal glutamine residue to a histidine residue, abolishing the Q/M cleavage site between VPg and the 24K proteinase. This mutant was designated Q28->H.

The VPg mutants were introduced in cDNA clone pTB1G, which contains a full-length copy of CPMV RNA1 behind the T7 promoter. *In vitro* transcripts of wt pTB1G and mutant clones were used to transfect cowpea mesophyll protoplasts. Two days post infection (dpi), the protoplasts were fixed and stained with antibodies raised against the CPMV 110K protein and the percentage of fluorescent cells was calculated. Because viral proteins accumulate to detectable levels only when replication of the virus takes place, the percentage of fluorescent cells is a measure for infectivity (183). As is evident from Figure 2, transcripts from none of

the mutant VPg containing constructs were infectious where as T7 transcripts of the wt cDNA of RNA1 infected at least 15 percent of the cowpea protoplasts. Apparently viral RNA replication is very sensitive for changes at the N-terminal end of VPg.

The proteolytic processing of the mutant polyproteins was examined *in vitro* to determine whether the lethal phenotype was due to an intrinsic defect in the functioning of VPg or to changes in the cleavage site, which could alter or prevent the cleavage by the 24-K proteinase. For this purpose the mutations were introduced in pTB84, a cDNA clone of CPMV RNA1 lacking the 32K coding region and a large part of the coding region of the 87K core polymerase (Fig 3A; (135)). Previous studies have shown that in this construct *in vitro* cleavage at the 58K-VPg site is more efficient than in full-length clones. Transcripts of these clones were translated *in vitro* and the samples were allowed to incubate 18 h. to accomplish processing by the viral 24K proteinase. The 88kDa translation product encoded by wt pTB84 and the mutant constructs was readily cleaved into the 84K protein at the Q/G site between 24K and the truncated 87K (Fig. 3B, upper panel). No difference in cleavage efficiency was apparent at this site between wild-type and the VPg mutants. Cleavage at the Q/S of the 58K-VPg junction and of the Q/M of VPg-24K occurred less efficiently than cleavage at the Q/G of 24K-87K and only rather faint bands corresponding to the 58K and 60K product were observed with wild-type pTB84 (Fig. 3B, lower panel, lane 1). The intensity of the 58K band for mutants SR-

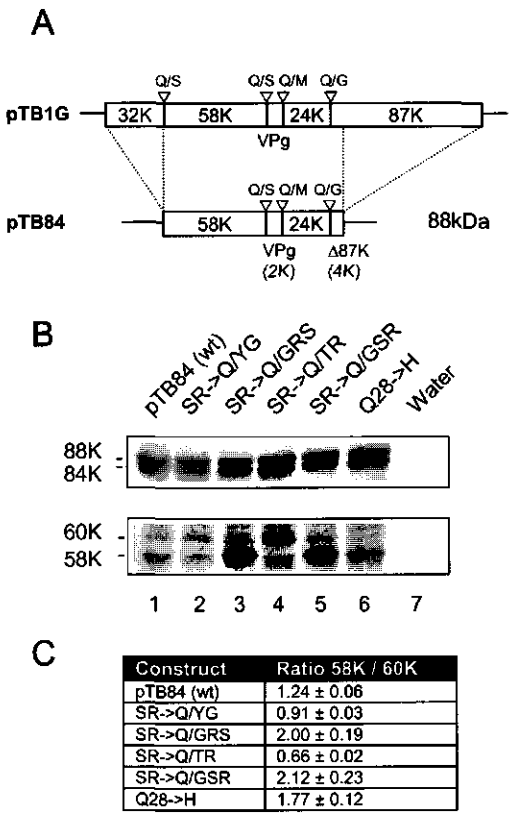

C

Construct	Ratio 58K / 60K
pTB84 (wt)	1.24 ± 0.06
SR->Q/YG	0.91 ± 0.03
SR->Q/GRS	2.00 ± 0.19
SR->Q/TR	0.66 ± 0.02
SR->Q/GSR	2.12 ± 0.23
Q28->H	1.77 ± 0.12

Figure 3 *In vitro* translation and processing of CPMV VPg mutants. A. Schematic diagram of plasmids pTB1G and pTB84 used for transcription with phage T7 polymerase. Mutations were introduced in pTB84 and transcripts were used for *in vitro* translation to determine processing at the cleavage sites. The open reading frame in the RNA molecule (open bar) and the cleavage sites are indicated as well as the apparent molecular masses of the final cleavage products. B. *In vitro* translation of RNA transcribed from pTB84 (containing wt VPg) and from the VPg mutants introduced in this vector in the presence of 35S methionine. The proteins were separated on a 10% PAAGE SDS gel. Water: no RNA added. C. Quantification of the ratio of 60K compared to 58K after *in vitro* translation and processing. Radioactivity corresponding to the 60K and 58K protein band was determined by scanning the gel with a phosphorimager. The values represent the amount of 58K protein divided by the amount of 60K protein and are the mean values of three separate experiments. The standard deviation is indicated.

>Q/GSR and SR->Q/GRS, which both contain a change of the cleavage site from Q/S to Q/G, is higher compared to wild-type. Since the 60K bands of these mutants are comparable in intensity this results in a higher ratio of 58K/60K compared to wild-type indicative of a more efficient cleavage between 58K and VPg (Fig. 3C). In contrast, replacement of the Q/S cleavage site to Q/T as is the case in mutant SR->Q/TR, resulted in a sharp increase in the amount of 60K protein (Fig. 3B, lower panel, lane 4). This is reflected in a reduction of the 58K/60K ratio (Fig. 3C) and suggests that cleavage at the 58K-VPg junction is inhibited. The amounts of 60K and 58K of mutant SR->Q/YG resembled that of wild-type although a small decrease in the amount of 58K was observed resulting in a slight decrease of the ratio 58K/60K (Fig 3B, lower panel, lane 2; Fig. 3C). Almost no 60K was detected in mutant Q28->H that contains a mutation at the C-terminal cleavage site and the ratio 58K/60K increased concomitantly, showing that cleavage between VPg and 24K was much less efficient in this mutant (Fig. 3B, lower panel, lane 6; Fig. 3C).

From this data we conclude that the VPg mutants that contain the linking serine at position 2 or 3 are processed more efficiently between the 58K and the VPg than wild-type *in vitro*. If the function of the 60K proteins is other than being the precursor for VPg this might contribute to the lethal phenotype of these mutants. The processing of the SR->Q/YG mutant resembled wild-type. In the VPg mutants SR->Q/TR and Q28->H the cleavage efficiency is clearly reduced and this might contribute to the loss of infectivity of these mutants in cowpea protoplasts.

Mutations designed to substitute CPMV VPg with the related CPSMV VPg

Cowpea severe mosaic virus (CPSMV), a related comovirus, encodes a 28 amino acid VPg that differs from CPMV at 9 positions, mostly involving conserved amino acid changes (Fig. 4). The nine mutations were introduced in the VPg coding region of pTB1G either as a pair or as a triplet generating four mutant constructs (designated VPg^{A}, VPg^{B}, VPg^{C} and VPg^{D} see figure 4). In mutant VPg^{AB} the mutations of VPg^{A} and VPg^{B} are combined. Combination of the mutations present in VPg^{A}, VPg^{B}, VPg^{C} and VPg^{D} resulted in the complete replacement of CPMV VPg with CPSMV VPg and the clone encoding this chimeric virus was designated VPg^{CPSMV}. It is noteworthy that, in contrast to the set of mutants described in the previous section, these mutations do not affect the N-terminal serine residue linking VPg to RNA nor do they affect amino acids in the immediate vicinity of this serine. The infectivity of the mutants was again tested by transfecting cowpea protoplasts with *in vitro* transcripts and the percentage of infected cells was determined using immunofluorescence with anti-110K serum at 2 dpi. The infectivity of transcripts from mutant VPg^{A} was comparable to wild-type. In contrast, the mutants containing the chimeric VPg^{CPSMV} or the intermediate VPg^{C} were non-infectious whereas the infectivity of mutants VPg^{B}, VPg^{AB} and VPg^{D} was decreased to 20, 20, and 50 percent respectively compared to wild-type (Fig. 4). Western blot analysis of extracts of these protoplasts with anti-110K serum confirmed the immuno-fluorescence data and

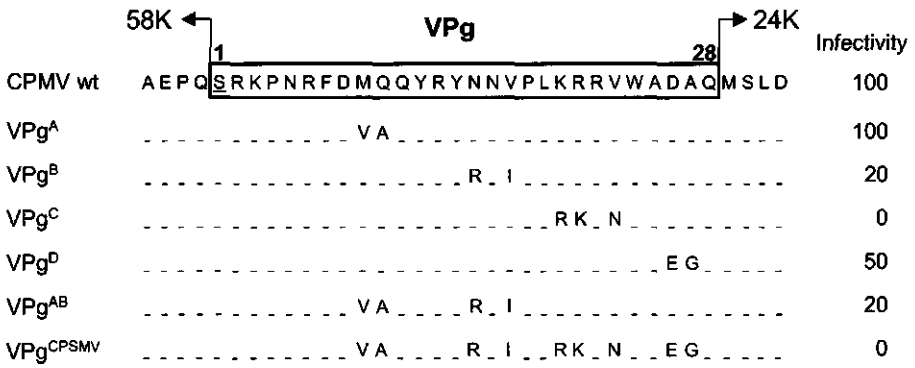

Figure 4 Diagram depicting mutations introduced to replace wild-type CPMV VPg with that of the related comovirus CPSMV. The amino acid sequence of CPSMV VPg differs from CPMV at nine positions and these mutations were introduced stepwise generating the intermediate clones VPg^{A}, VPg^{B}, VPg^{C}, VPg^{D} and Vpg^{AB}. VPg^{CPSMV} contains all nine mutations giving rise to a chimeric virus where the wild-type CPMV VPg is replaced by CPSMV VPg. The names of the mutants are given to the left side, and their appropriate changes are shown replacing the wild-type sequence (- - - -). Indicated to the right are the percentages of infected cowpea protoplasts upon transfection with the mutants as determined by immunofluorescence. The experiment was repeated at least twice and the percentage of infected cells obtained with wild-type RNA1 (typically 15% to 30%) was set to 100%.

displayed a similar reduction in accumulation of viral proteins of the VPg mutants (Fig. 5A; VPg^{D} [data not shown])

To test whether the alterations in VPg affected the ability of the mutants to infect cowpea plants, extracts of protoplasts that were infected with transcripts of the mutant VPg clones and RNA2 were used to mechanically inoculate cowpea leaves. Using this method, infection with mutant VPg^{A} produced symptoms similar to those with wild-type CPMV resulting in a yellow mosaic pattern on the primary inoculated leaves 2 dpi and on the upper systemic leaves 6 dpi (data not shown). The symptoms induced by infection with VPg^{B}, VPg^{AB}, and VPg^{D} were less severe than wild-type and developed 3 dpi on the primary inoculated leaves and 8 dpi (VPg^{B}) or 10 dpi (VPg^{AB} and VPg^{D}) on the systemic leaves (data not shown). As expected, no symptoms occurred on plants inoculated with extracts of protoplasts infected with mutants VPg^{C} or VPg^{CPSMV} (data not shown). From these data we can conclude that the mutations introduced in VPg^{C} and VPg^{CPSMV} completely abolished RNA replication suggesting that also changes of amino acids in CPMV VPg that are not conserved amongst the *Comoviridae* can have severe effects on virus viability. The mutations present in the other mutants showed a less severe effect on virus viability as they either debilitated (VPg^{B}, VPg^{AB} and VPg^{D}) or did not affect (VPg^{A}) replication and the ability to infect whole plants.

During the immunofluorescent analysis of the protoplasts infected with the VPg mutants with anti-110K serum we noted a different pattern in the case of mutant VPg^{D} in which the immunofluorescent label was distributed uniformly over the cytoplasm and not concentrated in specific areas as observed for wt RNA1 and the other mutants (data not shown). Previous

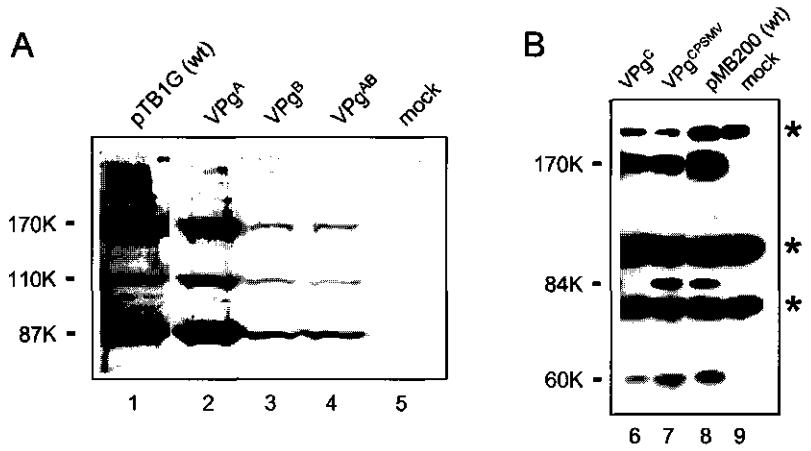

Figure 5 Immunoblot analysis of proteins produced in cowpea protoplasts by replicating VPg mutants (A) and by transient expression of non-replicating VPg mutants (B). The proteins were detected with anti-110K (A) or anti-VPg sera (B). The molecular masses of the viral proteins are indicated on the left and cowpea proteins that cross-react with anti-VPg are indicated by asterisks on the right. wt, wild-type

electron microscopy studies have revealed that the replication proteins accumulate in electron dense structures adjacent to clusters of small membranous vesicles that are the site of viral replication (33). Using light microcopy and immunofluorescent staining these structures appear as large shapeless bodies located near the nucleus in most infected cells. To confirm that mutations in VPg can alter the normal localization of the replication proteins, infected cowpea protoplasts were also analyzed for immunostaining with anti-VPg serum. The fluorescence in cowpea protoplasts transfected with wild-type RNA1, mutant VPg^{A}, VPg^{B} and VPg^{AB} was present in one or a few large shapeless bodies per cell (Fig. 6A and B and data not shown). The fluorescence in protoplasts transfected with mutant VPg^{D} was uniformly distributed over the cytoplasm (Fig. 6C) in agreement with the staining pattern observed with anti-110K serum.

The localization of the replication proteins of the non-infectious mutants VPg^{C} and VPg^{CPSMV} was further tested by introducing the mutations in a transient expression vector pMB200 that contains the coding sequence of the 200K polyprotein of RNA1 behind the CaMV 35S promoter. In protoplasts transfected with pMB200 or VPg^{C}, the fluorescence after immunostaining with anti-VPg and anti-110K serum was present in one or a few large shapeless bodies per cell (Fig. 6D and E and data not shown). Using anti-110K, the fluorescence pattern of mutant VPg^{CPSMV} resembled that of mutant VPg^{D} and the fluorescence label was distributed over the cytoplasm (Fig. 6F). No fluorescence was found using anti-VPg serum possibly due to reduced affinity of the antibody for the mutant VPg containing proteins. Western blot analysis using anti-VPg serum of extracts of protoplasts transfected with the transient expression constructs revealed that the accumulation of 170K, 84K and 60K proteins

in VPg^{CPSMV} and pMB200 transfected protoplasts is very similar, whereas in VPg^{C} transfected cells no 84K protein was detected and the amount of 60K protein was clearly reduced (Fig. 5B).

Taken together these results indicate that the two amino acid changes (an aspartic acid to glutamic acid residue at position 26 and an alanine to a glycine residue at position 27) present in both mutant VPg^{D} and VPg^{CPSMV} prevent the accumulation of replication proteins in distinct bodies near the nucleus; instead the replication proteins are now uniformly dispersed throughout the cytoplasm. Apparently formation of these bodies is not a prerequisite for replication as mutant VPg^{D} replicated in protoplasts and plants albeit at lower efficiency. Other mutations in VPg did not alter the localization pattern of the replication proteins including mutations in VPg^{C} that completely abolished RNA replication. The low levels of 84K and 60K proteins present in cells transfected with VPg^{C} suggest that the mutations present is this mutant had an effect on the stability of these proteins which could have contributed to the lack viability of this mutant, however this effect was not observed for VPg^{CPSMV} which is also not infectious and contains the same mutations.

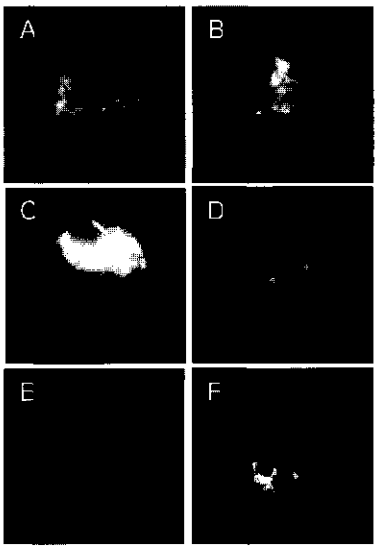

Figure 6 Effect of mutations in VPg on the distribution of CPMV replication proteins in cowpea protoplasts. The immunofluorescent images represent typical examples of fluorescent staining of protoplasts transfected with transcripts of pTB1G (A) and the mutants VPg^{AB} (B) and VPg^{D} (C) or with DNA constructs of the lethal mutants VPg^{C} (E) and VPg^{CPSMV} (F) that were introduced in pMB200 (D). Detection of the replication proteins was performed with anti-VPg (A-C) or anti-110K (D-F) serum and goat-anti-rabbit IgG conjugated with FITC.

Discussion

In this study we have performed a mutational analysis of the CPMV genome-linked protein VPg to discern the structural requirements necessary for proper functioning of VPg. We have shown that the structure of the N-terminal end of VPg, containing the serine residue involved in linking VPg to RNA, is crucial for virus replication but also other parts of VPg that are not conserved amongst comoviruses are important for viral infectivity. Furthermore VPg might be involved in protein-protein interactions with other replication proteins as was suggested by the altered localization pattern of the replication proteins in one of the mutants.

For the function of VPg linkage to a specific amino acid as well as the location of this amino acid within the VPg are essential. CPMV VPg attaches to its genomic RNA via the hydroxyl group of the serine residue at position 1. Changing this residue to tyrosine proved lethal for

the virus suggesting that the hydroxyl group presented by tyrosine is not accepted to form the linkage between VPg and the viral RNA although an additional mutation present in this mutant at position 2 could also have contributed to the lethal phenotype. Changing the linking serine residue of CPMV VPg to threonine also rendered the virus non-infectious. At the same time the processing between the 58K and VPg was severely inhibited in this mutant as was shown *in vitro*. Therefore the defect might be due to a lack of processing and we cannot rule out that the virus can accept the hydroxyl group of threonine to form the covalent bond between VPg and the RNA. The position of the linking amino acid within the VPg is critical to its function as can be concluded from the lethal phenotype of mutants SR->Q/GSR and SR->Q/GRS, where the linking serine was present at position 2 and 3 respectively. Processing at the 58K-VPg junction of these mutants occurred more efficiently than wild-type and this might contribute to the lethal phenotype. Clearly the functioning of CPMV VPg in virus replication is dependent on the identity and position of the amino acid that links the VPg to the viral RNA, which is in line with findings for the VPg of poliovirus and TVMV, a plant potyvirus. These viruses use the hydroxyl group of an internal tyrosine residue to link VPg to the viral RNA and it was shown that changing this tyrosine residue to serine, or changing the position within VPg results in a lethal phenotype (116, 144). Apparently the enzyme that catalyzes the esterification reaction between the hydroxyl group of the linking amino acid and the α-phosphate of uridine 5'-triphosphate (UTP) specifically recognizes tyrosine in the case of picorna- and potyviruses or serine in the case of nepo- and comoviruses. The specificity of these viral proteins for either tyrosine or serine is reminiscent of the specificity found in protein kinases that catalyze the phosphorylation of regulatory proteins, which also occurs via an esterification reaction of the hydroxyl group with the γ-phosphate. These kinases are divided in two, evolutionary distinct classes of the serine/threonine kinases and the tyrosine kinases.

It is not known whether the direct precursor protein of VPg is 60K or 112K and whether cleavage from its precursor is required for VPg functioning. The VPg mutant where the N-terminal serine residue was changed to threonine was disturbed in cleavage between 58K and VPg *in vitro* and was unable to replicate suggesting that proteolytic processing at that site is required. Changing the glutamine residue of the cleavage site at the C-terminal end to a histidine resulted in a virus that was severely disturbed in cleavage between VPg and the 24K proteinase. This mutation also proved lethal, strongly suggesting that VPg must be cleaved from its precursor in order to fulfill its role in replication. This is in line with results reported for the pea enation mosaic virus (PEMV), a member of the *Picornavirus*-like supergroup, where deletion of the N-terminal or the C-terminal cleavage site of the 28 amino acid VPg led to a loss of infectivity (166). Also a poliovirus VPg mutant defective in processing at the C-terminal cleavage site was reported to be non-viable (87). Interestingly, complete processing of VPg at the C-terminal cleavage site is not required for the potyviral VPg because both the

24 kDa VPg and the 49 kDa VPg-proteinase (NIa) were shown to be covalently attached to the RNA during infection with wild-type TEV (117).

Amino acid comparisons has shown that the first six amino acids of the VPgs of the comoviruses CPMV, CPSMV, bean pod mottle virus and red clover mosaic virus are identical, indicating that the N-terminal region of VPg near the linking serine is highly conserved amongst the comoviruses (38). However in other parts of VPg differences exist. CPSMV encodes a VPg that differs from CPMV VPg at nine positions. Introduction of these nine mutations in CPMV resulted in a chimeric virus that was unable to replicate demonstrating that also non-conserved amino acids can play an important role in virus replication. This is in sharp contrast to experiments with poliovirus where the replacement of VPg with the related echovirus 9 VPg or with the more distantly related human rhinovirus 14 VPg did not affect virus viability (86, 126) even though the VPg amino acid sequence of the latter chimeric virus differed at 13 positions of the 23 amino acids with poliovirus VPg. Notably, although the sequence of VPg is less conserved amongst human picornaviruses, their 3D polymerases are more conserved than the 87K polymerases of CPMV and CPSMV. Since it was proposed that recognition of VPg by the viral polymerase is a crucial step in initiation of viral replication (127), it is probable that the VPgs of picornaviruses are structurally more conserved than those of the comoviruses despite the lower level of conservation at the amino acid level. Alternatively the picornaviral polymerase is more promiscuous to the VPg structure than comoviral polymerases. Previous experiments to determine the structure of CPMV VPg using 2-dimensional NMR yielded spectra with substantial overlap that were difficult to interpret (184). This may suggests that VPg does not adopt a defined folded structure in aqueous solution.

A set of intermediate mutants allowed us to determine which of the nine amino acids that differed between CPMV VPg and CPSMV VPg are crucial for CPMV infectivity. The three amino acid changes introduced in mutant C resulted in a complete abolishment of replication demonstrating the pivotal role of these amino acids in CPMV replication. It is noteworthy that two of the three mutations present in VPg^C involve changes in a basic cluster of three amino acids at position 20 to 22. One could hypothesize that these positively charged amino acids are critical to the function of VPg because they interact directly with the negative charges associated with the nucleotides of the viral RNA. However, it is unlikely that this hypothesis explains the lethal phenotype of VPg^C because the mutations introduced in VPg^C at these positions were conservative of nature (lysine to arginine at position 20 and arginine to lysine at position 21) and did not change the net charge of the basic cluster. Also for poliovirus VPg mutational analysis showed that there is no direct correlation between the net charge of VPg and the ability to replicate. All mutations altering the arginine residue at position 17, even an arginine-to-lysine substitution, resulted in non-infectious virus whereas the lysine residue at position 20 could even be changed in a negatively charged glutamic acid without affecting virus replication (87). Perhaps the mutations introduced in VPg^C did not disturb an interaction

of VPg with RNA but an interaction of VPg with another replication protein. CPMV VPg is believed to interact with the viral polymerase to undergo uridylation and act as a primer for RNA transcription analogous to poliovirus initiation of replication (127). For this virus it has been shown extensively by biochemical methods and the yeast two-hybrid system that multiple protein-protein interactions occur between the replication proteins, in particular between the precursor of VPg, 3AB and the polymerase 3D or its precursor 3CD ((207) and references therein).

In this light it is interesting that the mutations introduced in another mutant, VPg^D caused a markedly different localization pattern of the replication proteins as revealed by immunofluorescence microscopy. Instead of aggregating into shapeless bodies in distinct areas as the wild-type, the replication proteins were dispersed uniformly over the cytoplasm. The shapeless bodies observed by light microscopy are believed to correspond to the large regions of electron dense material seen by electron microscopy that are present adjacent to the small membranous vesicles that are the site of CPMV replication (33). A similar aberrant localization pattern of the replication proteins was previously reported in protoplasts transiently expressing CPMV RNA1 mutants with either a deletion of the 32K coding region or a point mutation in the NTP binding site of the 60K protein (134, 183). Our results with mutant VPg^D implicate that besides the NTB-binding domain also the VPg region of 60K plays a role in formation of the electron dense structures. Based on the altered localization pattern of the different mutants and the observation that 60K associates with the 32K protein in infected cells (48), we propose that 32K and 60K are involved in an interaction that leads to multimerization and aggregation of the viral replication complexes in the electron dense structures. The significance of these electron dense structures for viral RNA replication is unclear. It has been proposed that the replication proteins accumulate in the electron dense structures either as inactive deposits or alternatively are maintained there in an active conformation for replication (183). The finding in our study that a mutation in CPMV VPg prevented formation of the electron dense structures without abolishing virus replication challenges the notion that the electron dense structures play an essential role in the viral replication. Instead the inclusion bodies might represent deposits of inactive non-structural proteins that are formed as a consequence of the expression strategy of the CPMV genome in a large polyprotein that does not allow differential regulation of replication proteins. A similar phenomenon is described for plant potyviruses where different nonstructural proteins accumulate in distinct inclusion bodies in the cytoplasm or in the nucleus, away from the site of replication (146) and references therein).

Materials and Methods

Construction of plasmids

To introduce mutations in the VPg coding region plasmid pTB1G (45) was used as starting material. Plasmid pTB1G contains the full-length cDNA of CPMV RNA1 from which infectious RNA can be generated using T7 RNA polymerase (45). The positions of restriction sites and nucleotides refer to the positions in the B-RNA sequence determined by (98). An SstI-BamHI fragment from pTB1G (positions 2301 to 3857) was inserted into the corresponding site of M13mp19. Site-directed mutagenesis was performed using the phosphorylated oligonucleotides shown in table 1 to introduce the different mutation according to the method described by (89). To facilitate selection of mutant clones, silent mutations were constructed that introduce a restriction site were indicated. In the case of SR->Q/YG, VPg^{D}, VPg^{AB} and VPg^{CPSMV} the mutations were introduced in mutant templates as indicated in table 1. Recombinant clones M13mp19 clones carrying the VPg mutations were analyzed by restriction enzyme mapping and dideoxy sequence analysis.

The SstI-BamHI fragments of the mutated M13mp19 clones were reinserted in the corresponding site of pTB1G. For *in vitro* translation assays, the mutant VPgs were introduced in pTB84 (135) as an SstI-AocI (3534) fragment. To produce the RNA1-encoded 200K polyprotein of the non-infectious VPg mutants in cowpea protoplasts, the mutations were introduced in pMB200 (183) that contains the RNA1 200K coding sequence under control of the CaMV 35S promoter. The NdeI (2080)-AocI fragment of pMB200 was exchanged with the NdeI-AocI fragments from the mutant clones.

In vitro transcription and translation

The procedure for *in vitro* transcription of viral cDNA and translation of RNA transcripts has been described earlier (136). The dried gels were exposed either to film or to a standard phosphor screen (Molecular Dynamics) for phosphorimager analysis. Band intensity was quantitated using a Storm phosphorimager (Molecular dynamics) and ImageQuant software.

Transfection of protoplasts and detection of RNA1-encoded proteins

Cowpea (*Vigna unguiculata L.*) mesophyll protoplasts were prepared and transfected by polyethylene glycol-mediated uptake as described previously (183). Transfected protoplasts were stained by the indirect fluorescent antibody technique (183) using anti-VPg (44) and anti-110K sera (181). After treatment with goat anti-rabbit antibodies conjugated to fluorescein isothiocyanate (FITC; Nordic), the protoplasts were examined by fluorescence microscopy.

For Western blot analysis protoplasts were collected 2 days post transfection by centrifugation at 100g for 2 min. Aliquots corresponding to 2 x 10^5 protoplasts were loaded on a 10% SDS-

Table 1. Oligonucleotides used in this study to introduce mutations in the coding sequence of VPg.

Mutant	Template	Oligonucleotide primer	R. site
SR->Q/YG	SR->Q/TR	CCTATTGGGCTTACGATATTGAGGCTC	--
SR->Q/GRS	Wt	CCTATTGGGCGATCGTCCTTGAGGCTC	*PvuI*
SR->Q/TR	Wt	CCTATTGGGCTTACGCGTTTGAGGCTC	*MluI*
SR->Q/GSR	Wt	GGGCTTTCTGGATCCTTGAGGCTCAG	*BamHI*
Q28->H	Wt	CCAAAGACATATGTGCGTCTGC	*NdeI*
VPg^{A}	Wt	GTATTGCGCGACGTCAAACCTATTGGG	*AatII*
VPg^{B}	Wt	CTCTTGAGAGGAATATTACGGTACCTGTATTGC	*KpnI*
VPg^{C}	Wt	GTGCGTCTGCCCAATTTCTTTTGCGCAGAGGAACATTG	*FspI*
VPg^{D}	Q28->H	CCAAAGACATTTGTCCCTCTGCCCAAACTC	--
VPg^{AB}	VPg^{A}	CTCTTGAGAGGAATATTACGGTACCTGTATTGC	*KpnI*
VPg^{CPSMV}	VPg^{ABD}	CTCTGCCCAATTTCTTTTGCGCAGAGGAATATTAC	*FspI*

polyacrylamide gel and electrophoresed. Immunoblots of these gels were prepared as described previously (183) using the antisera mentioned above.

Acknowledgements

We gratefully acknowledge Jeroen Pouwels for technical assistance and comments. Ton Bisseling is acknowledged for critically reading the manuscript. J.C. was supported by the Netherlands foundation for chemical research (CW) with financial aid from the Netherlands Foundation for Scientific Research (NWO). A.K. was supported by a FEBS Long-term Fellowship.

CHAPTER 7

CONCLUDING REMARKS

Introduction

The starting-point of the research described in this thesis was the observation that CPMV infection causes the accumulation of numerous small membranous vesicles that are involved in viral replication. Since it has become increasingly clear that membranes play a central role in viral RNA replication of many positive-stranded viruses (as outlined in chapter 1) we set out to define the cellular components involved in the establishment of the membranous site of viral RNA replication. Furthermore, the role of individual viral proteins as well as host proteins in this process was investigated.

Membrane proliferation as prerequisite for viral replication

We have demonstrated by expression of the green fluorescent protein (GFP) fused to marker proteins for the endoplasmic reticulum (ER) and the cis- and trans-Golgi stacks, that ER, but not Golgi membranes, undergo dramatic morphological changes during CPMV infection of cowpea protoplasts and *N. benthamiana* plants (chapter 2). Early in infection, multiple small and mobile bodies of packed ER tubules that were connected to the cortical ER were observed, which later in infection coalesced to one or several large bodies often located near the nucleus. For the whole period of the infection, these "proliferated" ER membranes surrounded and traversed the cytopathic structures that contained replication proteins and viral RNA as was demonstrated using fluorescence *in situ* hybridization (chapter 3). Taken together, these results point to an important role of the ER in supplying the membranes required for replication.

The importance of newly formed membranes for CPMV-replication was further emphasized by the observation that cerulenin, an inhibitor of an early step in phosphoglycerolipid (PGL) biosynthesis (122), proved to be a potent inhibitor of CPMV replication. Since in plant cells the ER is the major site of PGL synthesis (19), we may speculate that the small membranous vesicles that are involved in viral replication are composed of newly formed PGLs synthesized at the ER. It would be interesting to test directly whether CPMV-infection leads to an increased production of PGLs in the host cell as was demonstrated for poliovirus (191).

The recent finding that brome mosaic virus replication is severely inhibited in yeast cells that contain increased levels of saturated versus unsaturated PGLs in their membranes as a result of a mutation of the host Δ9 fatty acid desaturase, suggests that not only membrane synthesis per se but also lipid composition is important for viral replication (95). The proposed strict dependence on specific membrane composition for successful viral replication would tentatively explain the remarkable diversity of intracellular membranes that are utilized by different viruses. In our experiments, replication of tobacco mosaic virus and alfalfa mosaic virus was not affected by cerulenin, which suggests that the replication of these viruses takes place on preexisting membranes. CPMV infection, in contrast, might modulate PGL biosynthesis to create membranes with a lipid composition favorable for CPMV

replication. One could envision that certain PGLs stimulate the activity of the replication complex by providing a regulatory role in different steps e.g. the switch between translation of a plus-strand RNA and replication of this template. It would be interesting to test such a relation by interfering with the PGL composition of intracellular membranes of the host cells. This might be achieved by exogenous addition of different PGLs to the medium of CPMV-infected protoplasts. On the other hand a genetic approach to overexpress or knock out genes involved in specific steps of the PGL biosynthesis pathway seems also feasible. Since this pathway is well characterized in plants (121) and the different enzymes involved are for the greater part identified (109), this approach would allow careful modulation of the intracellular lipid composition. Several plants that carry mutations in genes encoding enzymes of the PGL biosynthesis pathway and transgenic plants that overexpress the relevant genes have already been described in the literature (e.g. (36, 81, 115). Especially interesting is the *Arabidopsis* mutant *fab2*, which contains a mutation in the gene encoding a stearoyl-ACP-desaturase (S-ACP DES) and has an increased accumulation of saturated versus unsaturated PGLs (36, 97). Since the functional homologue of plant S-ACP DES is the afore-mentioned Δ9 fatty acid desaturase in yeast, protoplasts isolated from *fab2* may perhaps not support viral (CPMV) replication. Alternatively, post-transcriptional gene silencing (PTGS) of an endogenous target gene involved in lipid biosynthesis can be achieved in *N. benthamiana* by Agrobacterium-mediated transformation with a construct encoding a double-stranded RNA for a specific gene. Virus vectors carrying elements of the exon of plant host genes are also potent elicitors of PTGS (11). This virus-induced gene silencing (VIGS) approach is attractive because of the ability to silence the expression of genes in mature plants. The latter may be important for silencing genes involved in lipid biosynthesis because it is expected that complete silencing of some of these genes will result in an embryo lethal phenotype. Mature leaves of plants silenced by VIGS may be less sensitive to these effects since the cells of these leaves are fully differentiated. The tobacco rattle virus (TRV) vector used in our studies to express CPMV proteins (chapter 5) could be instrumental for future studies of silencing genes involved in lipid biosynthesis because it has been described that with this vector efficient VIGS of endogenous genes in *N. benthamiana* can be achieved (139).

Role of 32K and 60K in viral replication

The clear morphological changes of intracellular membranes induced by CPMV infection, the localization of viral RNA complexes to membranes and the dependence of viral replication on membrane synthesis implies that CPMV encoded proteins are able to induce modifications of intracellular membranes and to anchor the replication complex to these membranes. The 60K protein was earlier implicated in these processes since it has been observed that expression of 60K in insect cells using the baculovirus expression system leads to formation of small membranous vesicles in the cytoplasm with some resemblance to the vesicles in CPMV-infected plant cells (181). This was very suggestive and in line with

findings for the polioviral 60K homologous 2BC protein, that induces membrane rearrangements when expressed separately from other polioviral proteins. We have shown by expression of the 60K protein in plant cells using the TRV vector that 60K indeed is membrane associated and is preferentially targeted to the ER membrane surrounding the nucleus and to plastidial membranes (chapter 5). However it induced only moderate ER proliferations.

During the course of our study it was noted that 32K also associates with membranes and is targeted to cortical ER membranes. Besides, expression of 32K is accompanied by cortical ER proliferations (chapter 5). This is unexpected since previous studies mainly pointed to a role of 32K as a cofactor required for processing of the RNA2 encoded polyprotein (136). Besides, deletion of 32K from the RNA1 200K polyprotein resulted in a more rapid cleavage of the 170K processing intermediate both *in vivo* and *in vitro* suggesting that 32K inhibits processing of 200K (136). The ER proliferations caused by 32K are mainly cortical whereas the proliferation caused by 60K are in a region near the nucleus, which may suggests that both 32K and 60K are needed to induce the membrane alterations that are morphologically similar to the alterations induced by CPMV-infection. For poliovirus the combined action of two proteins was also implicated in the induction of vesicles since it was demonstrated recently that small membranous vesicles that were ultrastructurally similar to those in poliovirus-infected cells only were formed when 2BC and 3A are expressed in combination in mammalian cells (173). Whether the observed changes in ER morphology by 32K and 60K corresponds to formation of small membranous vesicles in the cytoplasm of infected cells is currently unknown. Attempts to observe the ultrastructure of plant cells expressing 32K and 60K using electron microscopy were unsuccessful because *N. benthamiana* epidermal cells contain a large vacuole and the cytoplasmic content is small, which complicated the analysis of these cells (data not shown).

Compared to 110K and 24K, the amount of 32K and 60K that accumulated was low in cowpea protoplasts and in *N. benthamiana* leaves when expressed separately from the other CPMV proteins (chapter 5). Furthermore prolonged expression led to cell death in *N. benthamiana*. This was surprising because unlike mammalian viruses that depend on lysis of the host cells for their spread and often encode lytic proteins (25) or proteins inducing apoptosis (149), plant viruses spread through plasmodemata and cell death early in infection can restrict viral movement. Moreover, during CPMV infection, 32K and 60K accumulate to considerable amount without causing cell death. During CPMV infection, 32K and 60K interact with each other (48) and are present mainly in electron dense material in the vicinity to the membranous vesicles as was shown using electron microscopy ((196) and data not shown). Aggregation in these structures may protect 32K and 60K from degradation and may also prevent 32K and 60K from causing cell death. It would be interesting to express 32K and 60K together in plant cells and test the effect on membrane proliferation, expression levels of 32K and 60K and cell death.

Model for formation of the site of CPMV replication

The principal conclusions of the preceding sections can be brought together in a model for the formation of the site of CPMV RNA replication. When a plant cell becomes infected with CPMV, the viral RNA is released from the particles and translation of RNA1 results in production of the 200K polyprotein, which is rapidly cleaved into the 32K and 170K proteins (48). 32K and 170K remain associated via interaction between 32K and the 60K region contained in the 170K protein, which inhibits further proteolytic cleavage of 170K (136). It now appears that 32K/170K protein is specifically targeted to ER membranes via a localization signal residing in 32K. Interaction of 32K with the ER membrane may change the 32K/170K interaction thereby triggering further proteolytic cleavage of the 170K protein. At this stage 60K is released and inserted in the ER membrane thereby anchoring the replication complex to the membrane and serving as precursor for VPg similar to what was suggested for the polioviral 3AB protein (50). Interaction of both 32K and 60K with ER membranes leads to increased lipid biosynthesis and the proliferation of ER membranes. This favors replication since it increases the total surface of membranes that is available for viral replication and in that way form a compartment that protects the viral RNA from degradation by ribonucleases. The membranes could furthermore act as a scaffold to limit diffusion and increase local concentrations of viral proteins and RNA Deposition of replication proteins in electron-dense structures near the membranous site of replication may add to this compartmentalization. At their turn, the multiple initiation sites in a CPMV infected cell quickly coalesce to one or a few large structures. This actin dependent process may represent a higher order of compartmentalization in the infected cell (chapter 3). It is interesting to note that the distribution of replication proteins in cowpea protoplasts infected with CPMV carrying a particular mutation in VPg (VPg^{D}) was dispersed over the cytoplasm instead of concentrated in a distinct structure composed of electron dense material (chapter 6). Replication of the mutant was decreased to 50% of wild-type, which may suggest that formation of electron-dense material is beneficial but not required for virus replication. It would be interesting to examine the subcellular site of replication in protoplasts infected with this mutant by FISH and whether ER vesiculation and proliferation still occurs.

Remaining questions

How 32K and 60K induce the dramatic alterations in membrane morphology during CPMV infection remains tantalizing. The C-terminal domain of 60K interacts in the yeast two-hybrid system with VAP27 (chapter 4). We demonstrated that VAP27 is localized in ER membranes upon transient expression. VAP was originally identified in *Alypsia* and has been proposed to be a SNARE-like protein that functions in a complex with VAMP in the fusion of synaptic vesicles with the plasma membrane (168). Characterization of mammalian and yeast homologues of VAP has suggested a more general role in vesicle trafficking because VAP proteins were expressed in many different tissues and were found to localize mainly to ER

membranes and to microtubules (82, 167, 194). It is tempting to assume that binding of 60K with VAP27 disturbs the proposed function of VAP27 in fusion of the transport vesicles with the ER membrane and results in accumulation of the small membranous vesicles involved in CPMV replication. This would be in agreement with a recent report for poliovirus were it was shown, using immunofluorescence confocal microscopy combined with deconvolution analysis, that the small membranous vesicles, that occur during poliovirus infection and can be stained with 2BC antibodies, bud from the ER and colocalize with the COPII components Sec13 and Sec31 suggesting that poliovirus-induced vesicles are homologous to the vesicles of the anterograde membrane transport pathway (153). It should be noted however that binding of 60K with VAP27 still needs to be confirmed in CPMV-infected cells and further experiments are required to demonstrate the functionality of this interaction for the viral life cycle. Moreover a specific interaction of 60K with a SNARE-like protein does not account for the clear membrane alterations that occur when 32K is expressed in the absence of 60K. Rather than interfering with a specific protein involved in a specific vesicle transport pathway, the tight association of 32K and 60K with the membrane itself could trigger a stress response of the infected cell leading to vesiculation. We have tested whether the unfolded protein response, that occurs when improperly folded proteins overcrowd the ER membranes (63), could be involved by monitoring the level of BiP mRNA (chapter 3). Since BiP was not upregulated during CPMV infection it is unlikely that the UPR is involved in formation of the vesicles. A major challenge now will be to unravel how CPMV-encoded proteins activate the molecular pathways leading to ER proliferation and vesiculation.

REFERENCES

1. **Ahola, T., A. Lampio, P. Auvinen, and L. Kaariainen**. 1999. Semliki Forest virus mRNA capping enzyme requires association with anionic membrane phospholipids for activity. EMBO J. **18:**3164-3172.
2. **Aldabe, R., A. Barco, and L. Carrasco**. 1996. Membrane permeabilization by poliovirus proteins 2B and 2BC. J. Biol. Chem. **271:**23134-23137.
3. **Aldabe, R., and L. Carrasco**. 1995. Induction of membrane proliferation by poliovirus proteins 2C and 2BC. Biochem. Biophys. Res. Commun. **206:**64-76.
4. **Argos, P., G. Kamer, M. J. Nicklin, and E. Wimmer**. 1984. Similarity in gene organization and homology between proteins of animal picornaviruses and a plant comovirus suggest common ancestry of these virus families. Nucleic Acids Res. **12:**7251-7267.
5. **Assink, A. M., H. Swaans, and A. Van Kammen**. 1973. The localization of virus-specific double-stranded RNA of cowpea mosaic virus in subcellular fractions of infected *Vigna* leaves. Virology. **53:**384-391.
6. **Baluska, F., J. Jasik, H. G. Edelmann, T. Salajova, and D. Volkmann**. 2001. Latrunculin B-induced plant dwarfism: Plant cell elongation is F-actin- dependent. Dev. Biol. **231:**113-124.
7. **Barco, A., and L. Carrasco**. 1995. A human virus protein, poliovirus protein 2BC, induces membrane proliferation and blocks the exocytic pathway in the yeast Saccharomyces cerevisiae. EMBO J. **14:**3349-3364.
8. **Barco, A., and L. Carrasco**. 1998. Identification of regions of poliovirus 2BC protein that are involved in cytotoxicity. J. Virol. **72:**3560-3570.
9. **Barton, D. J., E. P. Black, and J. B. Flanegan**. 1995. Complete replication of poliovirus *in vitro*: preinitiation RNA replication complexes require soluble cellular factors for the synthesis of VPg-linked RNA. J. Virol. **69:**5516-5527.
10. **Baskin, T. I., J. E. Wilson, A. Cork, and R. E. Williamson**. 1994. Morphology and microtubule organization in *Arabidopsis* roots exposed to oryzalin or taxol. Plant Cell Physiol. **35:**935-942.
11. **Baulcombe, D. C.** 1999. Fast forward genetics based on virus-induced gene silencing. Curr. Opin. Plant Biol. **2:**109-113.
12. **Beachy, R. N., and M. Heinlein**. 2000. Role of P30 in replication and spread of TMV. Traffic. **1:**540-544.
13. **Bertens, P., J. Wellink, R. Goldbach, and A. van Kammen**. 2000. Mutational analysis of the cowpea mosaic virus movement protein. Virology. **267:**199-208.

14. **Bienz, K., D. Egger, and L. Pasamontes**. 1987. Association of polioviral proteins of the P2 genomic region with the viral replication complex and virus-induced membrane synthesis as visualized by electron microscopic immunocytochemistry and autoradiography. Virology. **160:**220-226.

15. **Blumenthal, T.** 1980. Interaction of host-coded and virus-coded polypeptides in RNA phage replication. Proc. R. Soc. Lond. B. Biol. Sci. **210:**321-335.

16. **Boevink, P., K. Oparka, S. Santa Cruz, B. Martin, A. Betteridge, and C. Hawes**. 1998. Stacks on tracks: the plant Golgi apparatus traffics on an actin/ER network. Plant J. **15:**441-447.

17. **Boevink, P., S. Santa Cruz, K. Oparka, and C. Hawes**. 1996. Virus-mediated delivery of the green fluorescent protein to the endoplasmic reticulum of tobacco cells. Plant J. **10:**935-941.

18. **Bolten, R., D. Egger, R. Gosert, G. Schaub, L. Landmann, and K. Bienz**. 1998. Intracellular localization of poliovirus plus- and minus-strand RNA visualized by strand-specific fluorescent *In situ* hybridization. J. Virol. **72:**8578-8585.

19. **Browse, J. A., and C. R. Somerville**. 1991. Glycerolipid metabolism, biochemistry and regulation. Annu. Rev. Plant Mol. Biol. **42:**467-506.

20. **Buck, K. W.** 1996. Comparison of the replication of positive-stranded RNA viruses of plants and animals. Adv. Virus Res. **47:**159-251.

21. **Buck, K. W.** 1999. Replication of tobacco mosaic virus RNA. Philos. Trans. R. Soc. Lond. B. Biol. Sci. **354:**613-627.

22. **Burgyan, J., L. Rubino, and M. Russo**. 1996. The 5'-terminal region of a tombusvirus genome determines the origin of multivesicular bodies. J. Gen. Virol. **77:**1967-1974.

23. **Burkhard, P., J. Stetefeld, and S. V. Strelkov**. 2001. Coiled coils: a highly versatile protein folding motif. Trends Cell Biol. **11:**82-88.

24. **Carette, J. E., M. Stuiver, J. Van Lent, J. Wellink, and A. Van Kammen**. 2000. Cowpea mosaic virus infection induces a massive proliferation of endoplasmic reticulum but not Golgi membranes and is dependent on *de novo* membrane synthesis. J. Virol. **74:**6556-6563.

25. **Carrasco, L.** 1995. Modification of membrane permeability by animal viruses. Adv. Virus Res. **45:**61-112.

26. **Chen, J., and P. Ahlquist**. 2000. Brome mosaic virus polymerase-like protein 2a is directed to the endoplasmic reticulum by helicase-like viral protein 1a. J. Virol. **74:**4310-4318.

27. **Cho, M. W., N. Teterina, D. Egger, K. Bienz, and E. Ehrenfeld**. 1994. Membrane rearrangement and vesicle induction by recombinant poliovirus 2C and 2BC in human cells. Virology. **202:**129-145.

28. **Clark, A. J., P. Bertens, J. Wellink, M. Shanks, and G. P. Lomonossoff**. 1999. Studies on hybrid comoviruses reveal the importance of three-dimensional structure for processing of the viral coat proteins and show that the specificity of cleavage is greater *in trans* than *in cis*. Virology. **263:**184-194.

29. **Das, T., M. Mathur, A. K. Gupta, G. M. Janssen, and A. K. Banerjee**. 1998. RNA polymerase of vesicular stomatitis virus specifically associates with translation elongation factor-1 alphabetagamma for its activity. Proc. Natl. Acad. Sci. USA. **95:**1449-1454.

30. **Davis, S. J., and R. D. Vierstra**. 1998. Soluble, highly fluorescent variants of green fluorescent protein (GFP) for use in higher plants. Plant Mol. Biol. **36:**521-528.

31. **De Graaf, M., and E. M. J. Jaspars**. 1994. Plant viral RNA synthesis in cell-free systems. Annu. Rev. Phytopathol. **32:**311-335.

32. **De Zoeten, G. A.** 1966. California tobacco rattle virus, its intracellular appearance, and the cytology of the infected cell. Phytopathology. **56:**744-754.

33. **De Zoeten, G. A., A. M. Assink, and A. Van Kammen**. 1974. Association of cowpea mosaic virus-induced double-stranded RNA with a cytopathological structure in infected cells. Virology. **59:**341-355.

34. **De Zoeten, G. A., G. Gaard, and F. B. Diez**. 1972. Nuclear vesiculation associated with pea enation mosaic virus-infected plant tissue. Virology. **48:**638-647.

35. **De Varennes, A., and A. J. Maule**. 1985. Independent replication of cowpea mosaic virus bottom component RNA: *in vivo* instabililty of the viral RNAs. Virology. **144:**495-501.

36. **Delhaize, E., D. M. Hebb, K. D. Richards, J. M. Lin, P. R. Ryan, and R. C. Gardner**. 1999. Cloning and expression of a wheat (Triticum aestivum L.) phosphatidylserine synthase cDNA. Overexpression in plants alters the composition of phospholipids. J. Biol. Chem. **274:**7082-7088.

37. **Denecke, J., M. H. Goldman, J. Demolder, J. Seurinck, and J. Botterman**. 1991. The tobacco luminal binding protein is encoded by a multigene family. Plant Cell. **3:**1025-1035.

38. **Di, R., C. C. Hu, and S. A. Ghabrial**. 1999. Complete nucleotide sequence of bean pod mottle virus RNA1: sequence comparisons and evolutionary relationships to other comoviruses. Virus Genes. **18:**129-137.

39. **Doedens, J., L. A. Maynell, M. W. Klymkowsky, and K. Kirkegaard**. 1994. Secretory pathway function, but not cytoskeletal integrity, is required in poliovirus infection. Arch. Virol. Suppl. **9:**159-172.

40. **Doedens, J. R., T. H. Giddings, Jr., and K. Kirkegaard**. 1997. Inhibition of endoplasmic reticulum-to-Golgi traffic by poliovirus protein 3A: genetic and ultrastructural analysis. J. Virol. **71:**9054-9064.

41. **Doedens, J. R., and K. Kirkegaard**. 1995. Inhibition of cellular protein secretion by poliovirus proteins 2B and 3A. EMBO J. **14:**894-907.

42. **Dolja, V. V., H. J. McBride, and J. C. Carrington**. 1992. Tagging of plant potyvirus replication and movement by insertion of beta-glucuronidase into the viral polyprotein. Proc. Natl. Acad. Sci. USA. **89:**10208-10212.

43. **Echeverri, A. C., and A. Dasgupta**. 1995. Amino terminal regions of poliovirus 2C protein mediate membrane binding. Virology. **208:**540-553.

44. **Eggen, R., A. Kaan, R. Goldbach, and A. Van Kammen**. 1988. Cowpea mosaic virus RNA replication in crude membrane fractions from infected cowpea and chenopodium armaranticolor. J. Gen. Virol. **69:**2711-2720.

45. **Eggen, R., J. Verver, J. Wellink, A. De Jong, R. Goldbach, and A. van Kammen**. 1989. Improvements of the infectivity of *in vitro* transcripts from cloned cowpea mosaic virus cDNA: impact of terminal nucleotide sequences. Virology. **173:**447-455.

46. **Fields, S., and R. Sternglanz**. 1994. The two-hybrid system: an assay for protein-protein interactions. Trends Genet. **10:**286-292.

47. **Franssen, H., J. Leunissen, R. Goldbach, G. Lomonossoff, and D. Zimmern**. 1984. Homologous sequences in non-structural proteins from cowpea mosaic virus and picornaviruses. EMBO J. **3:**855-861.

48. **Franssen, H., M. Moerman, G. Rezelman, and R. Goldbach**. 1984. Evidence that the 32,000-Dalton protein encoded by bottom-component RNA of cowpea mosaic virus is a proteolytic processing enzyme. J. Virol. **50:**183-190.

49. **Gaire, F., C. Schmitt, C. Stussi-Garaud, L. Pinck, and C. Ritzenthaler**. 1999. Protein 2A of grapevine fanleaf nepovirus is implicated in RNA2 replication and colocalizes to the replication site. Virology. **264:**25-36.

50. **Giachetti, C., and B. L. Semler**. 1991. Role of a viral membrane polypeptide in strand-specific initiation of poliovirus RNA synthesis. J. Virol. **65:**2647-2654.

51. **Gidekel, M., B. Jimenez, and L. Herrera-Estrella**. 1996. The first intron of the *Arabidopsis* thaliana gene coding for elongation factor 1 beta contains an enhancer-like element. Gene. **170:**201-206.

52. **Goldbach, R., G. Rezelman, P. Zabel, and A. Van Kammen**. 1982. Expression of the bottom-component RNA of cowpea mosaic virus: evidence that the 60-kilodalton VPg precursor is cleaved into single VPg and a 58-kilodalton polypeptide. J. Virol. **42:**630-635.

53. **Goldbach, R., G. Rezelman, P. Zabel, and A. van Kammen**. 1982. Expression of the bottom-component RNA of cowpea mosaic virus: evidence that the 60-kilodalton VPg precursor is cleaved into single VPg and a 58-kilodalton polypeptide. J. Virol. **42:**630-635.

54. **Goldbach, R., and J. Wellink** 1996. Comoviruses: molecular biology and replication, p. 35-76, The plant viruses, polyhedral virions and bipartite RNA genomes, vol. 5. Plenum Press, New York.

55. **Gopinath, K., J. Wellink, C. Porta, K. M. Taylor, G. P. Lomonossoff, and A. van Kammen**. 2000. Engineering cowpea mosaic virus RNA-2 into a vector to express heterologous proteins in plants. Virology. **267:**159-173.

56. **Gorbalenya, A. E., E. V. Koonin, and Y. I. Wolf**. 1990. A new superfamily of putative NTP-binding domains encoded by genomes of small DNA and RNA viruses. FEBS Lett. **262:**145-148.

57. **Grief, C., L. Galler, L. M. Cortes, and O. M. Barth**. 1997. Intracellular localization of dengue-2 RNA in mosquito cell culture using electron microscopic *in situ* hybridization. Arch. Virol. **142:**2347-2357.

58. **Grimley, P. M., I. K. Berezesky, and R. M. Friedman**. 1968. Cytoplasmic structures associated with an arbovirus infection: loci of viral ribonucleic acid synthesis. J. Virol. **2:**1326-1338.

59. **Guinea, R., and L. Carrasco**. 1991. Effects of fatty acids on lipid synthesis and viral RNA replication in poliovirus-infected cells. Virology. **185:**473-476.

60. **Guinea, R., and L. Carrasco**. 1990. Phospholipid biosynthesis and poliovirus genome replication, two coupled phenomena. EMBO J. **9:**2011-2016.

61. **Haizel, T., T. Merkle, A. Pay, E. Fejes, and F. Nagy**. 1997. Characterization of proteins that interact with the GTP-bound form of the regulatory GTPase Ran in *Arabidopsis*. Plant J. **11:**93-103.

62. **Hall, D. J., and A. C. Palmenberg**. 1996. Cleavage site mutations in the encephalomyocarditis virus P3 region lethally abrogate the normal processing cascade. J. Virol. **70:**5954-5961.

63. **Hampton, R. Y.** 2000. ER stress response: getting the UPR hand on misfolded proteins. Curr. Biol. **10:**R518-521.

64. **Harris, K. S., W. Xiang, L. Alexander, W. S. Lane, A. V. Paul, and E. Wimmer**. 1994. Interaction of poliovirus polypeptide 3CDpro with the 5' and 3' termini of the poliovirus genome. Identification of viral and cellular cofactors needed for efficient binding. J. Biol. Chem. **269:**27004-27014.

65. **Haseloff, J., K. R. Siemering, D. C. Prasher, and S. Hodge**. 1997. Removal of a cryptic intron and subcellular localization of green fluorescent protein are required to mark transgenic *Arabidopsis* plants brightly. Proc. Natl. Acad. Sci. USA. **94:**2122-2127.

66. **Hayes, R. J., and K. W. Buck**. 1990. Complete replication of a eukaryotic virus RNA *in vitro* by a purified RNA-dependent RNA polymerase. Cell. **63:**363-368.

67. **Heath, M. C.** 2000. Hypersensitive response-related death. Plant Mol. Biol. **44:**321-334.

68. **Hibi, T., G. Rezelman, and A. Van Kammen**. 1975. Infection of cowpea mesophyll protoplasts with cowpea mosaic virus. Virology. **64:**308-318.

69. **Hugle, T., F. Fehrmann, E. Bieck, M. Kohara, H. G. Krausslich, C. M. Rice, H. E. Blum, and D. Moradpour**. 2001. The hepatitis C virus nonstructural protein 4B is an integral endoplasmic reticulum membrane protein. Virology. **284:**70-81.

70. **Irurzun, A., L. Perez, and L. Carrasco**. 1992. Involvement of membrane traffic in the replication of poliovirus genomes: effects of brefeldin A. Virology. **191:**166-175.

71. **Ishihara, N., S. Yamashina, M. Sakaguchi, K. Mihara, and T. Omura**. 1995. Malfolded cytochrome P-450(M1) localized in unusual membrane structures of the endoplasmic reticulum in cultured animal cells. J. Biochem. (Tokyo). **118:**397-404.

72. **Ishikawa, M., J. Diez, M. Restrepo-Hartwig, and P. Ahlquist**. 1997. Yeast mutations in multiple complementation groups inhibit brome mosaic virus RNA replication and transcription and perturb regulated expression of the viral polymerase-like gene. Proc. Natl. Acad. Sci. USA. **94:**13810-13815.

73. **Ishikawa, M., S. Naito, and T. Ohno**. 1993. Effects of the tom1 mutation of *Arabidopsis* thaliana on the multiplication of tobacco mosaic virus RNA in protoplasts. J. Virol. **67:**5328-5338.

74. **Ishikawa, M., F. Obata, T. Kumagai, and T. Ohno**. 1991. Isolation of mutants of *Arabidopsis* thaliana in which accumulation of tobacco mosaic virus coat protein is reduced to low levels. Mol. Gen. Genet. **230:**33-38.

75. **Jaegle, M., J. Wellink, and R. Goldbach**. 1987. The genome-linked protein of cowpea mosaic virus is bound to the 5' terminus of virus RNA by a phosphodiester linkage to serine. J. Gen. Virol. **68:**627-632.

76. **James, P., J. Halladay, and E. A. Craig**. 1996. Genomic libraries and a host strain designed for highly efficient two- hybrid selection in yeast. Genetics. **144:**1425-1436.

77. **Janda, M., and P. Ahlquist**. 1993. RNA-dependent replication, transcription, and persistence of brome mosaic virus RNA replicons in S. cerevisiae. Cell. **72:**961-970.

78. **Jelitto-Van Dooren, E. P., S. Vidal, and J. Denecke**. 1999. Anticipating endoplasmic reticulum stress. A novel early response before pathogenesis-related gene induction. Plant Cell. **11:**1935-1944.

79. **Jespersen, H. M., I. V. Kjaersgard, L. Ostergaard, and K. G. Welinder**. 1997. From sequence analysis of three novel ascorbate peroxidases from *Arabidopsis* thaliana to structure, function and evolution of seven types of ascorbate peroxidase. Biochem. J. **326:**305-310.

80. **Jingami, H., M. S. Brown, J. L. Goldstein, R. G. Anderson, and K. L. Luskey**. 1987. Partial deletion of membrane-bound domain of 3-hydroxy-3-methylglutaryl coenzyme A reductase eliminates sterol-enhanced degradation and prevents formation of crystalloid endoplasmic reticulum. J. Cell Biol. **104:**1693-1704.

81. **Kachroo, P., J. Shanklin, J. Shah, E. J. Whittle, and D. F. Klessig**. 2001. A fatty acid desaturase modulates the activation of defense signaling pathways in plants. Proc. Natl. Acad. Sci. USA. **98:**9448-9453.

82. **Kagiwada, S., K. Hosaka, M. Murata, J. Nikawa, and A. Takatsuki**. 1998. The Saccharomyces cerevisiae SCS2 gene product, a homolog of a synaptobrevin-associated protein, is an integral membrane protein of the endoplasmic reticulum and is required for inositol metabolism. J. Bacteriol. **180:**1700-1708.

83. **Kasteel, D., J. Wellink, J. Verver, J. van Lent, R. Goldbach, and A. van Kammen**. 1993. The involvement of cowpea mosaic virus M RNA-encoded proteins in tubule formation. J. Gen. Virol. **74:**1721-1724.

84. **Kochevar, D. T., and R. G. Anderson**. 1987. Purified crystalloid endoplasmic reticulum from UT-1 cells contains multiple proteins in addition to 3-hydroxy-3-methylglutaryl coenzyme A reductase. J. Biol. Chem. **262:**10321-10326.

85. **Kost, B., P. Spielhofer, and N. H. Chua**. 1998. A GFP-mouse talin fusion protein labels plant actin filaments *in vivo* and visualizes the actin cytoskeleton in growing pollen tubes. Plant J. **16:**393-401.

86. **Kuhn, R. J., H. Tada, M. F. Ypma-Wong, J. J. Dunn, B. L. Semler, and E. Wimmer**. 1988. Construction of a "mutagenesis cartridge" for poliovirus genome-linked viral protein: isolation and characterization of viable and nonviable mutants. Proc. Natl. Acad. Sci. USA. **85:**519-523.

87. **Kuhn, R. J., H. Tada, M. F. Ypma-Wong, B. L. Semler, and E. Wimmer**. 1988. Mutational analysis of the genome-linked protein VPg of poliovirus. J. Virol. **62:**4207-4215.

88. **Kujala, P., A. Ikaheimonen, N. Ehsani, H. Vihinen, P. Auvinen, and L. Kaariainen**. 2001. Biogenesis of the Semliki Forest virus RNA replication complex. J. Virol. **75:**3873-3884.

89. **Kunkel, T. A.** 1985. Rapid and efficient site-specific mutagenesis without phenotypic selection. Proc. Natl. Acad. Sci. USA. **82:**488-492.

90. **Laage, R., J. Rohde, B. Brosig, and D. Langosch**. 2000. A conserved membrane-spanning amino acid motif drives homomeric and supports heteromeric assembly of presynaptic SNARE proteins. J. Biol. Chem. **275:**17481-17487.

91. **Lampio, A., I. Kilpelainen, S. Pesonen, K. Karhi, P. Auvinen, P. Somerharju, and L. Kaariainen**. 2000. Membrane binding mechanism of an RNA virus-capping enzyme. J. Biol. Chem. **275:**37853-37859.

92. **Lapierre, L. A., P. L. Tuma, J. Navarre, J. R. Goldenring, and J. M. Anderson**. 1999. VAP-33 localizes to both an intracellular vesicle population and with occludin at the tight junction. J. Cell Sci. **112:**3723-3732.

93. **Laurent, F., G. Labesse, and P. de Wit**. 2000. Molecular cloning and partial characterization of a plant VAP33 homologue with a major sperm protein domain. Biochem. Biophys. Res. Commun. **270:**286-292.

94. **Lee, H. I., S. Gal, T. C. Newman, and N. V. Raikhel**. 1993. The *Arabidopsis* endoplasmic reticulum retention receptor functions in yeast. Proc. Natl. Acad. Sci. USA. **90:**11433-11437.

95. **Lee, W. M., M. Ishikawa, and P. Ahlquist**. 2001. Mutation of host delta9 fatty acid desaturase inhibits brome mosaic virus RNA replication between template recognition and RNA synthesis. J. Virol. **75:**2097-2106.

96. **Li, H. W., A. P. Lucy, H. S. Guo, W. X. Li, L. H. Ji, S. M. Wong, and S. W. Ding**. 1999. Strong host resistance targeted against a viral suppressor of the plant gene silencing defence mechanism. EMBO J. **18:**2683-2691.

97. **Lightner, J., J. Wu, and J. Browse**. 1994. A mutant of *Arabidopsis* with increased levels of staeric acid. Plant Physiol. **106:**1443-1451.

98. **Lomonossoff, G., and M. Shanks**. 1983. The nucleotide sequence of cowpea mosaic virus B RNA. EMBO J. **2:**2253-2258.

99. **Lomonossoff, G., M. Shanks, and D. Evans**. 1985. The structure of cowpea mosaic virus replicative form RNA. Virology. **144:**351-362.

100. **Louvet, O., F. Doignon, and M. Crouzet**. 1997. Stable DNA-binding yeast vector allowing high-bait expression for use in the two-hybrid system. Biotechniques. **23:**816-818, 820.

101. **MacFarlane, S. A., and A. H. Popovich**. 2000. Efficient expression of foreign proteins in roots from tobravirus vectors. Virology. **267:**29-35.

102. **Mackenzie, J. M., M. K. Jones, and E. G. Westaway**. 1999. Markers for trans-Golgi membranes and the intermediate compartment localize to induced membranes with distinct replication functions in flavivirus-infected cells. J. Virol. **73:**9555-9567.

103. **Marc, J., C. L. Granger, J. Brincat, D. D. Fisher, T. Kao, A. G. McCubbin, and R. J. Cyr**. 1998. A GFP-MAP4 reporter gene for visualizing cortical microtubule rearrangements in living epidermal cells. Plant Cell. **10:**1927-1940.

104. **Martelli, G. P., and M. Russo** 1985. Virus-host relationships, symptomatological and ultrastructural aspects, p. 163-205. *In* R. I. B. Francki (ed.), Polyhedral virions with tripartite genomes. Plenum Press, New York.

105. **Martin, M. T., M. T. Cervera, J. A. Garcia, and P. Bonay**. 1995. Properties of the active plum pox potyvirus RNA polymerase complex in defined glycerol gradient fractions. Virus Res. **37:**127-137.

106. **Mas, P., and R. N. Beachy**. 1999. Replication of tobacco mosaic virus on endoplasmic reticulum and role of the cytoskeleton and virus movement protein in intracellular distribution of viral RNA. J. Cell Biol. **147:**945-958.

107. **Maurel, C., J. Reizer, J. I. Schroeder, and M. J. Chrispeels**. 1993. The vacuolar membrane protein gamma-TIP creates water specific channels in Xenopus oocytes. EMBO J. **12:**2241-2247.

108. **Maynell, L. A., K. Kirkegaard, and M. W. Klymkowsky**. 1992. Inhibition of poliovirus RNA synthesis by brefeldin A. J. Virol. **66:**1985-1994.

109. **Mekhedov, S., O. M. de Ilarduya, and J. Ohlrogge**. 2000. Toward a functional catalog of the plant genome. A survey of genes for lipid biosynthesis. Plant Physiol. **122:**389-402.

110. **Miller, J. H.** 1972. Experiments in molecular genetics. Cold Spring Harbor Laboratory, Cold Spring Harbor, NY.

111. **Minella, O., O. Mulner-Lorillon, V. De Smedt, S. Hourdez, P. Cormier, and R. Belle**. 1996. Major intracellular localization of elongation factor-1. Cell. Mol. Biol. (Noisy-le-grand). **42:**805-810.

112. **Miyawaki, A., J. Llopis, R. Heim, J. M. McCaffery, J. A. Adams, M. Ikura, and R. Y. Tsien**. 1997. Fluorescent indicators for Ca2+ based on green fluorescent proteins and calmodulin. Nature. **388:**882-887.

113. **Moche, M., G. Schneider, P. Edwards, K. Dehesh, and Y. Lindqvist**. 1999. Structure of the complex between the antibiotic cerulenin and its target, beta-ketoacyl-acyl carrier protein synthase. J. Biol. Chem. **274:**6031-6034.

114. **Molla, A., A. V. Paul, and E. Wimmer**. 1993. Effects of temperature and lipophilic agents on poliovirus formation and RNA synthesis in a cell-free system. J. Virol. **67:**5932-5938.

115. **Mou, Z., Y. He, Y. Dai, X. Liu, and J. Li**. 2000. Deficiency in fatty acid synthase leads to premature cell death and dramatic alterations in plant morphology. Plant Cell. **12:**405-418.

116. **Murphy, J. F., P. G. Klein, A. G. Hunt, and J. G. Shaw**. 1996. Replacement of the tyrosine residue that links a potyviral VPg to the viral RNA is lethal. Virology. **220:**535-538.

117. **Murphy, J. F., R. E. Rhoads, A. G. Hunt, and J. G. Shaw**. 1990. The VPg of tobacco etch virus RNA is the 49-kDa proteinase or the N- terminal 24-kDa part of the proteinase. Virology. **178:**285-288.

118. **Murphy, J. F., W. Rychlik, R. E. Rhoads, A. G. Hunt, and J. G. Shaw**. 1991. A tyrosine residue in the small nuclear inclusion protein of tobacco vein mottling virus links the VPg to the viral RNA. J. Virol. **65:**511-513.

119. **Nebenfuhr, A., L. A. Gallagher, T. G. Dunahay, J. A. Frohlick, A. M. Mazurkiewicz, J. B. Meehl, and L. A. Staehelin**. 1999. Stop-and-go movements of plant Golgi stacks are mediated by the acto- myosin system. Plant Physiol. **121:**1127-1142.

120. **Ohkuma, M., S. M. Park, T. Zimmer, R. Menzel, F. Vogel, W. H. Schunck, A. Ohta, and M. Takagi**. 1995. Proliferation of intracellular membrane structures upon homologous overproduction of cytochrome P-450 in Candida maltosa. Biochim. Biophys. Acta. **1236:**163-169.

121. **Ohlrogge, J., and J. Browse**. 1995. Lipid biosynthesis. Plant Cell. **7:**957-970.

122. **Omura, S.** 1976. The antibiotic cerulenin, a novel tool for biochemistry as an inhibitor of fatty acid synthesis. Bacteriol. Rev. **40:**681-697.

123. **Osman, T. A., and K. W. Buck**. 1996. Complete replication *in vitro* of tobacco mosaic virus RNA by a template- dependent, membrane-bound RNA polymerase. J. Virol. **70:**6227-6234.

124. **Packter, N. M., and P. K. Stumpf**. 1975. Fat metabolism in higher plants. The effect of cerulenin on the synthesis of medium- and long-chain acids in leaf tissue. Arch. Biochem. Biophys. **167:**655-667.

125. **Paul, A. V., A. Molla, and E. Wimmer**. 1994. Studies of a putative amphipathic helix in the N-terminus of poliovirus protein 2C. Virology. **199:**188-199.

126. **Paul, A. V., E. Rieder, D. W. Kim, J. H. van Boom, and E. Wimmer**. 2000. Identification of an RNA hairpin in poliovirus RNA that serves as the primary template in the *in vitro* uridylylation of VPg. J. Virol. **74:**10359-10370.

127. **Paul, A. V., J. H. van Boom, D. Filippov, and E. Wimmer**. 1998. Protein-primed RNA synthesis by purified poliovirus RNA polymerase. Nature. **393:**280-284.

128. **Pedersen, K. W., Y. van der Meer, N. Roos, and E. J. Snijder**. 1999. Open reading frame 1a-encoded subunits of the arterivirus replicase induce endoplasmic reticulum-derived double-membrane vesicles which carry the viral replication complex. J. Virol. **73:**2016-2026.

129. **Peranen, J., and L. Kaariainen**. 1991. Biogenesis of type I cytopathic vacuoles in Semliki Forest virus- infected BHK cells. J. Virol. **65:**1623-1627.

130. **Peranen, J., P. Laakkonen, M. Hyvonen, and L. Kaariainen**. 1995. The alphavirus replicase protein nsP1 is membrane-associated and has affinity to endocytic organelles. Virology. **208:**610-620.

131. **Perez, L., R. Guinea, and L. Carrasco**. 1991. Synthesis of Semliki Forest virus RNA requires continuous lipid synthesis. Virology. **183:**74-82.

132. **Peters, S. A.** 1994. Thesis Wageningen University.

133. **Peters, S. A., J. M. Mesnard, I. M. Kooter, J. Verver, J. Wellink, and A. van Kammen**. 1995. The cowpea mosaic virus RNA 1-encoded 112 kDa protein may function as a VPg precursor *in vivo*. J. Gen. Virol. **76:**1807-1813.

134. **Peters, S. A., J. Verver, E. A. Nollen, J. W. van Lent, J. Wellink, and A. van Kammen**. 1994. The NTP-binding motif in cowpea mosaic virus B polyprotein is essential for viral replication. J. Gen. Virol. **75:**3167-3176.

135. **Peters, S. A., W. G. Voorhorst, J. Wellink, and A. van Kammen.** 1992. Processing of VPg-containing polyproteins encoded by the B-RNA from cowpea mosaic virus. Virology. **191:**90-97.

136. **Peters, S. A., W. G. Voorhorst, J. Wery, J. Wellink, and A. van Kammen.** 1992. A regulatory role for the 32K protein in proteolytic processing of cowpea mosaic virus polyproteins. Virology. **191:**81-89.

137. **Pih, K. T., V. Kabilan, J. H. Lim, S. G. Kang, H. L. Piao, J. B. Jin, and I. Hwang.** 1999. Characterization of two new channel protein genes in *Arabidopsis*. Mol. Cells. **9:**84-90.

138. **Pinck, M., J. Reinbolt, A. M. Loudes, M. Le Ret, and L. Pinck.** 1991. Primary structure and location of the genome-linked protein (VPg) of grapevine fanleaf nepovirus. FEBS Lett. **284:**117-119.

139. **Ratcliff, F., A. M. Martin-Hernandez, and D. C. Baulcombe.** 2001. Technical Advance. Tobacco rattle virus as a vector for analysis of gene function by silencing. Plant J. **25:**237-245.

140. **Reichel, C., and R. N. Beachy.** 1998. Tobacco mosaic virus infection induces severe morphological changes of the endoplasmic reticulum. Proc. Natl. Acad. Sci. USA. **95:**11169-11174.

141. **Restrepo-Hartwig, M., and P. Ahlquist.** 1999. Brome mosaic virus RNA replication proteins 1a and 2a colocalize and 1a independently localizes on the yeast endoplasmic reticulum. J. Virol. **73:**10303-10309.

142. **Restrepo-Hartwig, M. A., and P. Ahlquist.** 1996. Brome mosaic virus helicase- and polymerase-like proteins colocalize on the endoplasmic reticulum at sites of viral RNA synthesis. J. Virol. **70:**8908-8916.

143. **Rezelman, G., H. Franssen, R. Goldbach, T. S. Ie, and A. van Kammen.** 1982. Limits to the independence of bottom component RNA of cowpea mosaic virus. J. Gen. Virol. **60:**335-342.

144. **Reuer, Q., R. J. Kuhn, and E. Wimmer.** 1990. Characterization of poliovirus clones containing lethal and nonlethal mutations in the genome-linked protein VPg. J. Virol. **64:**2967-2975.

145. **Richards, O. C., R. Eggen, R. Goldbach, and A. van Kammen.** 1989. High-level synthesis of cowpea mosaic virus RNA polymerase and protease in Escherichia coli. Gene. **78:**135-146.

146. **Riedel, D., D. E. Lesemann, and E. Maiss.** 1998. Ultrastructural localization of nonstructural and coat proteins of 19 potyviruses using antisera to bacterially expressed proteins of plum pox potyvirus. Arch. Virol. **143:**2133-2158.

147. **Rothberg, P. G., T. J. Harris, A. Nomoto, and E. Wimmer.** 1978. O4-(5'-uridylyl)tyrosine is the bond between the genome-linked protein and the RNA of poliovirus. Proc. Natl. Acad. Sci. USA. **75:**4868-4872.

148. **Rottier, P. J., G. Rezelman, and A. van Kammen**. 1979. The inhibition of cowpea mosaic virus replication by actinomycin D. Virology. **92:**299-309.

149. **Roulston, A., R. C. Marcellus, and P. E. Branton**. 1999. Viruses and apoptosis. Annu. Rev. Microbiol. **53:**577-628.

150. **Rubino, L., and M. Russo**. 1998. Membrane targeting sequences in tombusvirus infections. Virology. **252:**431-437.

151. **Rubino, L., F. Weber-Lotfi, A. Dietrich, C. Stussi-Garaud, and M. Russo**. 2001. The open reading frame 1-encoded ('36K') protein of Carnation Italian ringspot virus localizes to mitochondria. J. Gen. Virol. **82:**29-34.

152. **Ruiz, M. T., O. Voinnet, and D. C. Baulcombe**. 1998. Initiation and maintenance of virus-induced gene silencing. Plant Cell. **10:**937-946.

153. **Rust, R. C., L. Landmann, R. Gosert, B. L. Tang, W. Hong, H. P. Hauri, D. Egger, and K. Bienz**. 2001. Cellular copii proteins are involved in production of the vesicles that form the poliovirus replication complex. J. Virol. **75:**9808-9818.

154. **Salas, M.** 1991. Protein-priming of DNA replication. Annu. Rev. Biochem. **60:**39-71.

155. **Sanderfoot, A. A., F. F. Assaad, and N. V. Raikhel**. 2000. The *Arabidopsis* genome. An abundance of soluble N-ethylmaleimide- sensitive factor adaptor protein receptors. Plant Physiol. **124:**1558-1569.

156. **Sanders, J., M. Brandsma, G. M. Janssen, J. Dijk, and W. Moller**. 1996. Immunofluorescence studies of human fibroblasts demonstrate the presence of the complex of elongation factor-1 beta gamma delta in the endoplasmic reticulum. J. Cell Sci. **109:**1113-1117.

157. **Sandoval, I. V., and L. Carrasco**. 1997. Poliovirus infection and expression of the poliovirus protein 2B provoke the disassembly of the Golgi complex, the organelle target for the antipoliovirus drug Ro-090179. J. Virol. **71:**4679-4693.

158. **Sansom, M. S., and R. J. Law**. 2001. Membrane proteins: Aquaporins--channels without ions. Curr. Biol. **11:**R71-73.

159. **Sarnow, P.** 1989. Role of 3'-end sequences in infectivity of poliovirus transcripts made *in vitro*. J. Virol. **63:**467-470.

160. **Schaad, M. C., P. E. Jensen, and J. C. Carrington**. 1997. Formation of plant RNA virus replication complexes on membranes: role of an endoplasmic reticulum-targeted viral protein. EMBO J. **16:**4049-4059.

161. **Schlegel, A., T. H. Giddings, Jr., M. S. Ladinsky, and K. Kirkegaard**. 1996. Cellular origin and ultrastructure of membranes induced during poliovirus infection. J. Virol. **70:**6576-6588.

162. **Schneider, F., R. Lessire, J. J. Bessoule, H. Juguelin, and C. Cassagne**. 1993. Effect of cerulenin on the synthesis of very-long-chain fatty acids in microsomes from leek seedlings. Biochim. Biophys. Acta. **1152:**243-252.

163. **Serebriiskii, I., J. Estojak, M. Berman, and E. A. Golemis**. 2000. Approaches to detecting false positives in yeast two-hybrid systems. Biotechniques. **28:**328-330, 332-326.

164. **Sidrauski, C., R. Chapman, and P. Walter**. 1998. The unfolded protein response: an intracellular signalling pathway with many surprising features. Trends Cell. Biol. **8:**245-249.

165. **Siemering, K. R., R. Golbik, R. Sever, and J. Haseloff**. 1996. Mutations that suppress the thermosensitivity of green fluorescent protein. Curr. Biol. **6:**1653-1663.

166. **Skaf, J. S., M. H. Schultz, H. Hirata, and G. A. de Zoeten**. 2000. Mutational evidence that the VPg is involved in the replication and not the movement of Pea enation mosaic virus-1. J. Gen. Virol. **81 Pt 4:**1103-1109.

167. **Skehel, P. A., R. Fabian-Fine, and E. R. Kandel**. 2000. Mouse VAP33 is associated with the endoplasmic reticulum and microtubules. Proc. Natl. Acad. Sci. USA. **97:**1101-1106.

168. **Skehel, P. A., K. C. Martin, E. R. Kandel, and D. Bartsch**. 1995. A VAMP-binding protein from Aplysia required for neurotransmitter release. Science. **269:**1580-1583.

169. **Smirnoff, N.** 2000. Ascorbic acid: metabolism and functions of a multi-facetted molecule. Curr. Opin. Plant Biol. **3:**229-235.

170. **Snijder, E. J., H. van Tol, N. Roos, and K. W. Pedersen**. 2001. Non-structural proteins 2 and 3 interact to modify host cell membranes during the formation of the arterivirus replication complex. J. Gen. Virol. **82:**985-994.

171. **Sosnovtsev, S., and K. Y. Green**. 1995. RNA transcripts derived from a cloned full-length copy of the feline calicivirus genome do not require VpG for infectivity. Virology. **210:**383-390.

172. **Staehelin, L. A.** 1997. The plant ER: a dynamic organelle composed of a large number of discrete functional domains. Plant J. **11:**1151-1165.

173. **Suhy, D. A., T. H. Giddings, Jr., and K. Kirkegaard**. 2000. Remodeling the endoplasmic reticulum by poliovirus infection and by individual viral proteins: an autophagy-like origin for virus-induced vesicles. J. Virol. **74:**8953-8965.

174. **Zabel, P., H. Weenen-Swaans, and A. van Kammen**. 1974. *In vitro* replication of cowpea mosaic virus RNA: I. Isolation and properties of the membrane-bound replicase. J. Virol. **14:**1049-1055.

175. **Zalloua, P. A., J. M. Buzayan, and G. Bruening**. 1996. Chemical cleavage of 5'-linked protein from tobacco ringspot virus genomic RNAs and characterization of the protein-RNA linkage. Virology. **219:**1-8.

176. **Takegami, T., R. J. Kuhn, C. W. Anderson, and E. Wimmer**. 1983. Membrane-dependent uridylylation of the genome-linked protein VPg of poliovirus. Proc. Natl. Acad. Sci. USA. **80:**7447-7451.

177. **Towner, J. S., T. V. Ho, and B. L. Semler**. 1996. Determinants of membrane association for poliovirus protein 3AB. J. Biol. Chem. **271:**26810-26818.

178. **Tu, H., L. Gao, S. T. Shi, D. R. Taylor, T. Yang, A. K. Mircheff, Y. Wen, A. E. Gorbalenya, S. B. Hwang, and M. M. Lai**. 1999. Hepatitis C virus RNA polymerase and NS5A complex with a SNARE-like protein. Virology. **263:**30-41.

179. **Ushiyama, R., and R. E. Matthews**. 1970. The significance of chloroplast abnormalities associated with infection by turnip yellow mosaic virus. Virology. **42:**293-303.

180. **Van Bokhoven, H., O. Le Gall, D. Kasteel, J. Verver, J. Wellink, and A. B. Van Kammen**. 1993. Cis- and trans-acting elements in cowpea mosaic virus RNA replication. Virology. **195:**377-386.

181. **van Bokhoven, H., J. W. van Lent, R. Custers, J. M. Vlak, J. Wellink, and A. van Kammen**. 1992. Synthesis of the complete 200K polyprotein encoded by cowpea mosaic virus B-RNA in insect cells. J. Gen. Virol. **73:**2775-2784.

182. **van Bokhoven, H., J. Wellink, M. Usmany, J. M. Vlak, R. Goldbach, and A. van Kammen**. 1990. Expression of plant virus genes in animal cells: high-level synthesis of cowpea mosaic virus B-RNA-encoded proteins with baculovirus expression vectors. J. Gen. Virol. **71:**2509-2517.

183. **van Bokhoven, H., J. Verver, J. Wellink, and A. van Kammen**. 1993. Protoplasts transiently expressing the 200K coding sequence of cowpea mosaic virus B-RNA support replication of M-RNA. J. Gen. Virol. **74:**2233-2241.

184. **van de Ven, F. J., P. O. Lycksell, A. van Kammen, and C. W. Hilbers**. 1990. Computer-aided assignment of the 1H-NMR spectrum of the viral-protein-genome-linked polypeptide from cowpea mosaic virus. Eur. J. Biochem. **190:**583-591.

185. **Van Der Heijden, M. W., J. E. Carette, P. J. Reinhoud, A. Haegi, and J. F. Bol**. 2001. Alfalfa mosaic virus replicase proteins P1 and P2 interact and colocalize at the vacuolar membrane. J. Virol. **75:**1879-1887.

186. **van der Meer, Y., E. J. Snijder, J. C. Dobbe, S. Schleich, M. R. Denison, W. J. Spaan, and J. K. Locker**. 1999. Localization of mouse hepatitis virus nonstructural proteins and RNA synthesis indicates a role for late endosomes in viral replication. J. Virol. **73:**7641-7657.

187. **van Kuppeveld, F. J., J. M. Galama, J. Zoll, P. J. van den Hurk, and W. J. Melchers**. 1996. Coxsackie B3 virus protein 2B contains cationic amphipathic helix that is required for viral RNA replication. J. Virol. **70:**3876-3886.

188. **van Kuppeveld, F. J., J. G. Hoenderop, R. L. Smeets, P. H. Willems, H. B. Dijkman, J. M. Galama, and W. J. Melchers**. 1997. Coxsackievirus protein 2B modifies endoplasmic reticulum membrane and plasma membrane permeability and facilitates virus release. EMBO J. **16:**3519-3532.

189. **Van Lent, J., J. Wellink, and R. Goldbach**. 1990. Evidence for the involvement of the 58K and 48K proteins in intracellular movement of cowpea mosaic virus. J. Gen. Virol. **71**:219-223.

190. **van Lent, J. W., J. T. Groenen, E. C. Klinge-Roode, G. F. Rohrmann, D. Zuidema, and J. M. Vlak**. 1990. Localization of the 34 kDa polyhedron envelope protein in Spodoptera frugiperda cells infected with Autographa californica nuclear polyhedrosis virus. Arch. Virol. **111**:103-114.

191. **Vance, D. E., E. M. Trip, and H. B. Paddon**. 1980. Poliovirus increases phosphatidylcholine biosynthesis in HeLa cells by stimulation of the rate-limiting reaction catalyzed by CTP: phosphocholine cytidylyltransferase. J. Biol. Chem. **255**:1064-1069.

192. **Vartapetian, A. B., Y. F. Drygin, K. M. Chumakov, and A. A. Bogdanov**. 1980. The structure of the covalent linkage between proteins and RNA in encephalomyocarditis virus. Nucleic Acids Res. **8**:3729-3742.

193. **Weir, M. L., A. Klip, and W. S. Trimble**. 1998. Identification of a human homologue of the vesicle-associated membrane protein (VAMP)-associated protein of 33 kDa (VAP-33): a broadly expressed protein that binds to VAMP. Biochem. J. **333**:247-251.

194. **Weir, M. L., H. Xie, A. Klip, and W. S. Trimble**. 2001. VAP-A Binds Promiscuously to both v- and tSNAREs. Biochem. Biophys. Res. Commun. **286**:616-621.

195. **Wellink, J., and A. van Kammen**. 1989. Cell-to-cell transport of cowpea mosaic virus requires both the 58K/48K proteins and the capsid proteins. J. Gen. Virol. **70**:2279-2286.

196. **Wellink, J., J. Van Lent, and R. Goldbach**. 1988. Detection of viral proteins in cytopathic structures in cowpea protoplasts infected with cowpea mosaic virus. J. Gen. Virol. **69**:751-755.

197. **Wellink, J., J. W. van Lent, J. Verver, T. Sijen, R. W. Goldbach, and A. van Kammen**. 1993. The cowpea mosaic virus M RNA-encoded 48-kilodalton protein is responsible for induction of tubular structures in protoplasts. J. Virol. **67**:3660-3664.

198. **Verver, J., J. Wellink, J. Van Lent, K. Gopinath, and A. Van Kammen**. 1998. Studies on the movement of cowpea mosaic virus using the jellyfish green fluorescent protein. Virology. **242**:22-27.

199. **Westaway, E. G., J. M. Mackenzie, M. T. Kenney, M. K. Jones, and A. A. Khromykh**. 1997. Ultrastructure of Kunjin virus-infected cells: colocalization of NS1 and NS3 with double-stranded RNA, and of NS2B with NS3, in virus- induced membrane structures. J. Virol. **71**:6650-6661.

200. **Wimmer, E., C. U. Hellen, and X. Cao**. 1993. Genetics of poliovirus. Annu. Rev. Genet. **27**:353-436.

201. **Wolk, B., D. Sansonno, H. G. Krausslich, F. Dammacco, C. M. Rice, H. E. Blum, and D. Moradpour**. 2000. Subcellular localization, stability, and trans-cleavage competence of the hepatitis C virus NS3-NS4A complex expressed in tetracycline-regulated cell lines. J. Virol. **74:**2293-2304.

202. **von Arnim, A. G., X. W. Deng, and M. G. Stacey**. 1998. Cloning vectors for the expression of green fluorescent protein fusion proteins in transgenic plants. Gene. **221:**35-43.

203. **Vos, P., M. Jaegle, J. Wellink, J. Verver, R. Eggen, A. Van Kammen, and R. Goldbach**. 1988. Infectious RNA transcripts derived from full-length DNA copies of the genomic RNAs of cowpea mosaic virus. Virology. **165:**33-41.

204. **Vos, P., J. Verver, M. Jaegle, J. Wellink, A. van Kammen, and R. Goldbach**. 1988. Two viral proteins involved in the proteolytic processing of the cowpea mosaic virus polyproteins. Nucleic Acids Res. **16:**1967-1985.

205. **Wu, S. X., P. Ahlquist, and P. Kaesberg**. 1992. Active complete *in vitro* replication of Nodavirus RNA requires glycerophospholipid. Proc. Natl. Acad. Sci. USA. **89:**11136-11140.

206. **Wu, S. X., and P. Kaesberg**. 1991. Synthesis of template-sense, single-strand Flockhouse virus RNA in a cell-free replication system. Virology. **183:**392-396.

207. **Xiang, W., A. Cuconati, D. Hope, K. Kirkegaard, and E. Wimmer**. 1998. Complete protein linkage map of poliovirus P3 proteins: interaction of polymerase 3Dpol with VPg and with genetic variants of 3AB. J. Virol. **72:**6732-6741.

208. **Yamanaka, T., T. Ohta, M. Takahashi, T. Meshi, R. Schmidt, C. Dean, S. Naito, and M. Ishikawa**. 2000. TOM1, an *Arabidopsis* gene required for efficient multiplication of a tobamovirus, encodes a putative transmembrane protein. Proc. Natl. Acad. Sci. USA. **97:**10107-10112.

NEDERLANDSE SAMENVATTING

Planten- en diervirussen met een RNA genoom vermenigvuldigen hun RNA genoom in het cytoplasma van geïnfecteerde cellen op specifieke membraanstructuren. (hoofdstuk 1). Het proces van RNA replicatie staat centraal in de levenscyclus van een RNA virus en de membraanstructuren zijn daarvoor essentieel. Cowpea mosaic virus (CPMV), het virus waar het onderzoek beschreven in dit proefschrift betrekking op heeft, is een goed voorbeeld van zo'n RNA virus. Infectie van cowpea planten (*Vigna unguiculata* L.) met CPMV leidt tot de vorming van kleine membraanblaasjes in het cytoplasma en met electronenmicroscopie is aangetoond dat de replicatie van CPMV-RNA hiermee is geassocieerd. Het doel van onderzoek was om meer inzicht te krijgen in de vorming van deze blaasjes en de cellulaire componenten die daar betrokken bij zijn. Ook is geprobeerd om na te gaan welke door het virus gecodeerde eiwitten en/of welke eiwitten gecodeerd door de waardplant van het virus, betrokken zijn bij de door CPMV geïnduceerde veranderingen in membraanstructuren.

CPMV behoort tot de groep van *Comovirussen* die een opmerkelijke overeenkomst vertonen met dierlijke *Picornavirussen* zoals bv. poliovirus. Cowpea is een tropisch voedselgewas dat door de lange peulen ook bekend is als kousenband. Het genoom van CPMV bestaat uit twee RNA moleculen die elk afzonderlijk zijn verpakt in een eiwitmantel. Aan het ene, het 5'-uiteinde van het RNA molecuul zit een klein eiwit gebonden (VPg) en het andere, het 3'-uiteinde heeft een poly(A) staart. Translatie van beide RNA moleculen leidt tot de synthese van een poly-eiwit dat proteolytisch geknipt wordt in verschillende functionele eiwitten. Het grootste RNA molecuul (RNA1 genoemd) codeert voor de eiwitten die essentieel zijn voor de replicatie van het virus en kan zich onafhankelijk van het andere, kleinere RNA molecuul (RNA2) vermenigvuldigen. Het RNA2 codeert voor de eiwitten betrokken bij het omhullen van het RNA molecuul met een mantel en een eiwit dat ervoor zorgt dat het virus zich van cel naar cel door de geïnfecteerde plant kan verspreiden. De typische membraanblaasjes die betrokken zijn bij replicatie van het virus worden ook gevonden in geïsoleerde plantencellen (protoplasten) die alleen met het RNA1 zijn geïnfecteerd hetgeen suggereert dat een of meerdere eiwitten die gecodeerd worden door RNA1 betrokken zijn bij inductie van de blaasjes.

Om meer inzicht te krijgen in welke intracellulaire membranen betrokken zijn bij de vorming van de membraanblaasjes is er gebruikt gemaakt van eiwitten die zich specifiek in de membranen van bepaalde organellen bevinden zoals het endoplasmatisch reticulum (ER), het Golgi apparaat etc. (hoofdstuk 2). Door deze merker eiwitten te koppelen aan het "green fluorescent protein" (GFP) konden de gevolgen van een CPMV-infectie op de morfologie van verschillende membraansystemen met een fluorescentiemicroscoop gevolgd worden. Uit deze experimenten bleek dat na een infectie met CPMV er in verschillende gebieden van het ER

woekering plaatsvindt. In deze gebieden werden ook de replicatie eiwitten van CPMV aangetroffen hetgeen suggereert dat de membraanblaasjes afkomstig zijn van deze ER woekering. De replicatie van CPMV bleek sterk geremd te worden door cerulenine, een remmer van *de novo* membraansynthese terwijl de replicatie van alfafa mozaiek virus en tabaks mozaiek virus bij dezelfde concentratie cerulenine niet verhinderd werd. Deze resultaten wijzen erop dat het ER de bron is van de membraanblaasjes en dat bovendien het ontstaan van deze blaasjes afhankelijk is van *de novo* lipide synthese.

De gebieden in CPMV geïnfecteerde protoplasten waar de replicatie plaatsvindt zijn verder gekarakteriseerd door gebruik te maken van fluorescente *in situ* hybridisatie (FISH) waarmee de lokalisatie van het virale RNA in de cel kan worden bepaald (hoofdstuk 3). Het bleek dat de replicatie van het virale RNA begint in verschillende kleine, duidelijk omsloten gebieden in de cel die vervolgens samen te vloeien tot een grote structuur die meestal in het midden van de cel naast de kern is gelegen. Experimenten met de remmers van het cytoskelet, oryzaline en latrunculine B, suggereerden dat het actine cytoskelet betrokken is bij de vorming van deze centrale structuur. De inductie van de ER membraan woekeringen leidde niet tot een opregulatie van BiP mRNA hetgeen erop duidt dat de "unfolded protein response" niet betrokken is bij dit proces.

Om te bepalen welke van de virale eiwitten verantwoordelijk zijn voor de membraan modificaties en de verankering van het replicatiecomplex aan de membranen, zijn individuele eiwitten gecodeert door RNA1 tot expressie gebracht in cowpea protoplasten en in tabaksbladeren met het tabaks ratel virus expressie systeem (hoofdstuk 5). Het 32K en het 60K eiwit bleken zich in kleine hoeveelheden op te hopen en waren aan membranen gebonden. Het 24K en het 110K daarentegen bleken los en vrij oplosbaar in het cytoplasma voor te komen. Verder bewerkstelligden 32K en 60K duidelijke veranderingen in de morfologie van het ER te bewerkstelligen wat aangeeft dat deze twee eiwitten, wellicht in combinatie, verantwoordelijk zijn voor de ER woekeringen die voorkomen in CPMV geïnfecteerde cellen. Afzonderlijke expressie van 32K of 60K met het tabaks ratel virus expressie systeem leidde tot necrotische plekken op geïnfecteerde bladeren. Dit was zeer opmerkelijk is omdat tijdens normale infectie met CPMV geen sprake is van celdood. De necrose kan het gevolg zijn van een specifieke afweerreactie van de plant zoals beschreven is voor veel andere plant pathogenen. Het zou ook zo kunnen zijn dat 32K of 60K door zich in de membraan te voegen de membraan poreus maakt waardoor de cel sterft. Dit mechanisme is beschreven voor het poliovirus eiwit 2BC wat sequentie homologie vertoont met het 60K.

Met het gist twee-hybride systeem zijn vijf gastheer eiwitten gevonden die aan het 60K eiwit binden en die 60K wellicht assisteren in de functie die het uitoefent tijdens de virale levenscyclus (hoofdstuk 4). Twee van de eiwitten (VAP27-1 en VAP27-2) vertoonden homologie met een dierlijk eiwitten die betrokken zijn bij eiwittransport tussen ER en het Golgi-apparaat. Expressie van de eiwitten in protoplasten toonde aan dat zij ook aanwezig

waren in het gewoekerde ER en dit zou mogelijk kunnen betekenen dat de interactie van 60K met deze eiwitten leid tot het ontstaan van de CPMV-geïnduceerde membraanveranderingen.

Het 60K eiwit is een directe precursor van het VPg eiwit dat covalent gebonden is aan het 5'-uiteinde van het virus RNA via de hydroxyl groep van het N-terminale serine aminozuur (hoofdstuk 6). Virussen met mutaties van dit aminozuur of van aminozuren in de directe nabijheid bleken niet infectieus te zijn in protoplasten. Sommige van deze mutaties verstoorden de klieving van het VPg met het 58K eiwit *in vitro* hetgeen zou kunnen hebben bijgedragen to het lethale fenotype. Verder zijn er mutaties aangebracht die het CPMV VPg veranderende in het VPg van een gerelateerd comovirus. Sommige van deze mutaties waren lethaal terwijl andere minder of geen effect hadden op virus replicatie. Dit duidt erop dat ook aminozuren die niet geconserveerd zijn tussen de comovirussen essentieel kunnen zijn voor de functie van VPg. De replicatie eiwitten van een van de mutanten hoopten zich niet meer op in de typische cytopatische structuur hetgeen de betrokkenheid van VPg in eiwit-eiwit interacties zou kunnen weerspiegelen.

In hoofdstuk 7 worden de resultaten samengevat en een model van CPMV geïnduceerde membraan modificaties gepresenteerd. Wanneer een plantencel geïnfecteerd wordt met CPMV komt het virale RNA uit zijn eiwitmantel en zal vertaling van RNA1 leiden tot productie van het 200K poly-eiwit dat geklieft wordt in het 32K en het 170K eiwit. In ons model blijft het 32K geassocieerd met het 170K via een interactie tussen 32K en het 60K gedeelte van 170K, waardoor verdere klieving geremd wordt. Het 32K/170K complex wordt specifiek gestuurd naar de ER membraan gestuurd via een lokalisatie signaal in het 32K. Interactie van 32K met het membraan zou effect kunnen hebben op de 32K/170K interactie waardoor verdere klieving van het 170K optreedt. Op dat moment wordt het 60K vrijgemaakt en in de ER membraan gevoegd waardoor het replicatie complex verankert is in dit membraan. Interactie van zowel 32K en 60K met de membranen leidt tot een verhoging van de lipide synthese en het woekeren van ER membranen. Dit zou de replicatie van CPMV kunnen bevorderen omdat er een compartiment gevormd wordt waarin het RNA beschermd is tegen degradatie. Tevens zouden de membranen kunnen bijdragen aan het verhogen van locale concentraties viraal RNA en replicatie eiwitten. Een grote uitdaging resteert nu om te ontrafelen hoe de CPMV gecodeerde eiwitten de moleculaire mechanismen activeren die leiden tot ER woekering en het vormen van de membraanblaasjes.

NAWOORD

Het nawoord is een goede gelegenheid om mensen te noemen die direct of indirect betrokken zijn geweest bij het onderzoek dat in dit proefschrift beschreven is.

De sfeer op de vakgroep Moleculaire Biologie heb ik altijd als bijzonder goed ervaren. Hoewel de onderwerpen binnen de vakgroep nogal verschilden was er altijd een "kritische massa" AIO's en postdocs bezig met vernieuwend onderzoek die voor mij een bron van ideeën en praktische tips vormden. Ik wil dan ook alle medewerkers en tijdelijke medewerkers van de vakgroep hiervoor bedanken. Aan de wieg van de vakgroep heeft Ab van Kammen gestaan en ik voel het als een voorrecht om tijdens zijn emiritaat de laatste promovendus te zijn die onder zijn supervisie promoveert. Beste Ab, bedankt voor de enthousiaste manier waarop je nieuwe resulaten van mijn onderzoek hebt ontvangen. De discussies die we hebben gevoerd over de interpretatie van de resultaten en over de wetenschap in het algemeen vond ik zeer stimulerend en het leidde vaak tot nieuwe inzichten bij mij. Verder zal ik op jouw aanraden in mijn nieuwe baan als postdoc ervoor waken teveel wetenschappelijk jargon op te schrijven. Joan, als co-promotor heb je een grote rol gespeeld in het tot stand komen van dit boekje. Ik heb het erg gewaardeerd dat bij jouw altijd de deur openstond (zowel letterlijk als figuurlijk) voor vragen en problemen en door je uitgebreide kennis van het CPMV-onderzoek wist je op de meeste vragen een meer dan adequaat antwoord. Ook in de laatste fase van mijn AIO-schap heb je door het snelle corrigeren van mijn manuscripten ervoor gezorgd dat de vaart erin kon blijven. Bedankt hiervoor. Kerstin, jouw handige, en in ieder geval RNAse-vrije, vingers zijn verantwoordelijk voor een niet onaanzienlijk deel van de resulaten beschreven in dit proefschrift. Ik vond de samenwerking altijd heel prettig. Je drang om nieuwe dingen te leren en toe te passen zal in je nieuwe baan goed van pas komen. Jan V., als collectief geheugen van het lab wist je altijd goede tips om de proef te laten slagen. Bedankt hiervoor en voor je hulp bij vele experimenten. Want je weet: als ik jouw niet had, dan. . . . . Verder wil ik Peter, Jeroen, Sizo en Gopi bedanken voor de gezellige tijd in en buiten het lab. Peter, ik denk met veel plezier terug aan de gezamelijke congresbezoeken aan Florida en Sydney. Het onderzoek dat je gedaan hebt aan de verspreiding van CPMV wordt nu vol enthousiasme doorgezet door Jeroen. Jeroen, het was altijd leuk om een pittige discussie met je te voeren over het werk of over de politiek. Sizo, I have enjoyed the interesting discussions we had on the topic of gene silencing and the role of HC-Pro in this. I am glad that you are in the position to continue to work on this subject in the United States and I wish you all the best. Gopi, your cloning skills (and especially speed) are still memorable in our lab and I have enjoyed working with you. I hope that after your research in the United States you will be able to obtain a permanent position in India. Verder

hebben vier studenten in het kader van een afstudeervak onderzoek gedaan aan de replicatie van CPMV. Marchel, Imke, Gert-Jan en Joost, bedankt voor jullie inzet en enthousiasme. Ton Bisseling wil ik bedanken voor de inbreng tijdens de werkbesprekingen. De sequence groep, met name Tony van Kampen wil ik bedanken voor alle sequenties die ze in het kader van dit onderzoek hebben bepaald. Janneke Saaijer en Aart van Ommeren bedankt voor het opkweken van de bentha's.

Verder dienen de stimulerende discussies met collega's van de vakgroep virologie in Wageningen (bedankt voor het opvangen van de CPMV nomaden tijdens de asbest crisis) en van de vakgroep plantenvirologie in Leiden niet onvermeld te blijven. Jan van Lent, bedankt voor het EM werk aan CPMV-geïnfecteerde cellen, waarbij er heel wat gespeurd moest worden naar vesicles en niet te vergeten bedankt voor het aanleveren van het fluorescentieplaatje dat dient als kaft-illustratie van dit proefschrift.

Natuurlijk kan de boog niet altijd gespannen staan en buiten het lab waren er dan ook vrienden die het leven van een AIO konden veraangenamen. Met de "Leidse connectie" (Bas, Camiel, Marc en Roeland) werd er onder het genot van een goed glas bier (of meerdere) over wetenschap en andere zaken gepraat. Met Frank was het altijd leuk om een "verantwoorde" film te kijken. Op de squashbaan (Cindy en Tinri) werd na de geestelijke arbeid ook lichamelijke arbeid verricht en dan waren er nog de WAIOO vergaderingen (Cindy, Eyke, Marijke en Marc) die ook altijd gezellig waren. Als laatste wil ik mijn broer Staf en mijn moeder bedanken voor de belangstelling, steun en liefde die jullie hebben gegeven in alle jaren.

CURRICULUM VITAE

Jan Eduard Carette werd op 1 oktober 1971 te Den Haag geboren. Hij behaalde het VWO diploma aan het Sint Maartens College te Voorburg in juni 1990. In september dat jaar startte hij met de studie Scheikunde aan de Rijksuniversiteit Leiden. Zijn studie werd afgesloten met onderzoek bij de vakgroep Plantenvirussen (Prof. J.F. Bol) en bij de vakgroep Virologie (divisie Medische Microbiologie, Prof. W. Spaan). In augustus 1996 behaalde hij zijn doctoraal diploma. In oktober 1996 is hij gestart met een promotieonderzoek bij het Laboratorium voor Moleculaire Biologie aan de Wageningen Universiteit onder begeleiding van Prof. A. van Kammen en Dr. J. Wellink. De resultaten van het onderzoek zijn beschreven in dit proefschrift. Sinds 1 september 2001 is hij werkzaam als postdoc bij de vakgroep Gentherapie divisie Medische Oncologie (Prof. H.M. Pinedo) aan de Vrije Universiteit te Amsterdam.

The work presented in this thesis was carried out at the Laboratory of Molecular Biology Department of Plant Sciences, Wageningen University, Wageningen , The Netherlands and was financially supported by the Council for Chemical Sciences (CW) of the Netherlands Organization of Scientific Research (NWO).

Origin of the membrane compartment for cowpea mosaic virus replication
Carette, Jan
Thesis Wageningen University, The Netherlands
With references - with summary in Dutch

Cover illustration: Fluorescence confocal micrograph of the endoplasmic reticulum in *N. Benthamiana* epidermal petal cells infected with CPMV as visualized by ER-GFP. The photograph was kindly provided by Jan van Lent, Laboratory of Virology, Wageningen University.